

Cosmic-Ray Anisotropies in the TeV-PeV Range

Markus Ahlers
Niels Bohr Institute

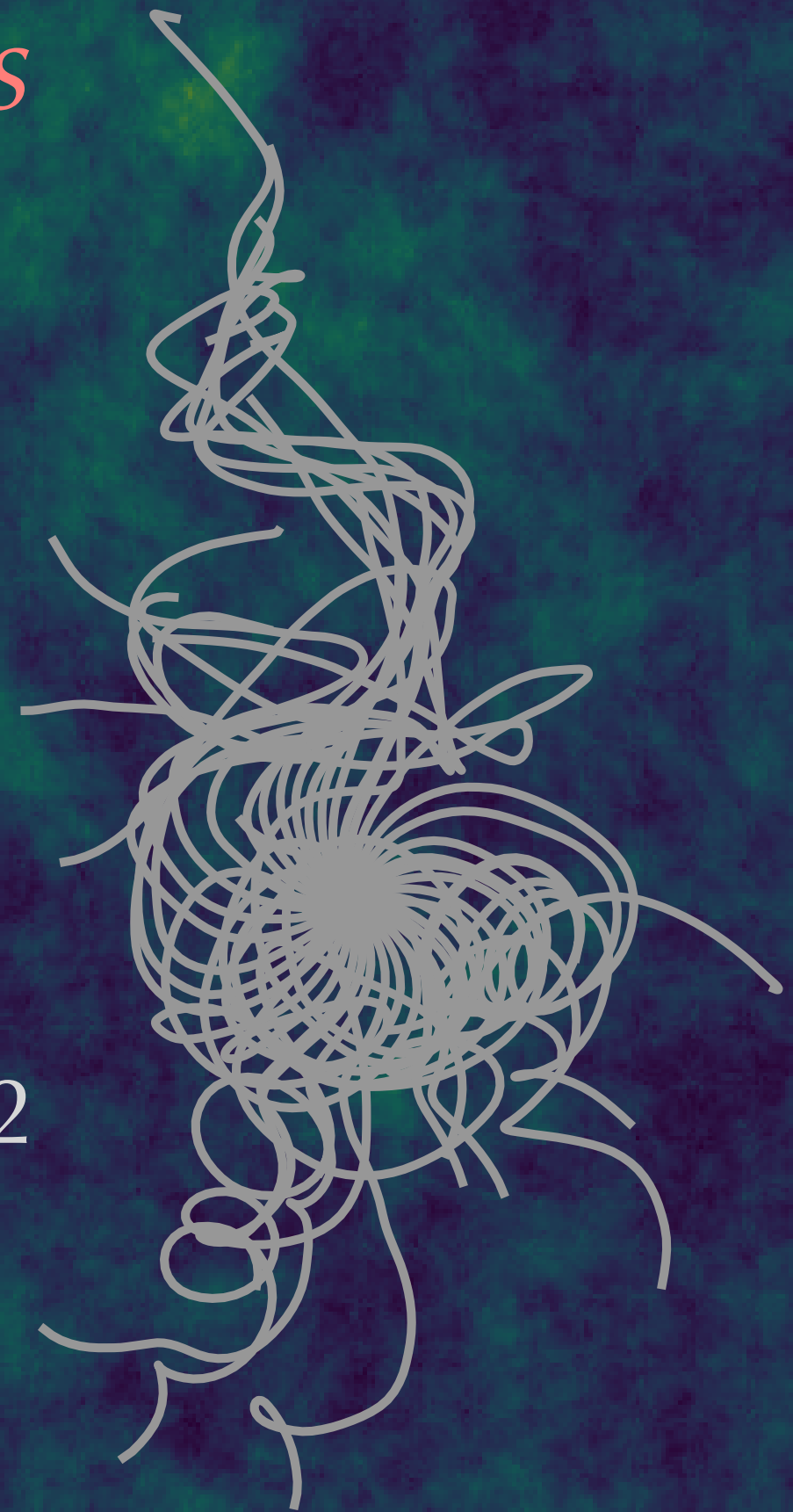
*International School of
Cosmic Ray Astrophysics*

EMFCSC, Erice, August 1-2, 2022

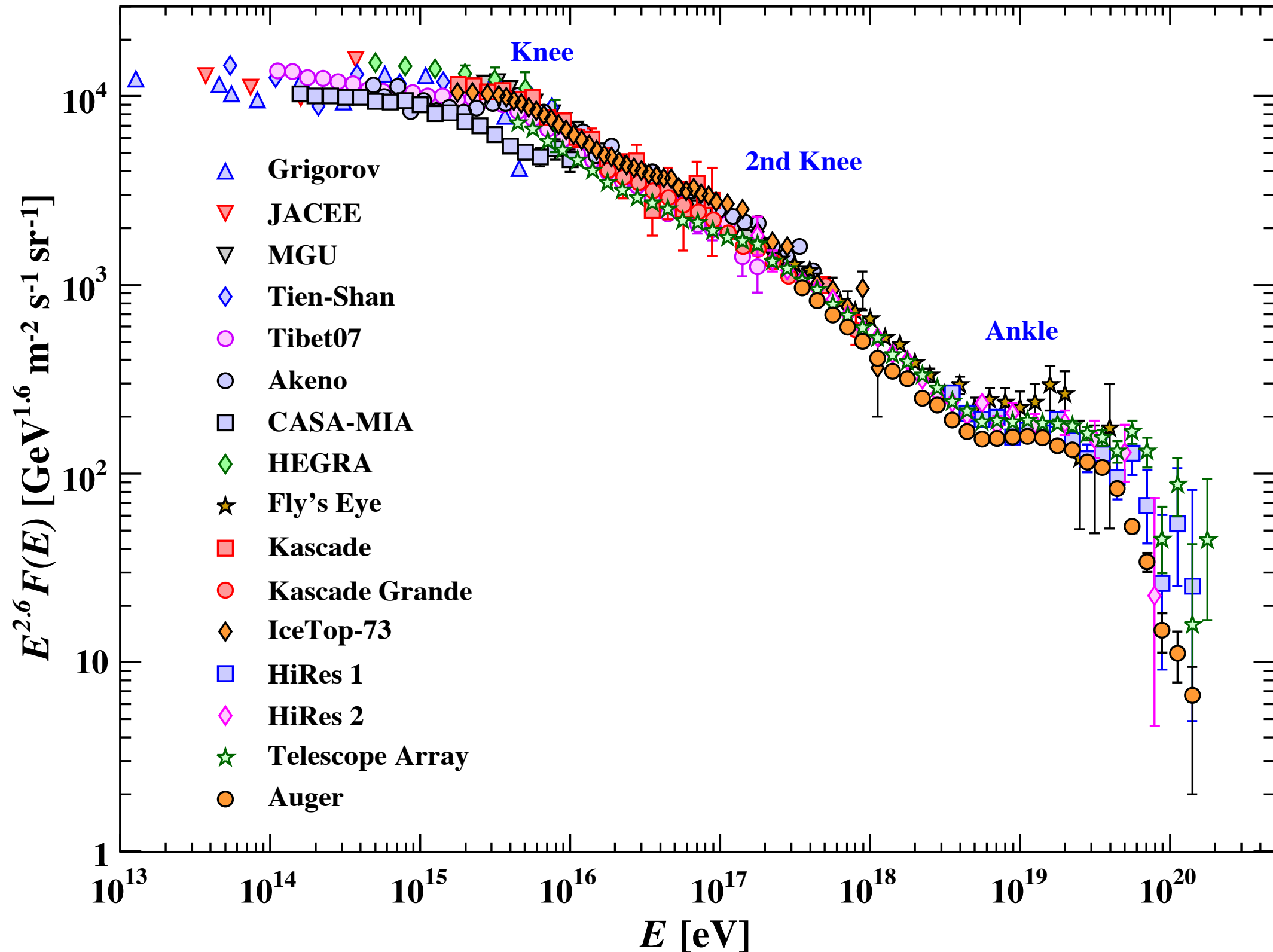
VILLUM FONDEN



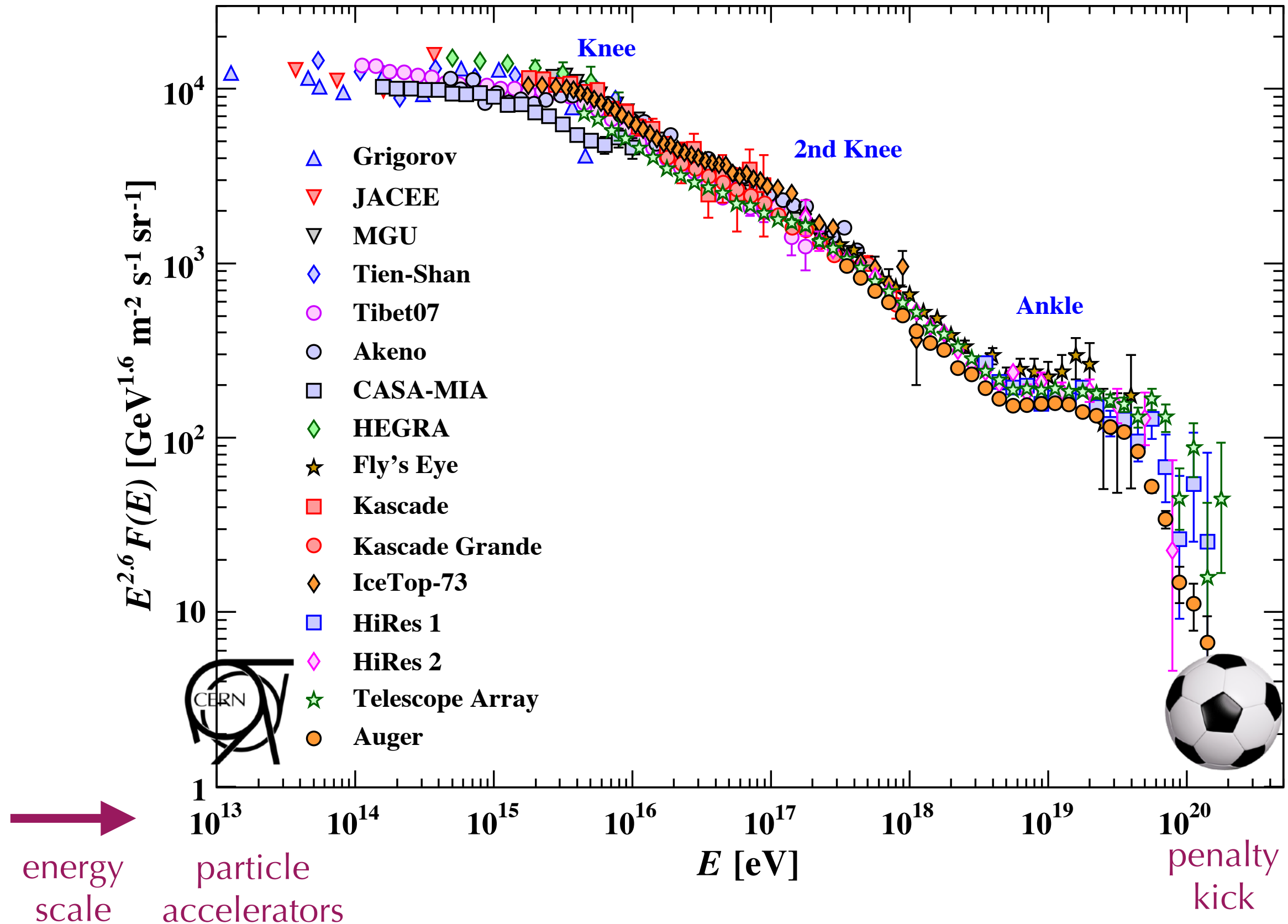
KØBENHAVNS
UNIVERSITET



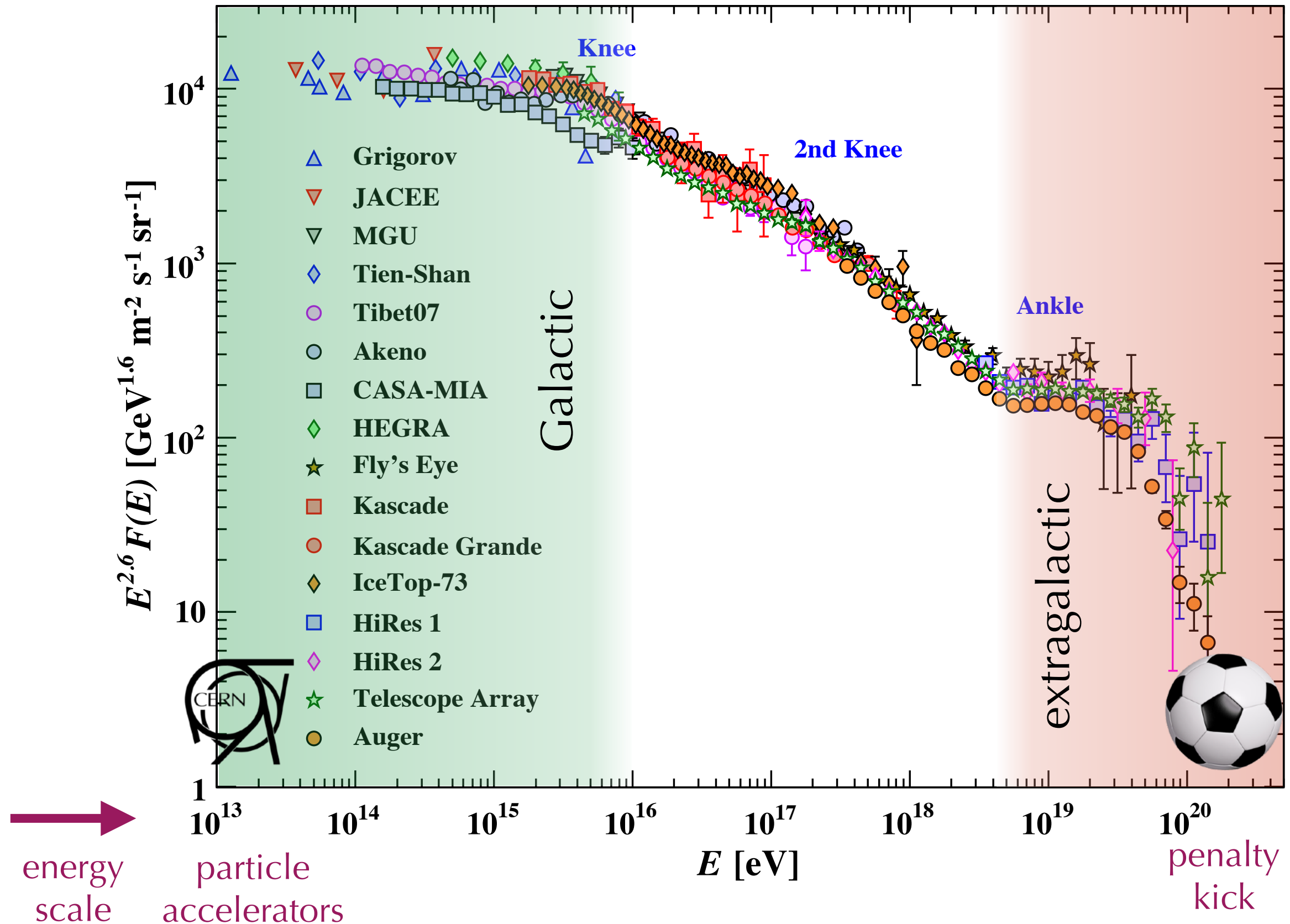
The Cosmic Ray Monopole



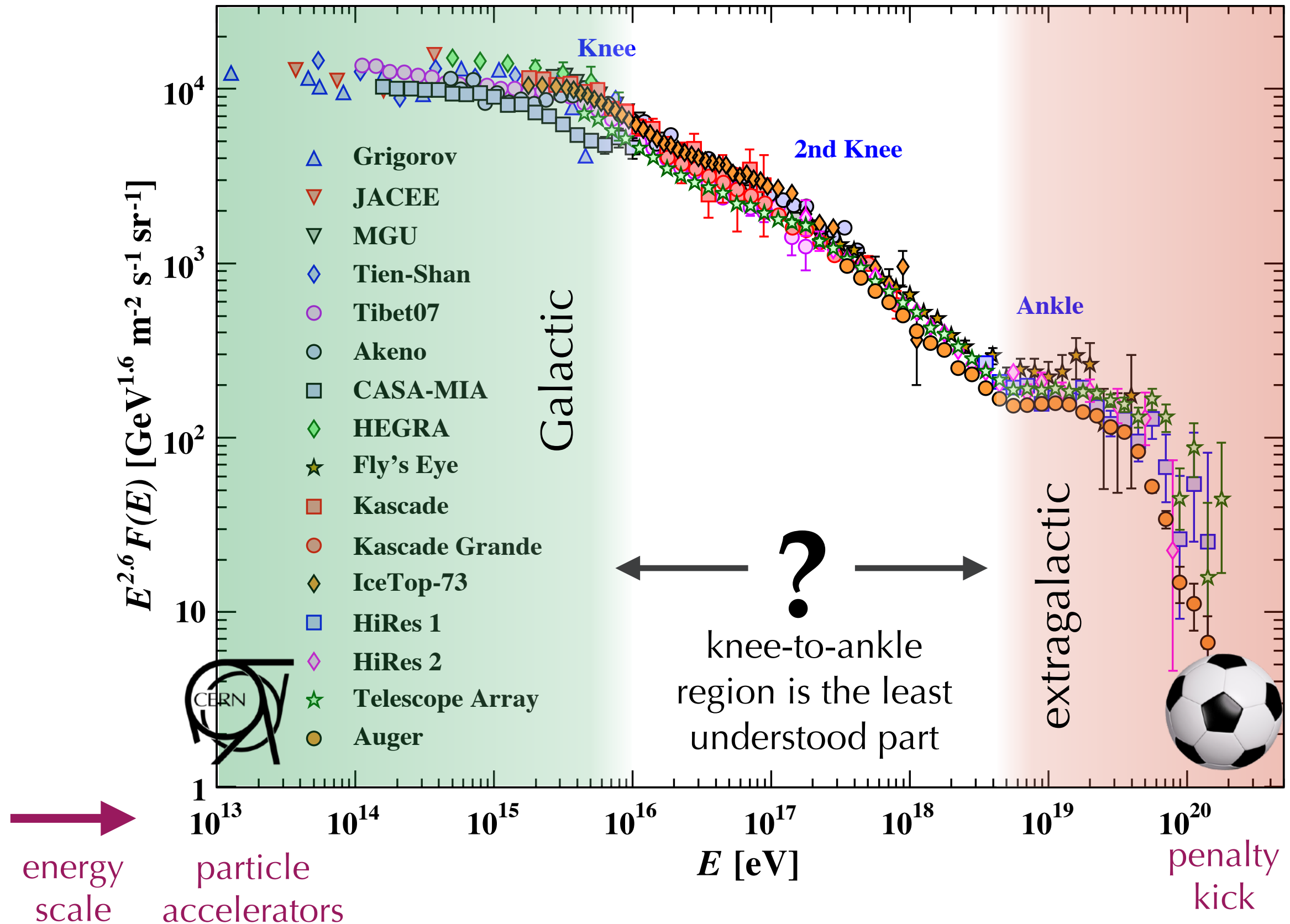
The Cosmic Ray Monopole



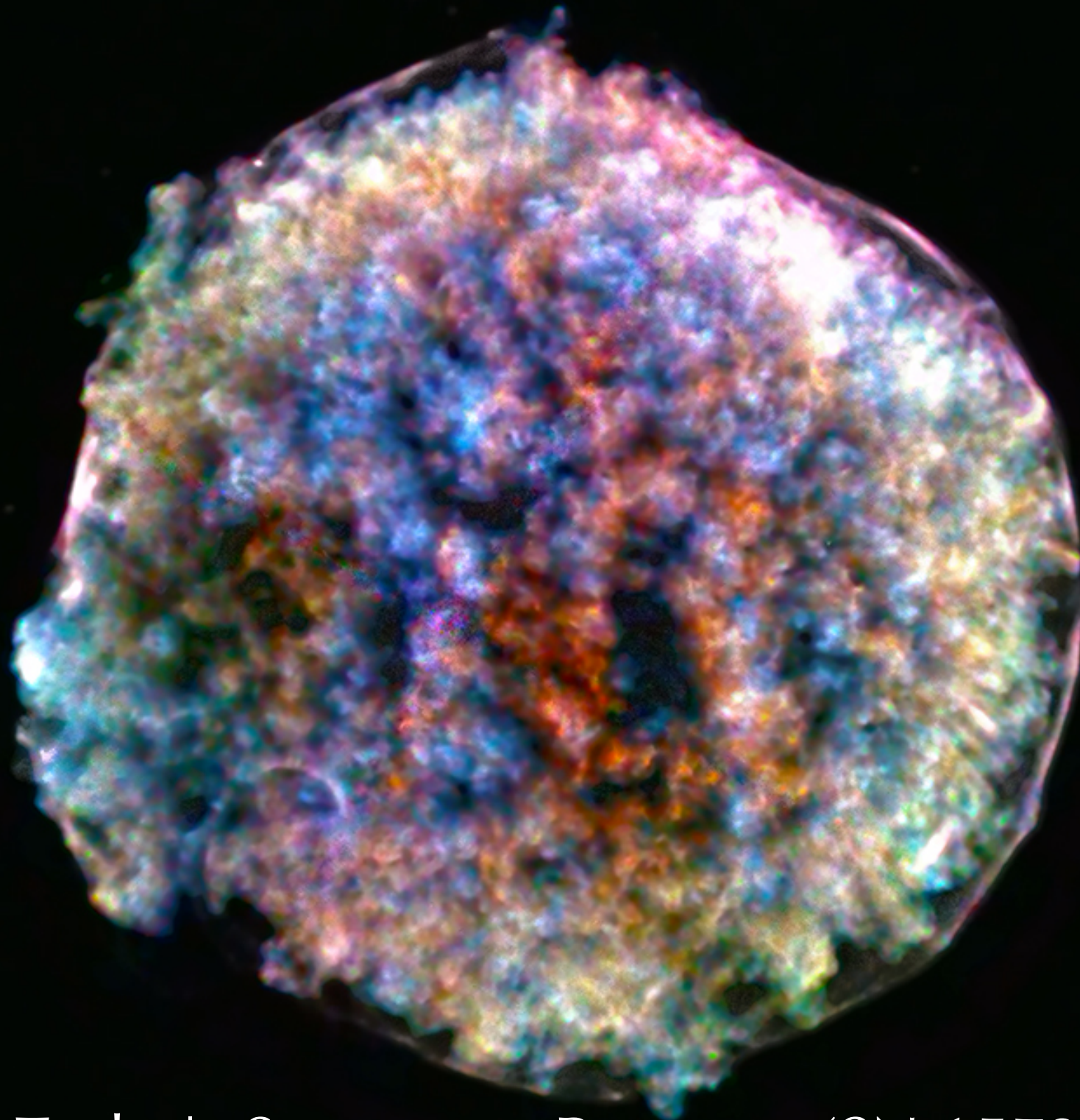
The Cosmic Ray Monopole



The Cosmic Ray Monopole



Supernova Remnants



Tycho's Supernova Remnant (SN 1572)

Galactic Cosmic Rays

- *Standard paradigm:*
Galactic CRs accelerated in
supernova remnants
- sufficient power: $\sim 10^{-3} M_{\odot}$
per 3 SNe per century
[Baade & Zwicky'34]

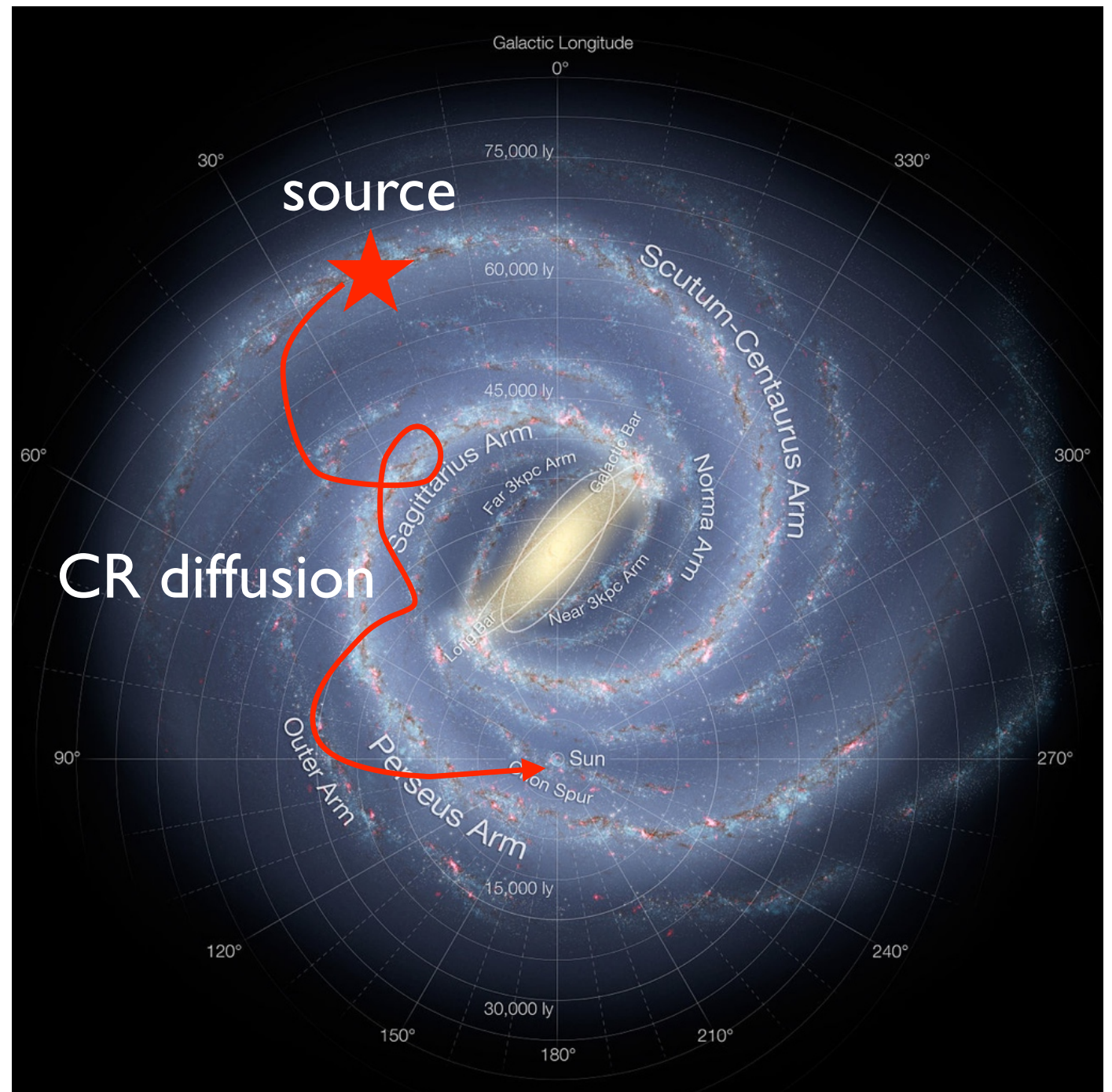
- diffusive shock acceleration:

$$n_{\text{CR}} \propto E^{-\Gamma}$$

- rigidity-dependent escape
from Galaxy:

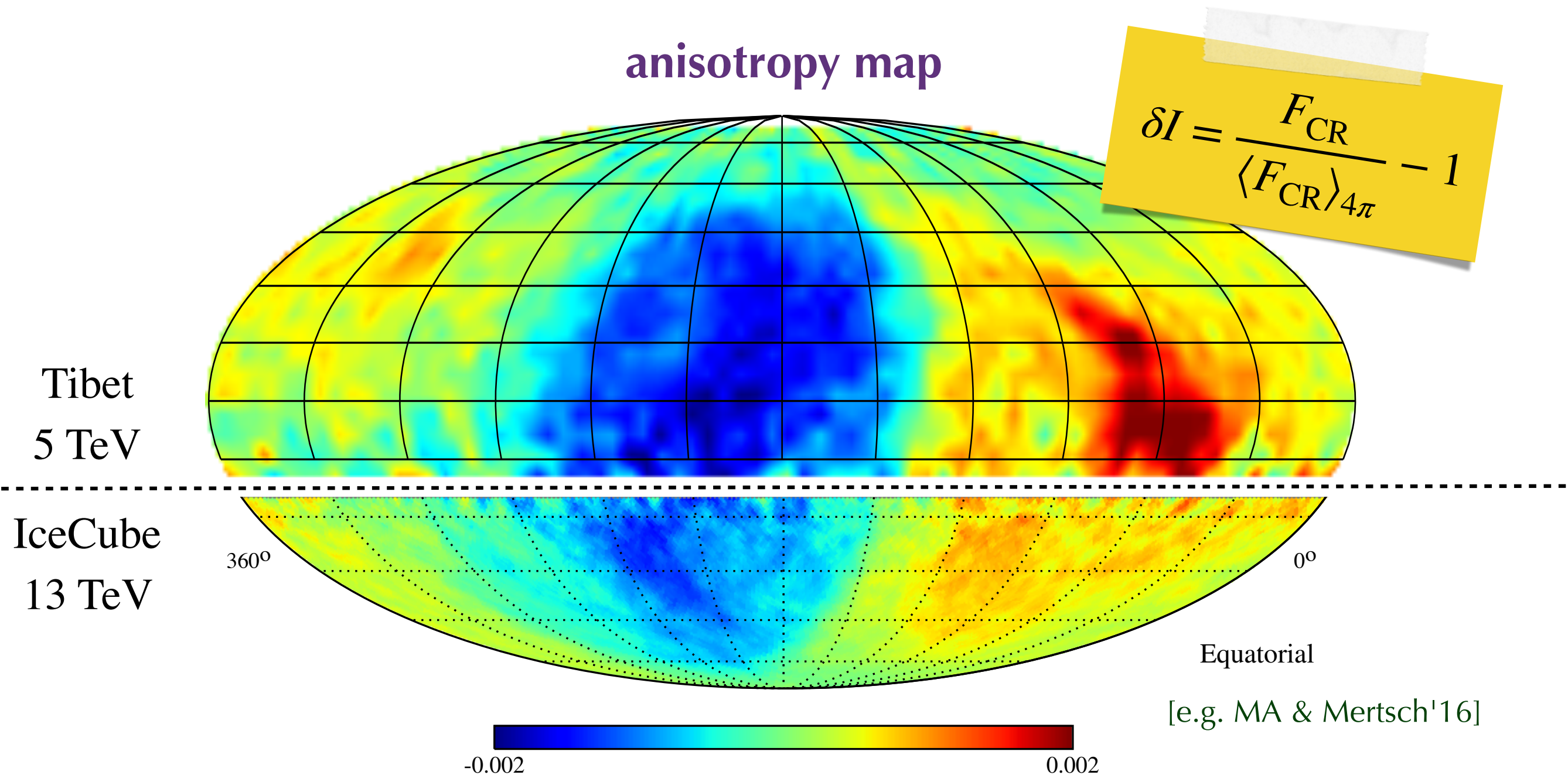
$$n_{\text{CR}} \propto E^{-\Gamma-\delta}$$

- mostly isotropic CR arrival
directions



Galactic Cosmic Rays Anisotropy

Cosmic ray anisotropies up to the level of **one-per-mille** at various energies
(Super-Kamiokande, Milagro, ARGO-YBJ, EAS-TOP, Tibet AS γ , IceCube, HAWC)

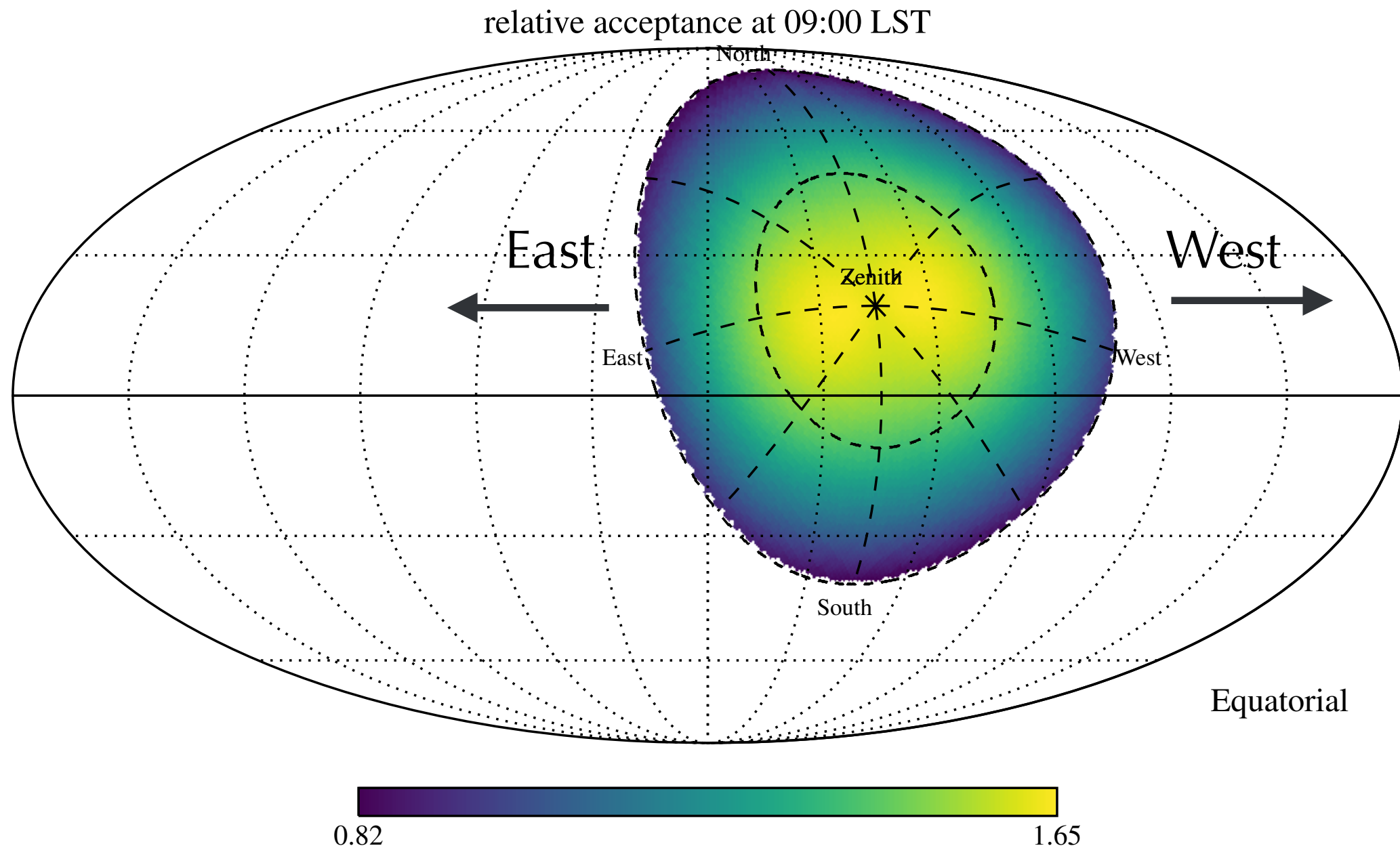


Galactic Cosmic Rays Anisotropy

Cosmic ray anisotropies up to the level of **one-per-mille** at various energies
(Super-Kamiokande, Milagro, ARGO-YBJ, EAS-TOP, Tibet AS γ , IceCube, HAWC)



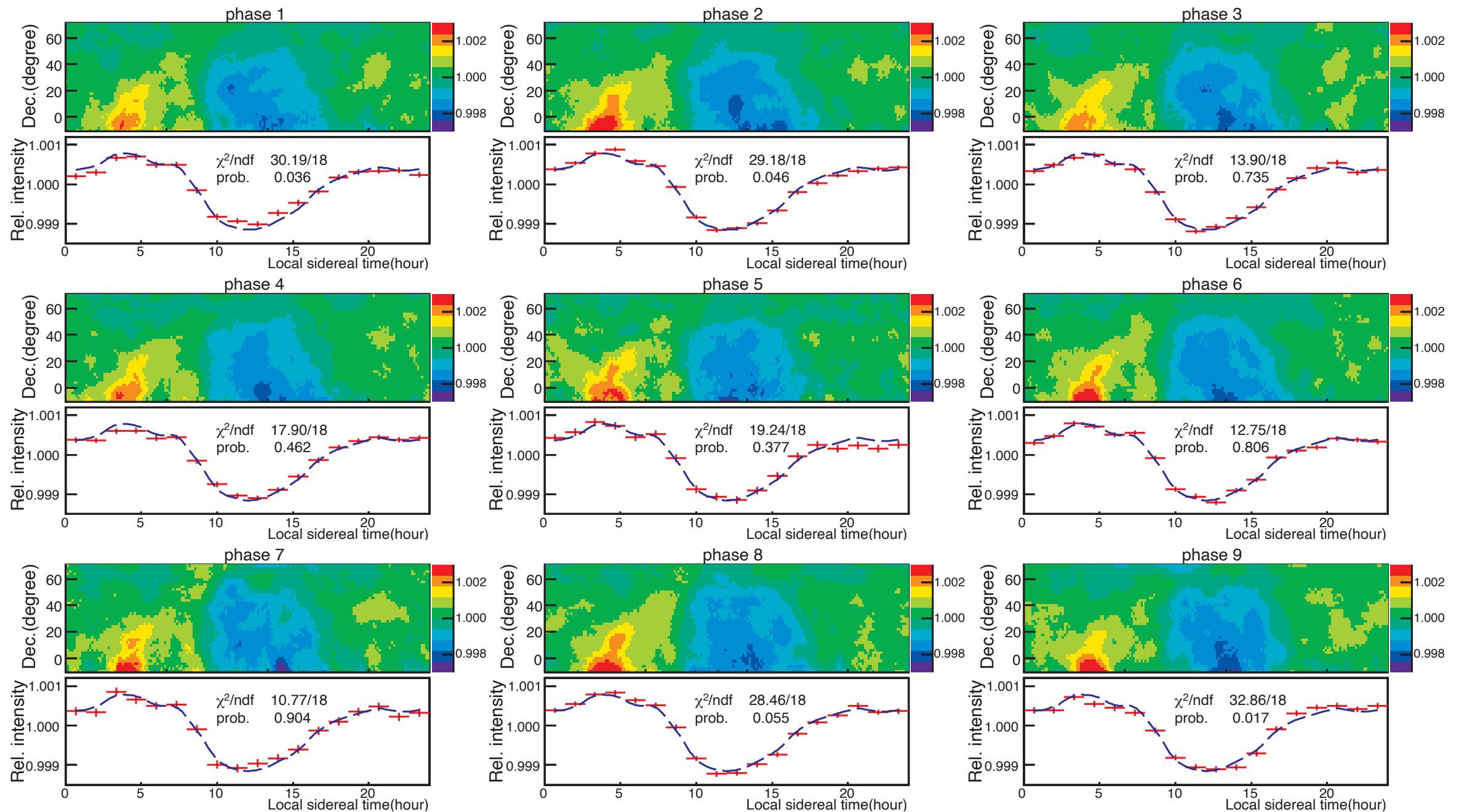
Ground-Based Observations



Field of View (FoV) of ground-based detector (e.g. HAWC at geographic latitude 19°) sweeps across the Sky over 24h.

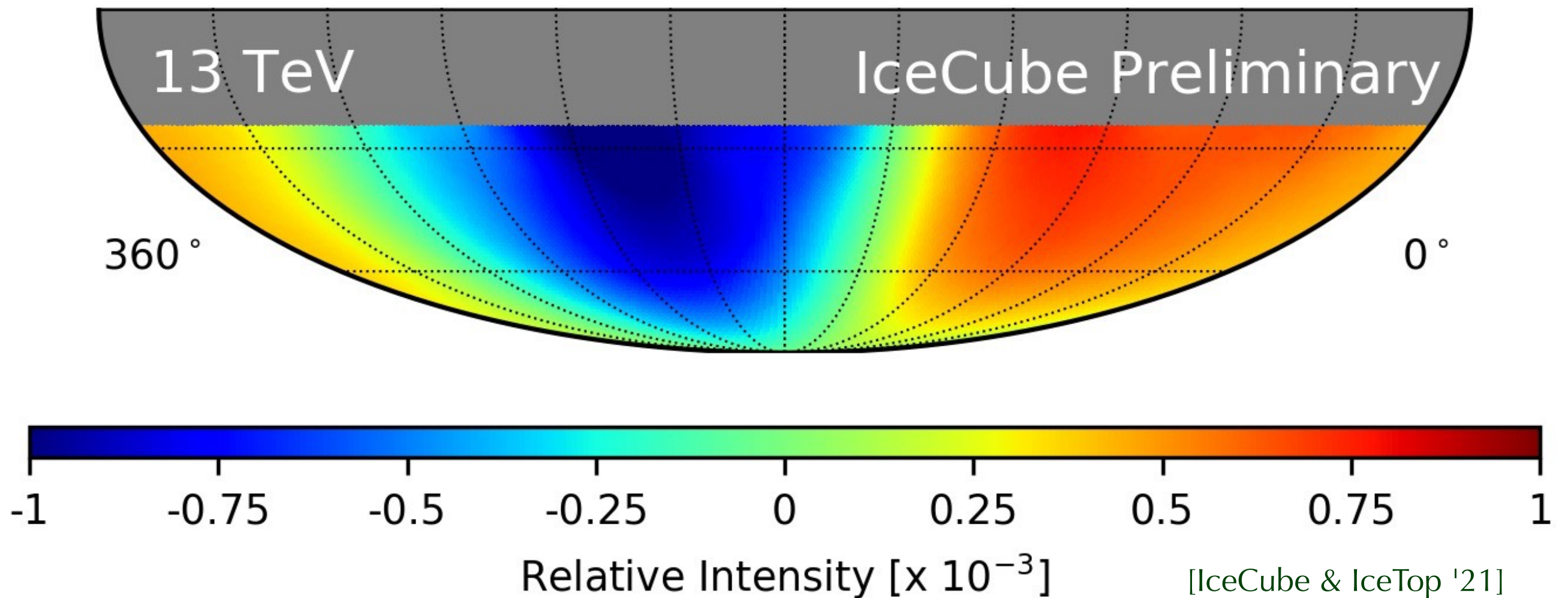
Galactic Cosmic Rays Anisotropy

No significant variation of TeV-PeV anisotropy over the time scale of $\mathcal{O}(10)$ years.



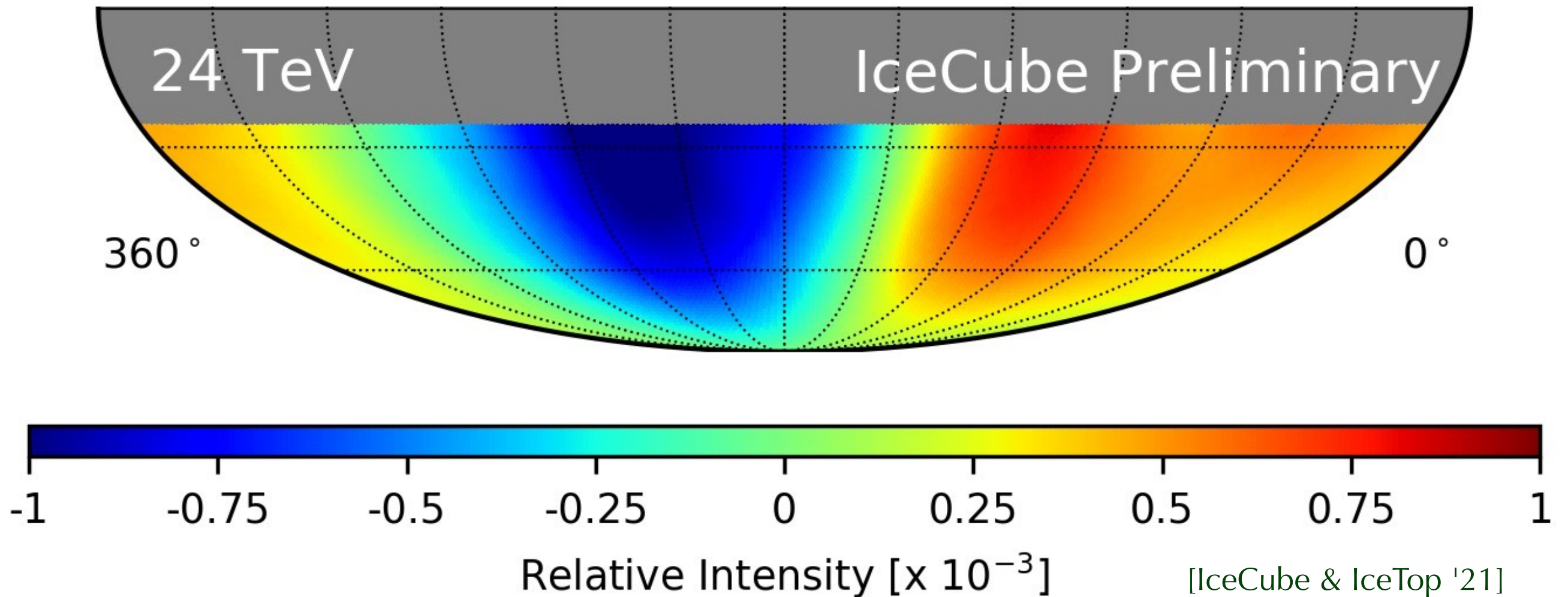
[Tibet-ASy '10]

Large-Scale Anisotropy



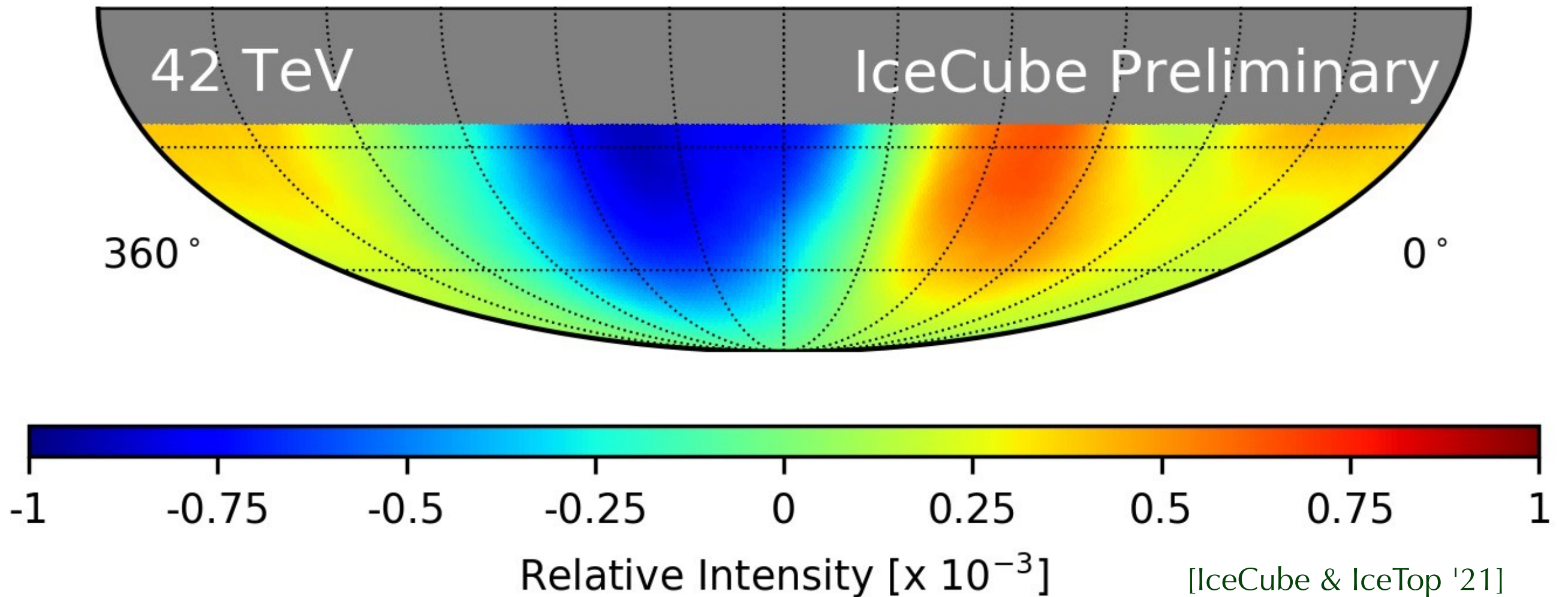
Amplitude of large-scale dipole anisotropy has strong energy dependence with a phase flip around 100 TeV.

Large-Scale Anisotropy



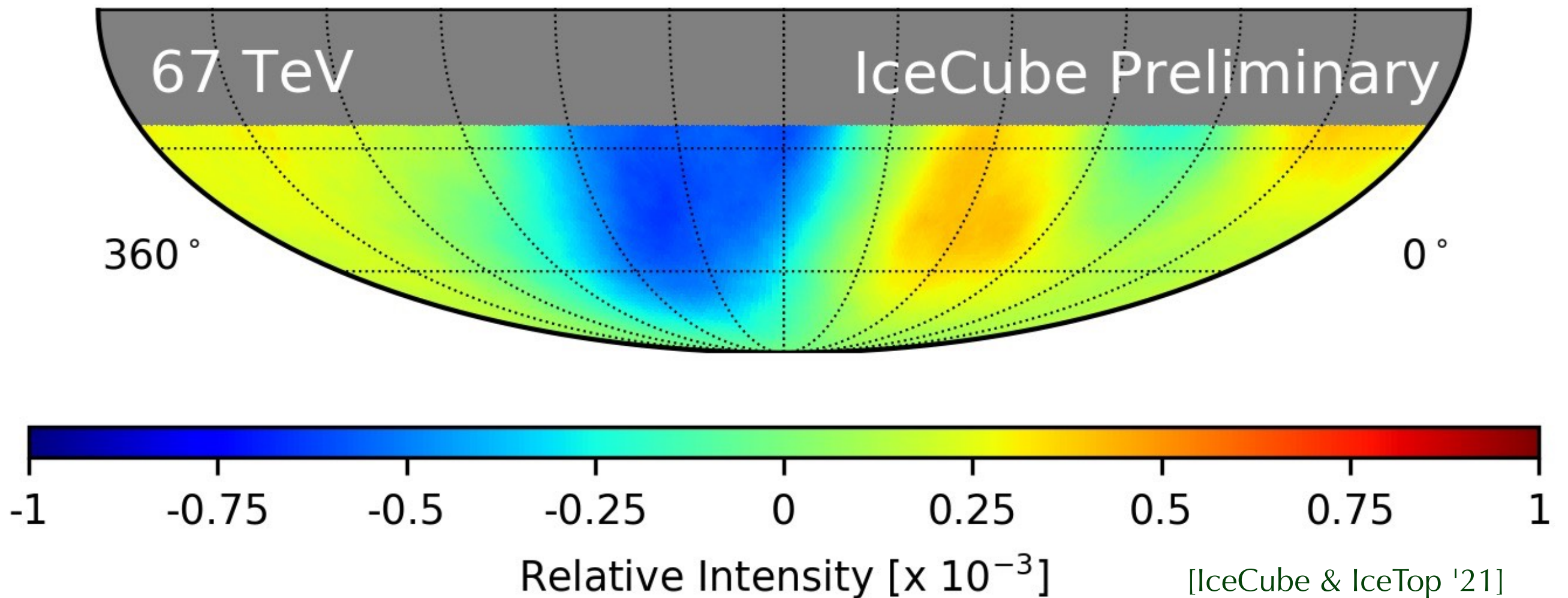
Amplitude of large-scale dipole anisotropy has strong energy dependence with a phase flip around 100 TeV.

Large-Scale Anisotropy



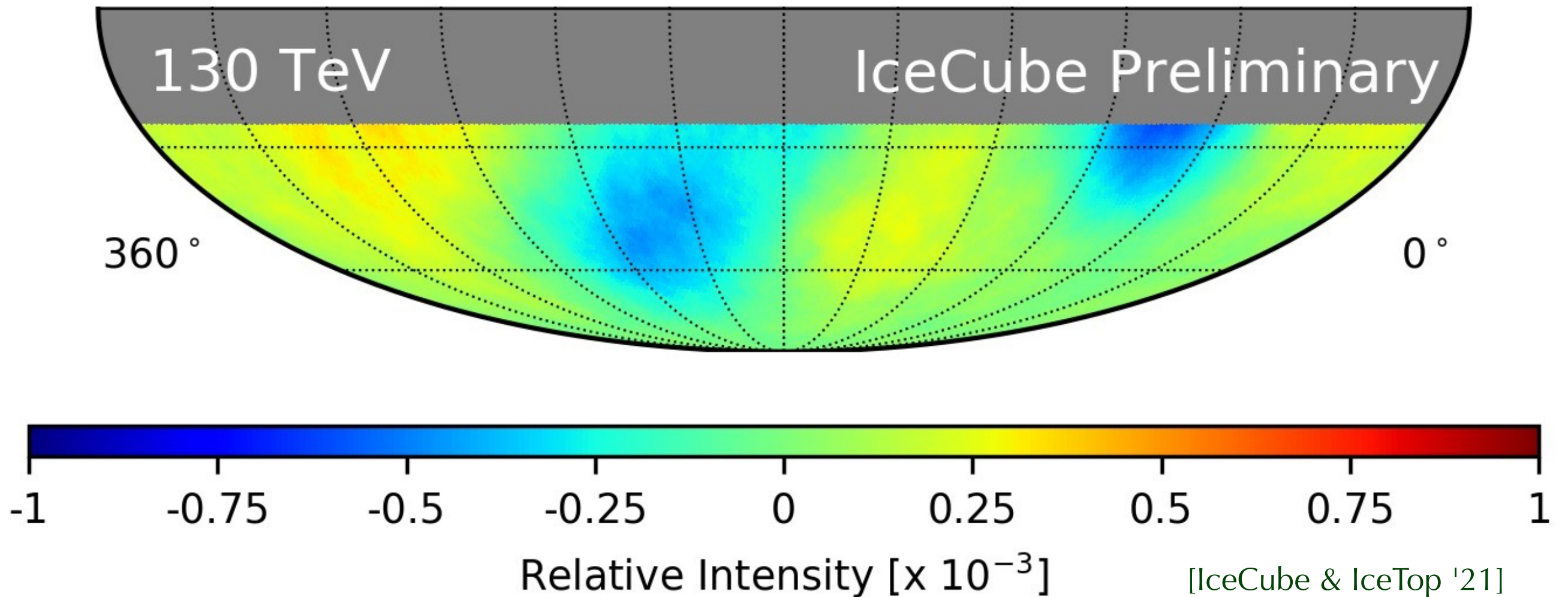
Amplitude of large-scale dipole anisotropy has strong energy dependence with a phase flip around 100 TeV.

Large-Scale Anisotropy



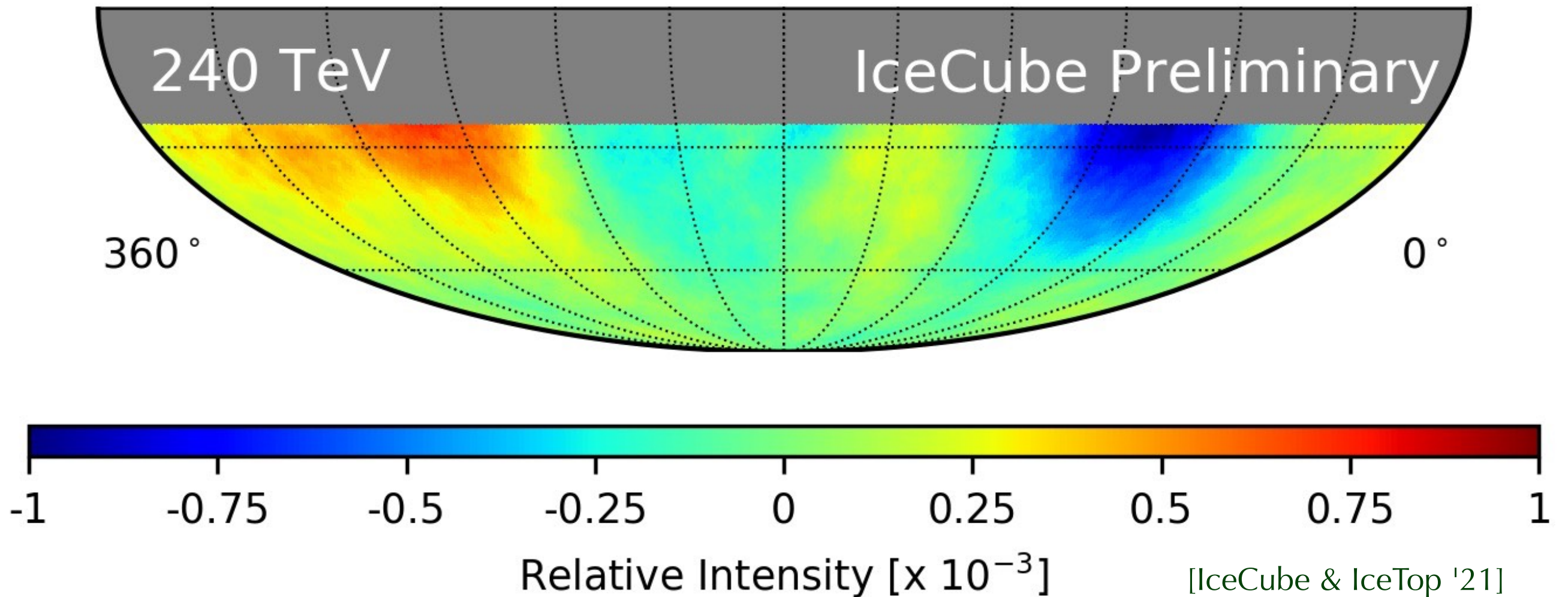
Amplitude of large-scale dipole anisotropy has strong energy dependence with a phase flip around 100 TeV.

Large-Scale Anisotropy



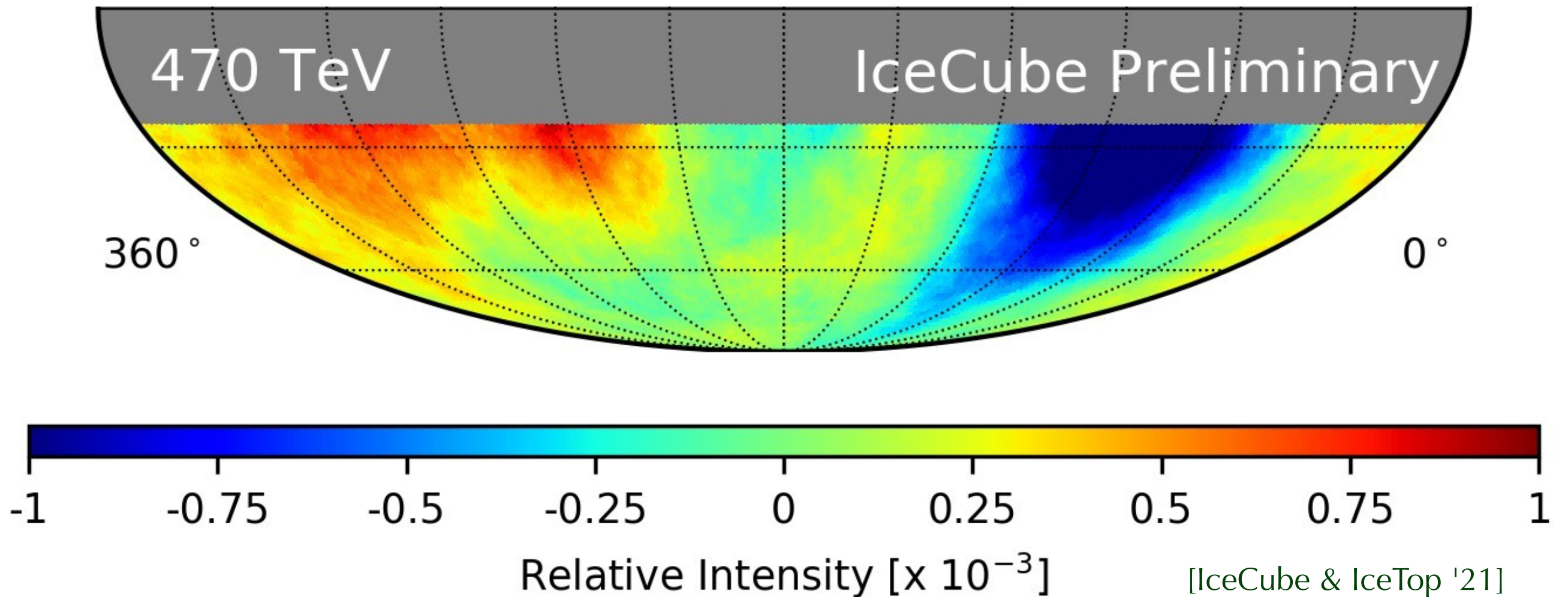
Amplitude of large-scale dipole anisotropy has strong energy dependence with a phase flip around 100 TeV.

Large-Scale Anisotropy



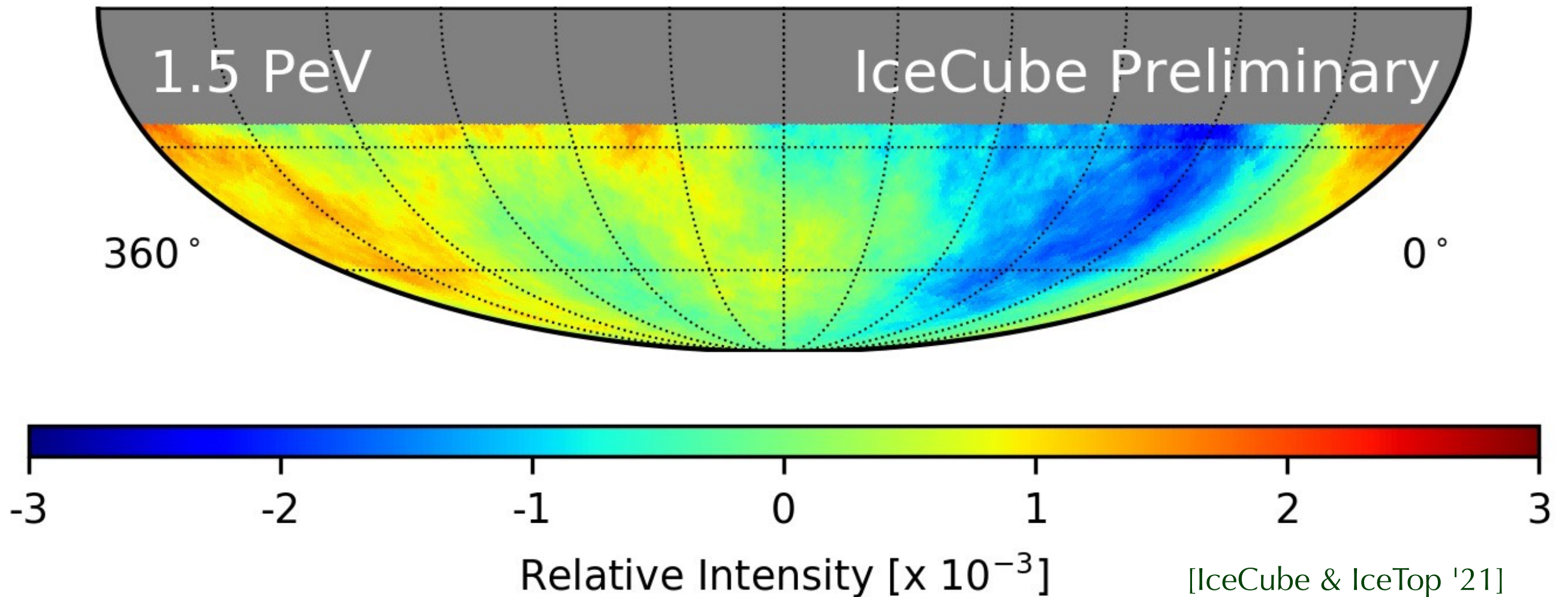
Amplitude of large-scale dipole anisotropy has strong energy dependence with a phase flip around 100 TeV.

Large-Scale Anisotropy



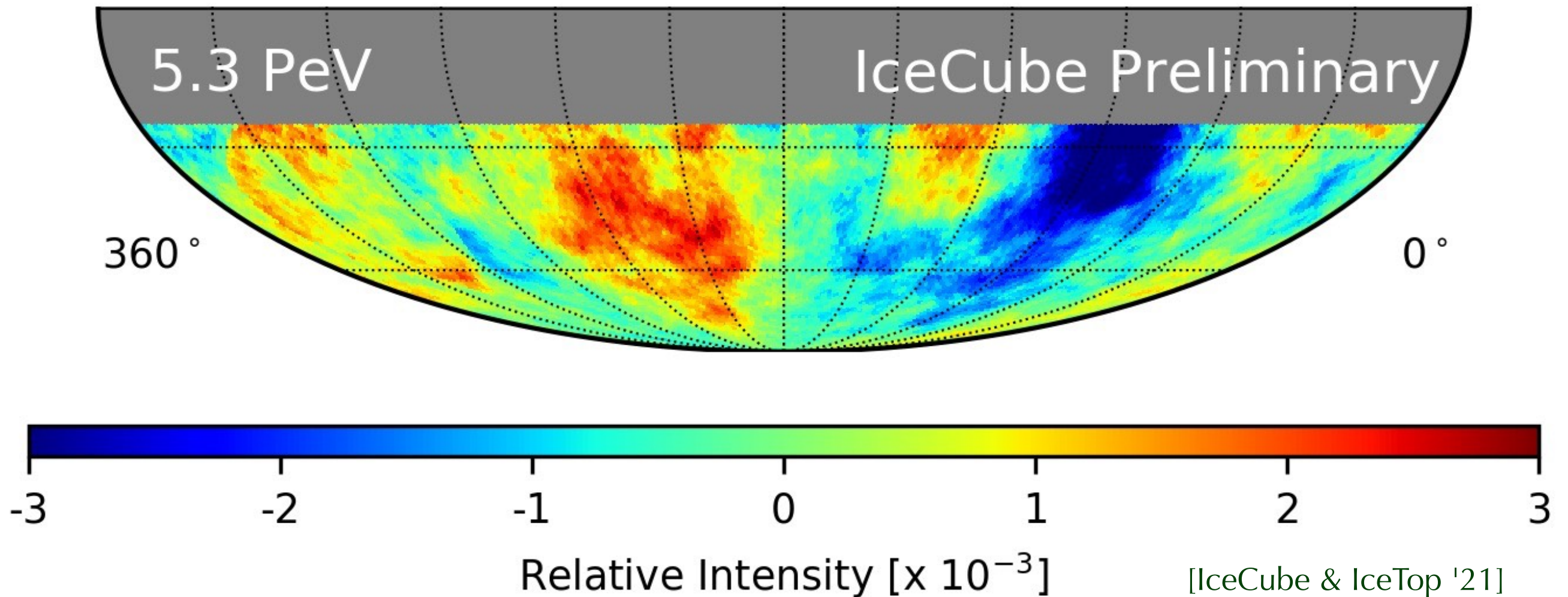
Amplitude of large-scale dipole anisotropy has strong energy dependence with a phase flip around 100 TeV.

Large-Scale Anisotropy



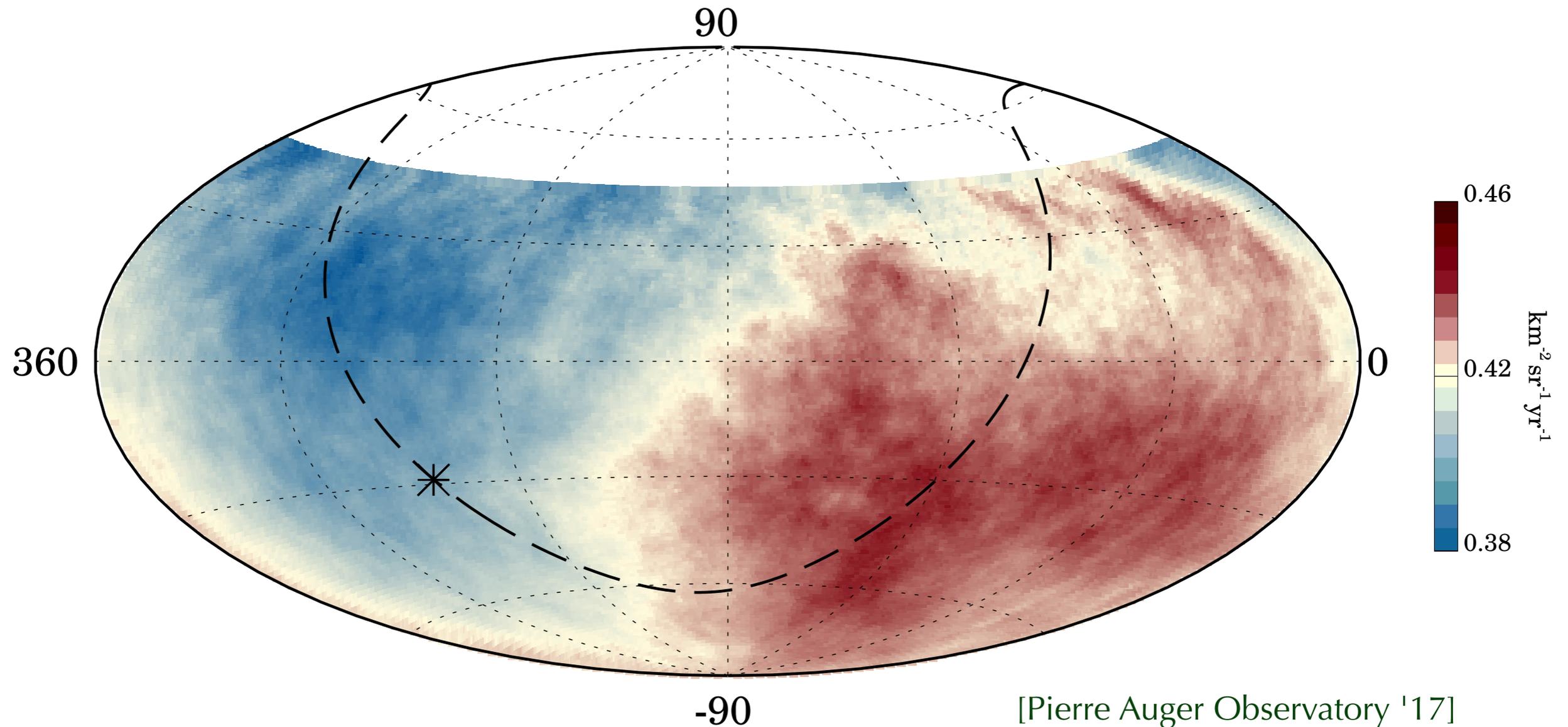
Amplitude of large-scale dipole anisotropy has strong energy dependence with a phase flip around 100 TeV.

Large-Scale Anisotropy



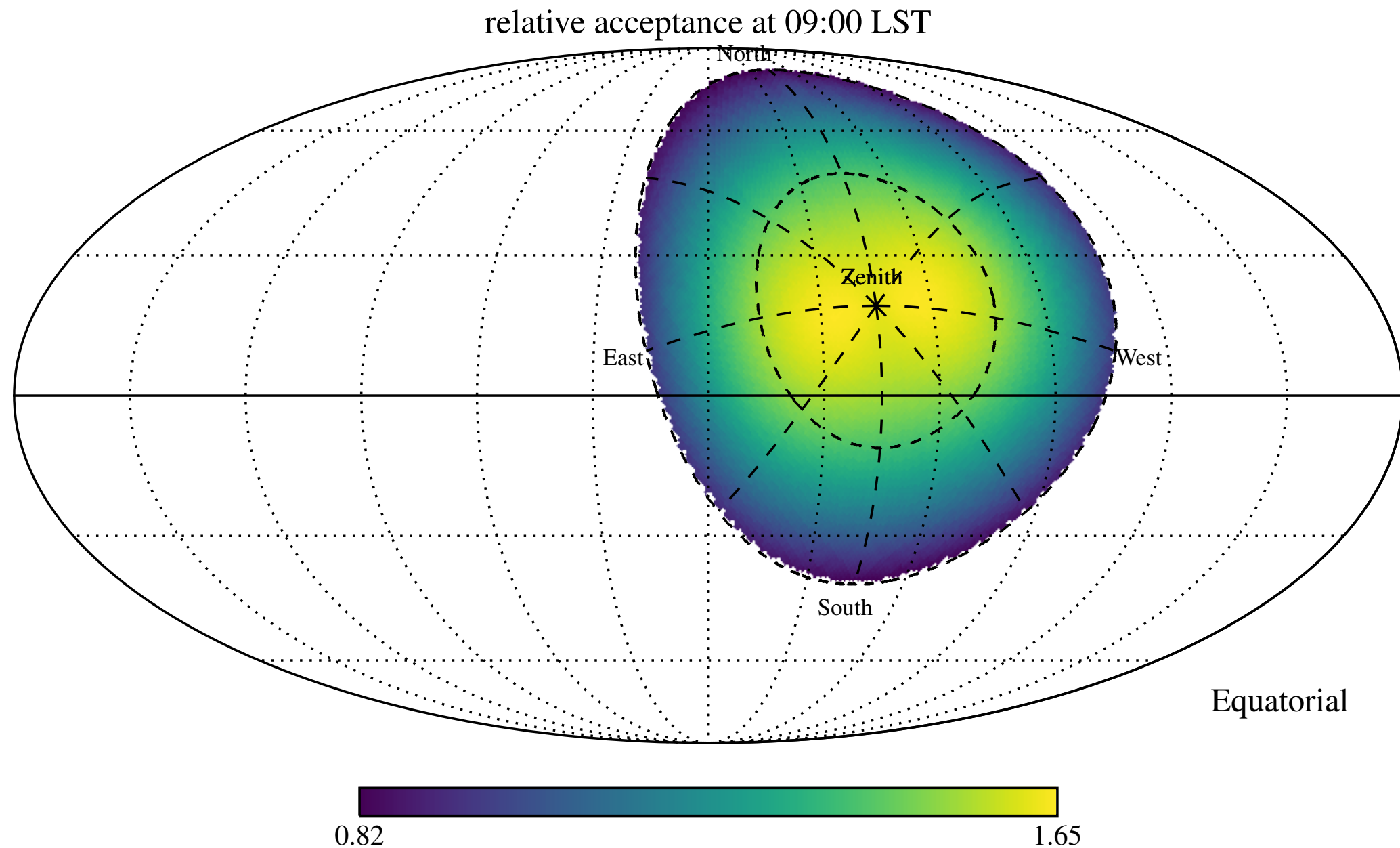
Amplitude of large-scale dipole anisotropy has strong energy dependence with a phase flip around 100 TeV.

Dipole Anisotropy of UHE CRs



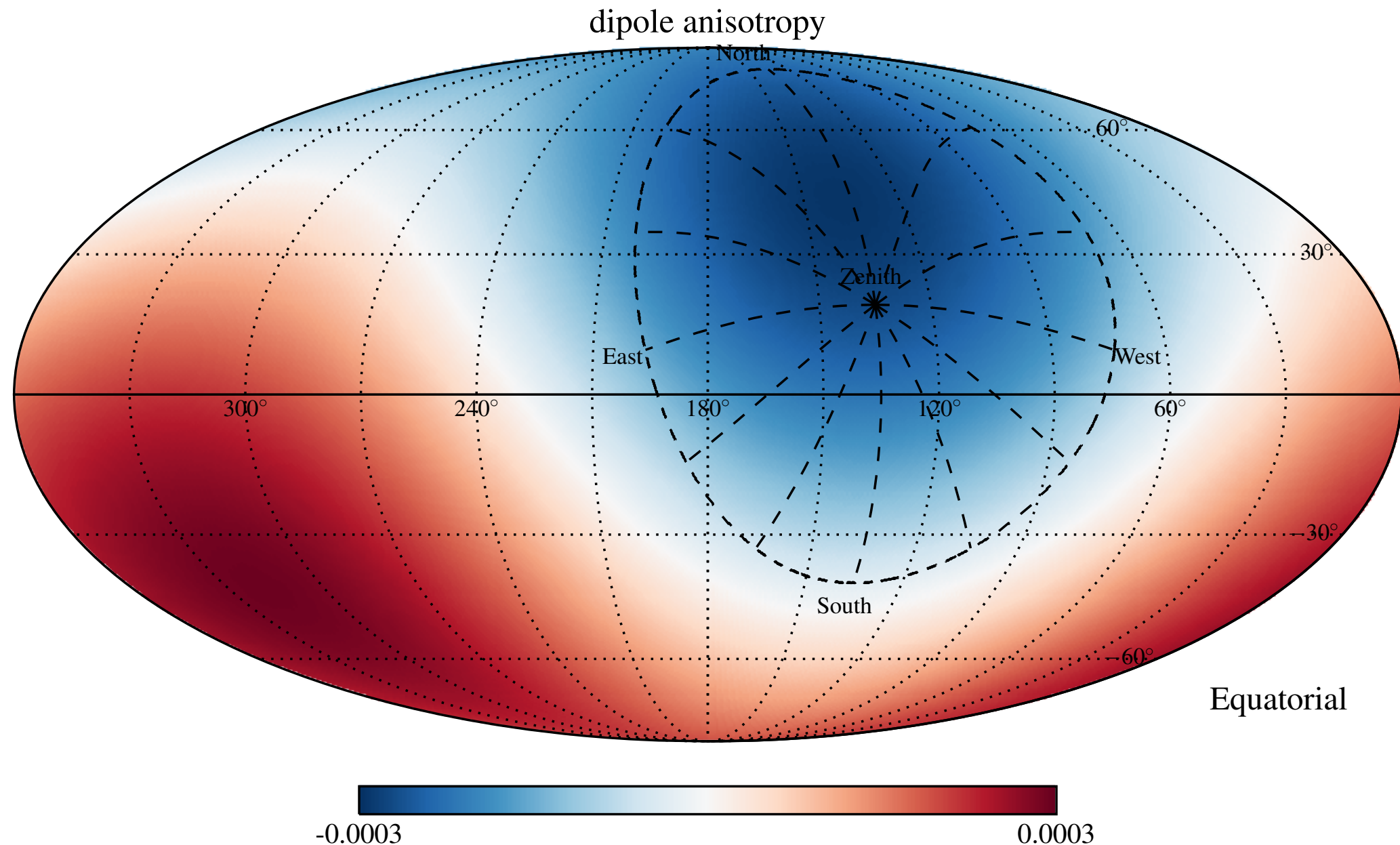
Energy [EeV]	Dipole component d_z	Dipole component d_{\perp}	Dipole amplitude d	Dipole declination δ_d [°]	Dipole right ascension α_d [°]
4 to 8	-0.024 ± 0.009	$0.006^{+0.007}_{-0.003}$	$0.025^{+0.010}_{-0.007}$	-75^{+17}_{-8}	80 ± 60
8	-0.026 ± 0.015	$0.060^{+0.011}_{-0.010}$	$0.065^{+0.013}_{-0.009}$	-24^{+12}_{-13}	100 ± 10

Issues with Reconstructions



Ground-based detectors need to be calibrated by the CR data it collects while it sweeps across the sky over 24h.

Issues with Reconstructions

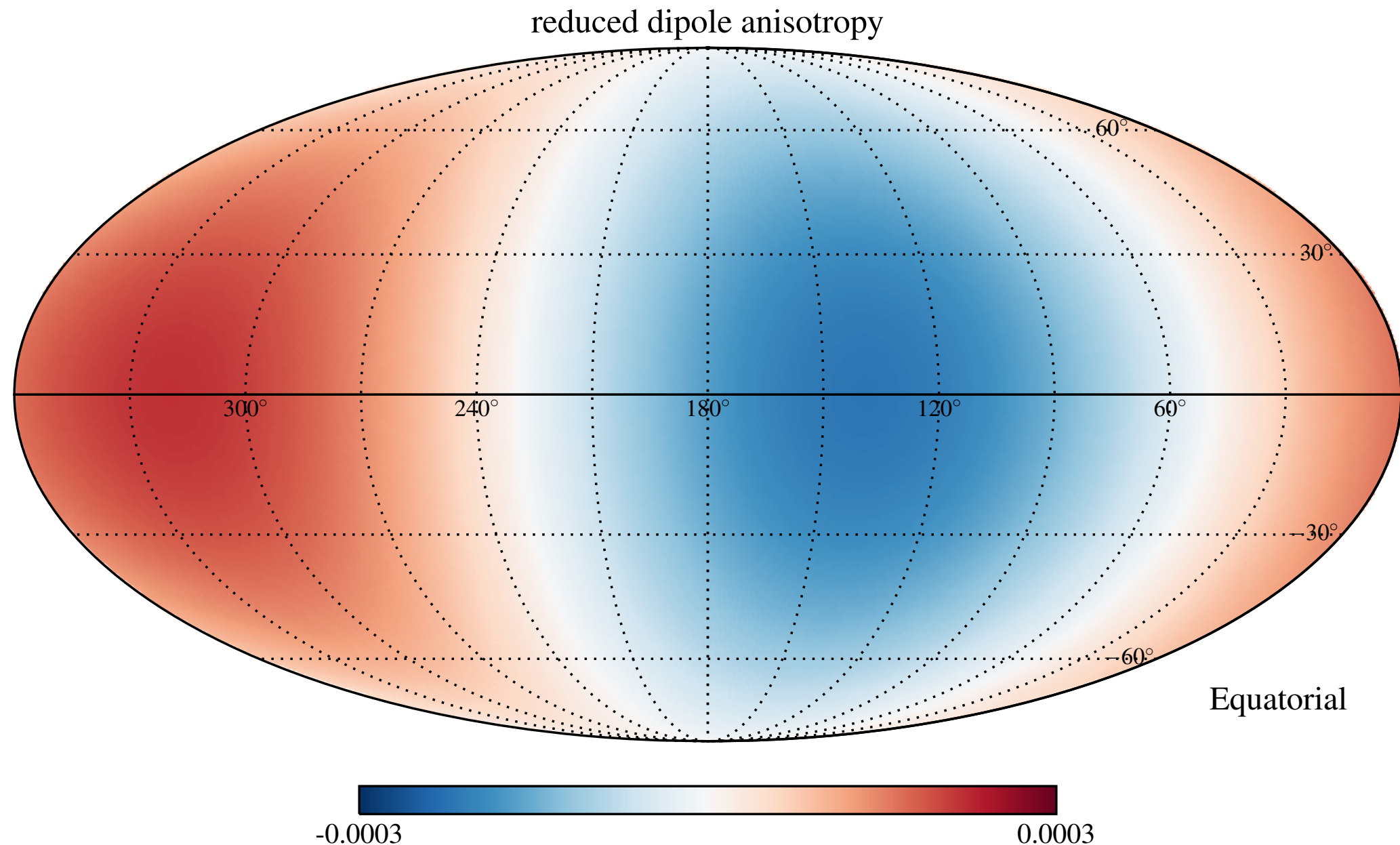


True CR dipole is defined by amplitude A and direction (α, δ) .

Observable dipole is projected onto equatorial plane: $A' = A \cos \delta$

[Iuppa & Di Sciacio'13; MA *et al.*'15]

Issues with Reconstructions

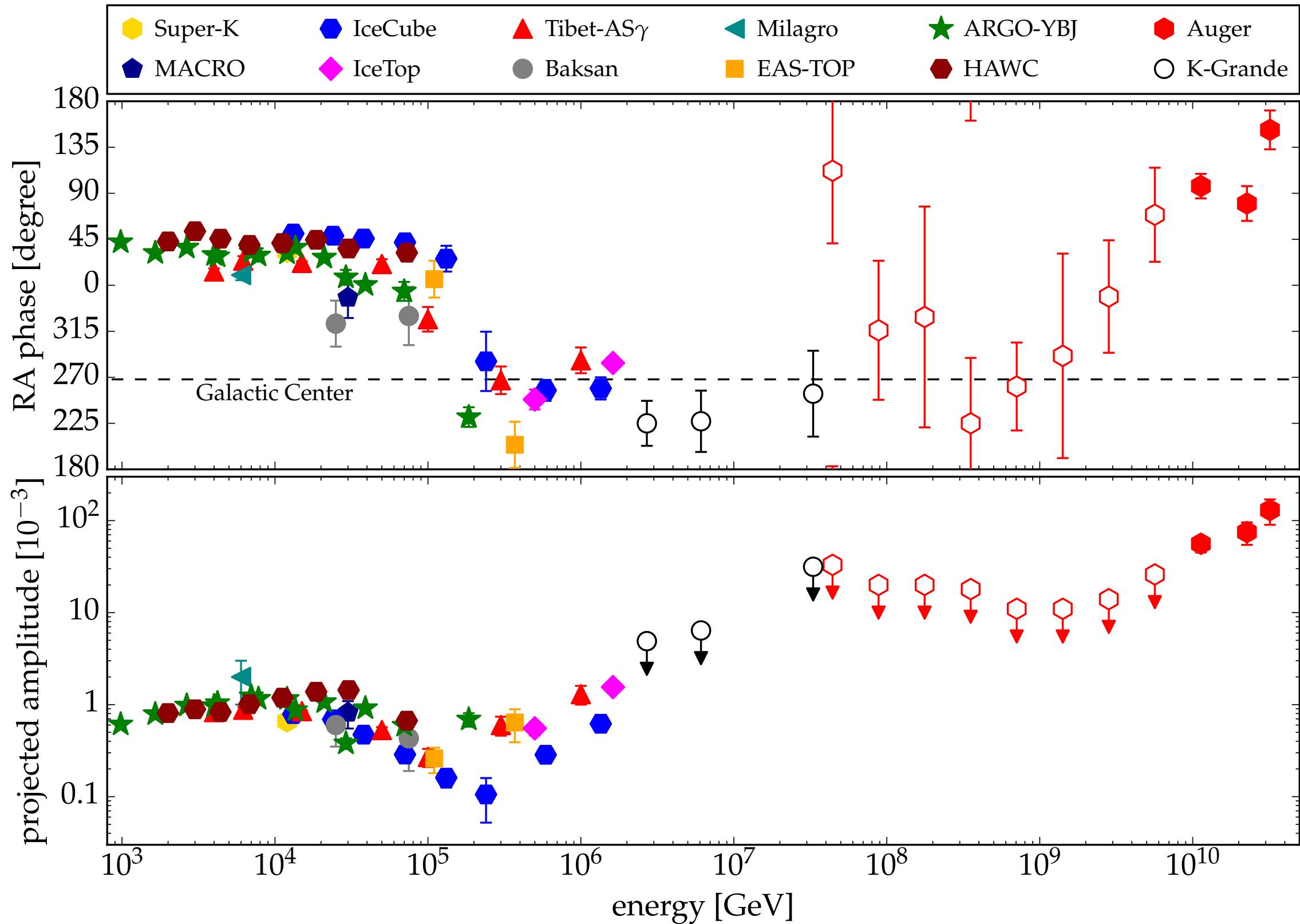


True CR dipole is defined by amplitude A and direction (α, δ) .

Observable dipole is projected onto equatorial plane: $A' = A \cos \delta$

[Iuppa & Di Sciacio'13; MA *et al.*'15]

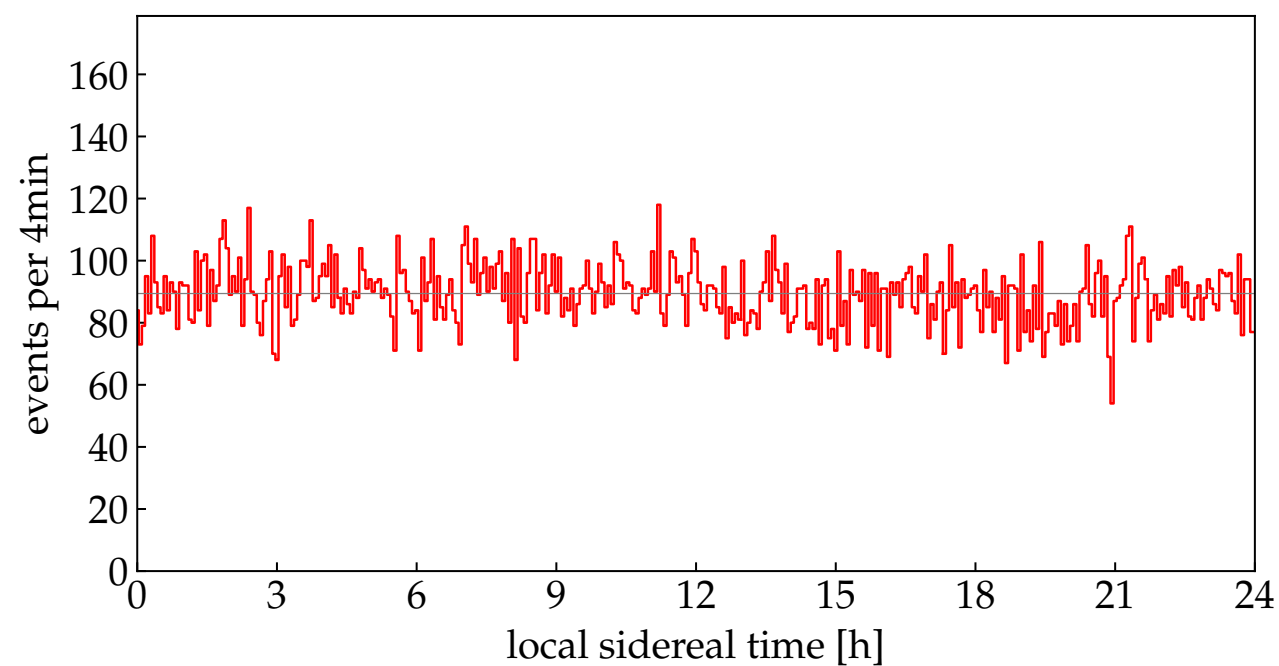
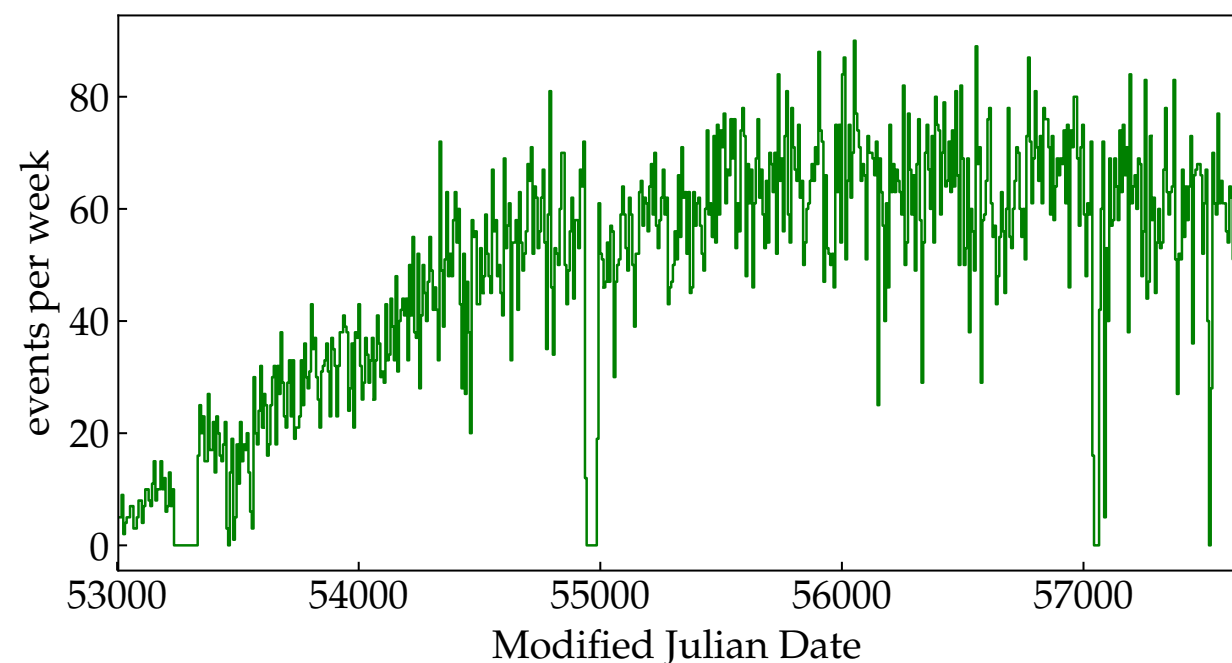
Dipole Anisotropy



Reconstruction

- data has **strong time dependence**
 - detector deployment/
maintenance
 - atmospheric conditions (day/
night, seasons)
 - power outages, etc.
- **local anisotropy** of detector:
 - non-uniform geometry
- two analysis strategies:
 - **Monte-Carlo & monitoring**
(limited by systematic
uncertainties)
 - **data-driven likelihood methods**
(limited by statistical
uncertainties)

Example: Auger data > 8 EeV



[Pierre Auger Observatory'17; MA'18]

East-West Method

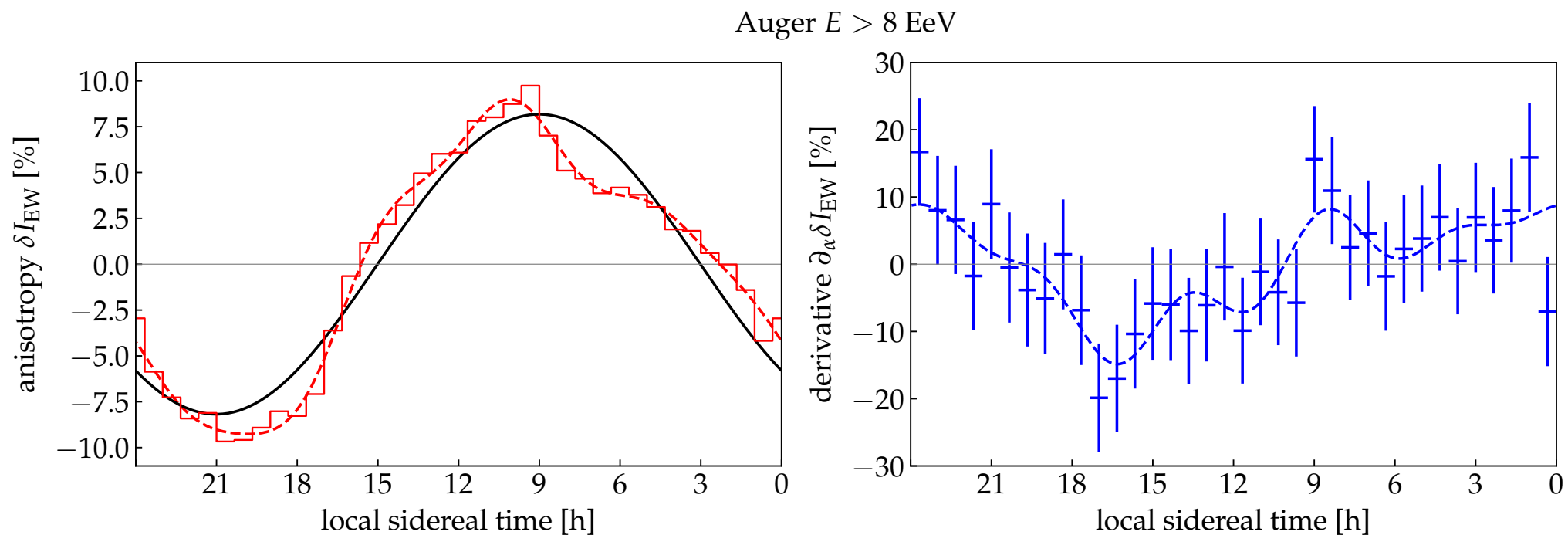
- Strong time variation of CR background level can be compensated by differential methods.

[e.g. Bonino *et al.*'11]

- **East-West asymmetry:**

$$A_{EW}(t) \equiv \frac{N_E(t) - N_W(t)}{N_E(t) + N_W(t)} \simeq \underbrace{\Delta\alpha \frac{\partial}{\partial\alpha} \delta I(\alpha, 0)}_{\text{assuming dipole!}} + \underbrace{\text{const}}_{\text{local asym.}}$$

- For instance, Auger data $> 8\text{EeV}$:



- best-fit dipole from EW method: $(8.2 \pm 1.4) \%$ and $\alpha_d = 135^\circ \pm 10^\circ$

Likelihood Reconstruction

- East-West method introduces cross-talk between higher multipoles, regardless of the field of view.
- Alternatively, data can be analyzed to simultaneously reconstruct:
 - **relative acceptance** $\mathcal{A}(\varphi, \theta)$ (in local coordinates)
 - **relative intensity** $\mathcal{F}(\alpha, \delta)$ (in equatorial coordinates)
 - **background rate** $\mathcal{N}(t)$ (in sidereal time)
- expected number of CRs observed in sidereal time bin τ and local "pixel" i :

$$\mu_{\tau i} = \mu(\mathcal{F}_{\tau i}, \mathcal{N}_{\tau}, \mathcal{A}_i)$$

- reconstruction **likelihood**:

[MA et al.'15]

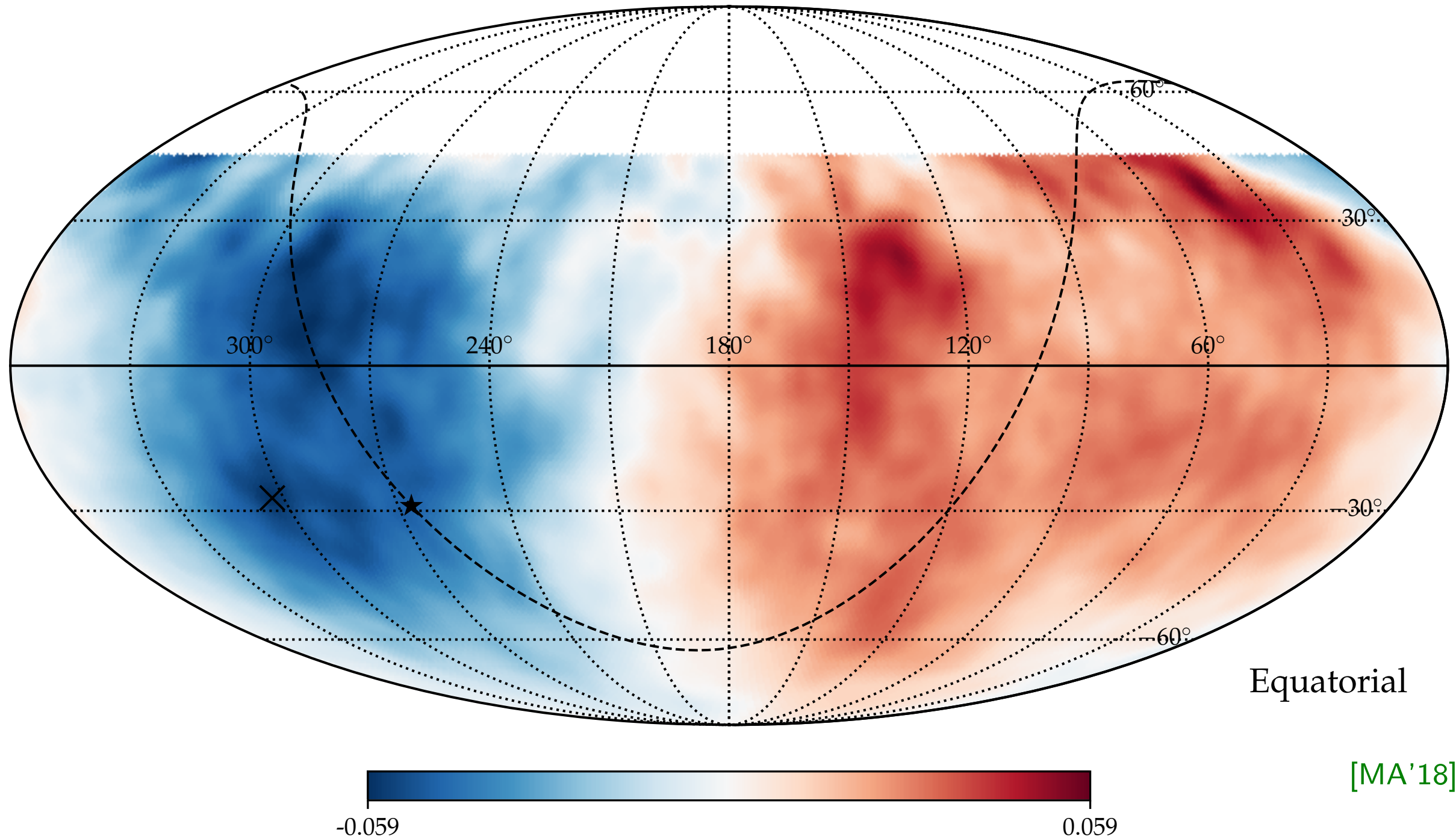
$$\mathcal{L}(\mathbf{n} | \mathcal{F}, \mathcal{N}, \mathcal{A}) = \prod_{\tau i} \frac{(\mu_{\tau i})^{n_{\tau i}} e^{-\mu_{\tau i}}}{n_{\tau i}!}$$

- Maximum LH can be reconstructed by iterative methods.
- used in joint IceCube & HAWC analysis

[IceCube & HAWC '18]

Likelihood Reconstruction

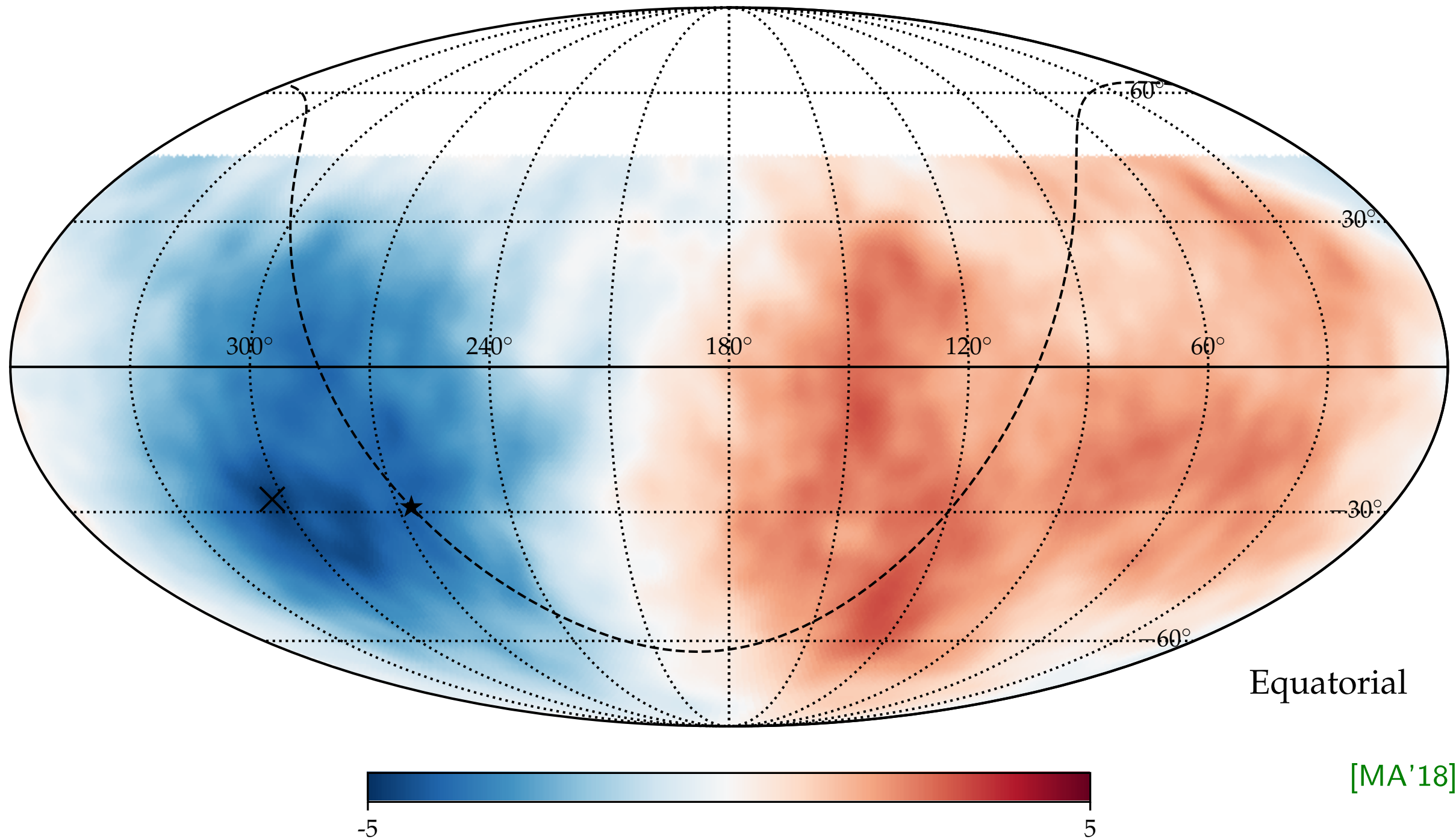
anisotropy ($E > 8 \text{ EeV}$, 45° smoothing)



Method can also be applied to high-energy data beyond the knee, e.g. Auger.

Likelihood Reconstruction

pre-trial significance ($E > 8 \text{ EeV}$, 45° smoothing, $\sigma_{\text{max}} = 4.86$)



[MA'18]

Method can also be applied to high-energy data beyond the knee, e.g. Auger.

Take-Away on Reconstruction

Data-driven methods of anisotropy reconstructions used by ground-based observatories in the TV-PV range are **only sensitive to equatorial dipole** (or, more generally, to all $m \neq 0$ multipole moments).

$$\Delta\delta_{\perp} \sim \frac{1}{\sqrt{N_{\text{CR}}}} \quad \mathcal{N} \sim \frac{4\pi}{N_{\text{CR}}}$$

Monte-Carlo-based methods of anisotropy reconstructions are sensitive to the full dipole, but are severely **limited by systematic uncertainties.**

Particles in Magnetic Fields

- natural Heaviside-Lorentz units:

$$\hbar = c = 1 \quad \mu_0 = \epsilon_0 = 1$$

- For instance, Coulomb force:

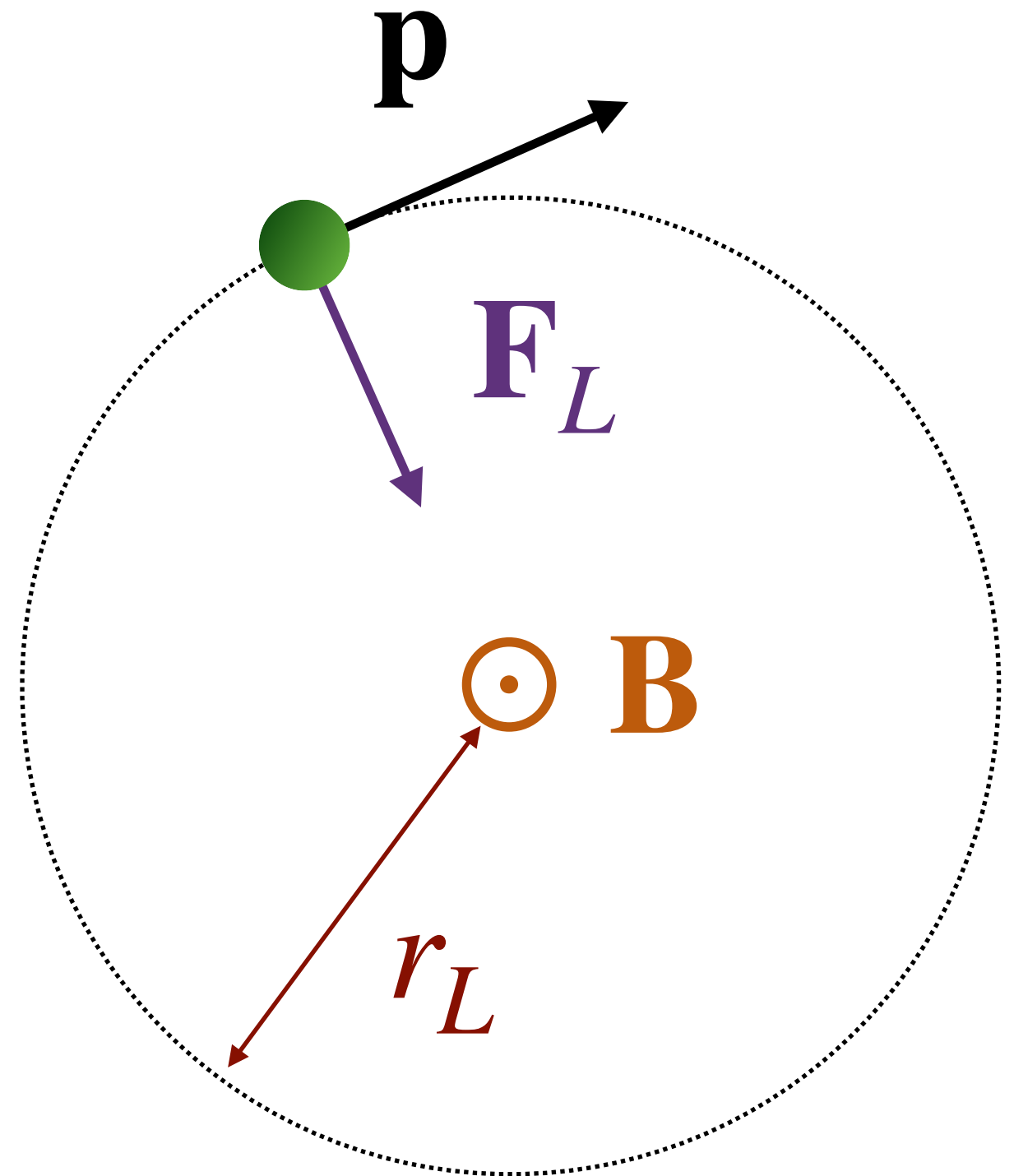
$$\mathbf{F} = \frac{q_1 q_2}{4\pi r^2} \mathbf{e}_r = \alpha \frac{Z_1 Z_2}{r^2} \mathbf{e}_r$$

- Lorentz force:

$$\mathbf{F} = q (\mathbf{E} + \boldsymbol{\beta} \times \mathbf{B})$$

- EoM in the absence of \mathbf{E} :

$$\dot{\mathbf{p}} = \mathbf{p} \times \boldsymbol{\Omega}$$



Particles in Magnetic Fields

- natural Heaviside-Lorentz units:

$$\hbar = c = 1 \quad \mu_0 = \epsilon_0 = 1$$

- For instance, Coulomb force:

$$\mathbf{F} = \frac{q_1 q_2}{4\pi r^2} \mathbf{e}_r = \alpha \frac{Z_1 Z_2}{r^2} \mathbf{e}_r$$

- Lorentz force:

$$\mathbf{F} = q (\mathbf{E} + \boldsymbol{\beta} \times \mathbf{B})$$

- EoM in the absence of \mathbf{E} :

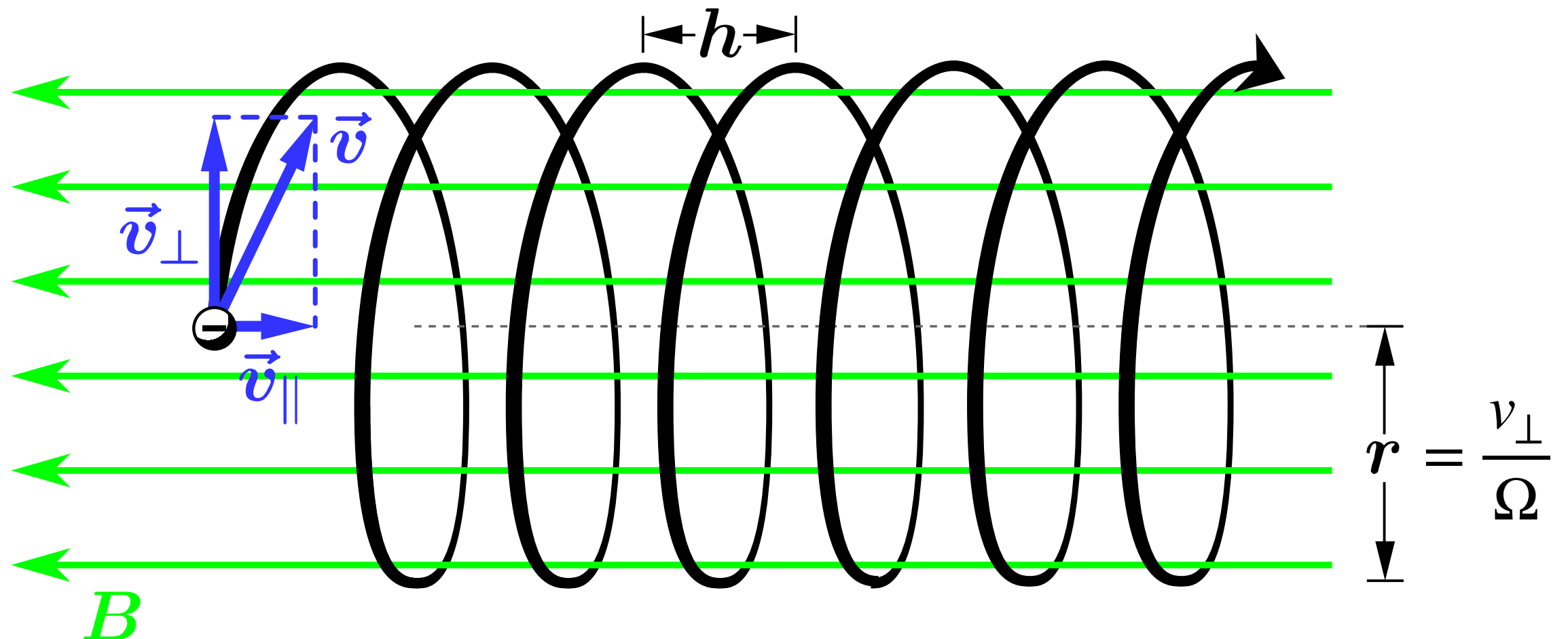
$$\dot{\mathbf{p}} = \mathbf{p} \times \boldsymbol{\Omega}$$

Larmor frequency: $\boldsymbol{\Omega} \equiv \frac{q}{\gamma m} \mathbf{B}$

Larmor radius: $r_L = \frac{\beta}{|\boldsymbol{\Omega}|} = \frac{\mathcal{R}}{|\mathbf{B}|}$

rigidity: $\mathcal{R} = \frac{|\mathbf{p}|}{q}$

Particle Gyration



The **pitch angle** θ between $\mathbf{v}(t)$ and \mathbf{B}_0 remains constant in time.

The path is a superposition of circular motion in the plane perpendicular to \mathbf{B}_0 and linear motion along \mathbf{B}_0 with velocity:

$$v_{\parallel} = \cos \theta v \equiv \mu v.$$

Larmor Radius

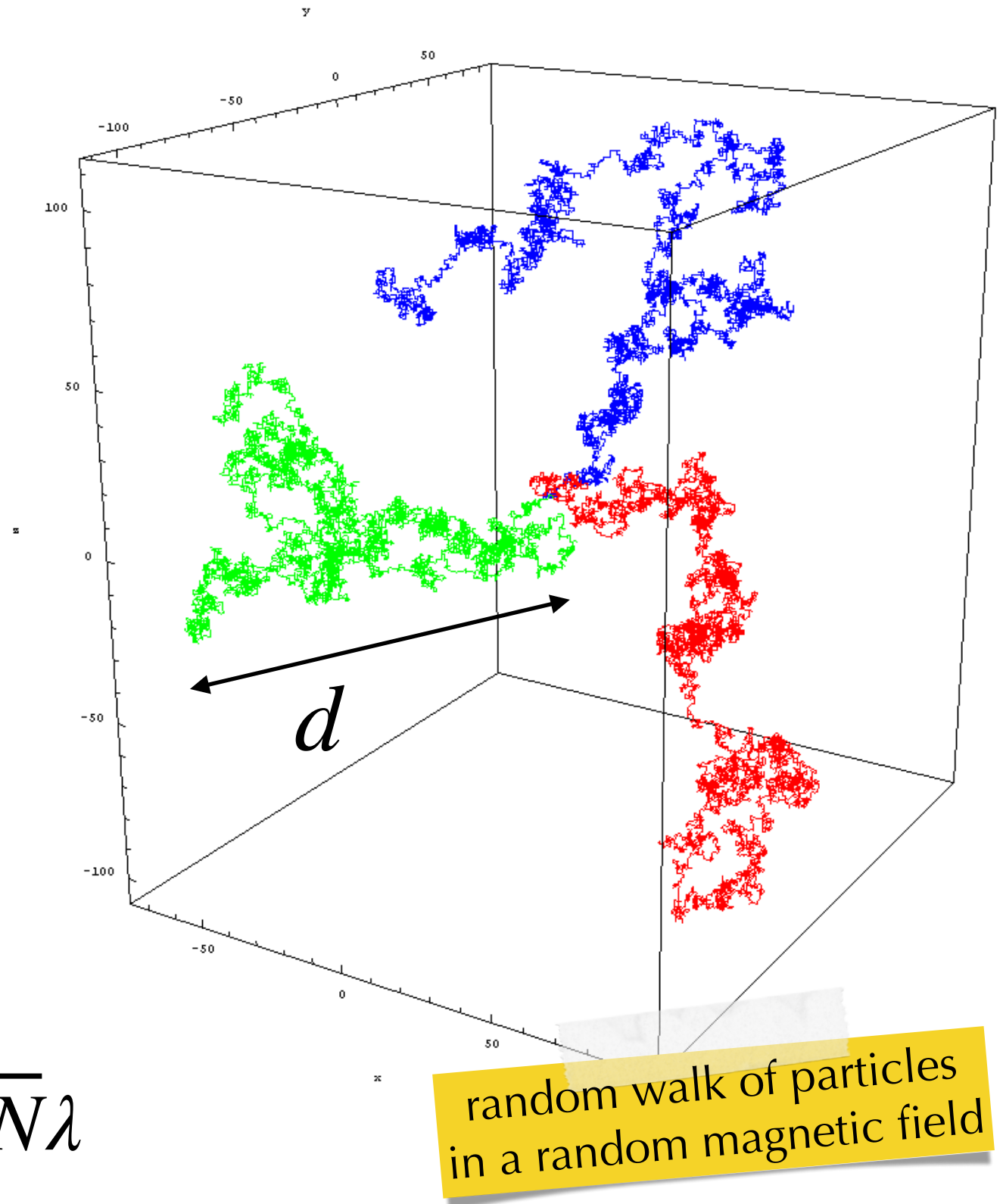
- Cosmic rays with the same **rigidity** \mathcal{R} follow same trajectories.
- We expect that cosmic ray anisotropies depend on rigidity, not energy.
- Low-energy cosmic rays are affected by the O(1 G) geomagnetic field.
- High-energy cosmic rays experience deflections in Galactic O(10^{-6} G) and extragalactic O(10^{-9} G) magnetic fields:

$$r_L \simeq 1.1 \text{pc} \frac{1 \mu\text{G}}{B} \frac{\mathcal{R}}{10^{15} \text{V}}$$

- In addition to regular magnetic fields, **random magnetic fields** introduce a random walk that can be treated as a **diffusive process**.

Cosmic Ray Diffusion

- Galactic and extragalactic magnetic fields have a random component (no preferred direction).
- Effectively, after some **characteristic distance** λ , a CR will be scattered into a random direction.
- Cosmic ray propagation follows a random walk.
- After N encounters the CR will have travelled an **average distance**: $d = \sqrt{N}\lambda$



Magnetic Turbulence

- In the following, we consider relativistic particles in magnetic fields with vanishing electric fields ($\mathbf{E} = 0$) due to the high conductivity of astrophysical plasmas:

$$\mathbf{B}(\mathbf{r}) = \underbrace{B_0 \mathbf{e}_z}_{\text{ordered}} + \underbrace{\delta \mathbf{B}(\mathbf{r})}_{\text{turbulent}}$$

- We also consider only **homogenous and isotropic turbulence**.
- Turbulence can be characterized by its **two-point correlation function**:

$$\langle \delta B_i(\mathbf{r}) \delta B_j(\mathbf{r}') \rangle = C_{ij}(\mathbf{r} - \mathbf{r}')$$

- To characterize the turbulence we look into the Fourier modes:

$$\delta B_i(\mathbf{r}) = \int d^3k \delta \tilde{B}_i(\mathbf{k}) e^{i\mathbf{k}\mathbf{r}}$$

Magnetic Turbulence

- Real valued fields obeying $\nabla \delta \mathbf{B} = 0$ require:

$$\delta \tilde{B}_j^*(\mathbf{k}) = \delta \tilde{B}_j(-\mathbf{k}) \quad \& \quad \mathbf{k} \delta \tilde{B}_j(\mathbf{k}) = 0$$

- The two-point correlation function can now be expressed in Fourier space:

$$\langle \delta \tilde{B}_i(\mathbf{k}) \delta \tilde{B}_i^*(\mathbf{k}') \rangle = \delta(\mathbf{k} - \mathbf{k}') \left(\delta_{ij} - \frac{k_i k_j}{k^2} \right) \frac{\mathcal{P}(k)}{4\pi k^2}$$

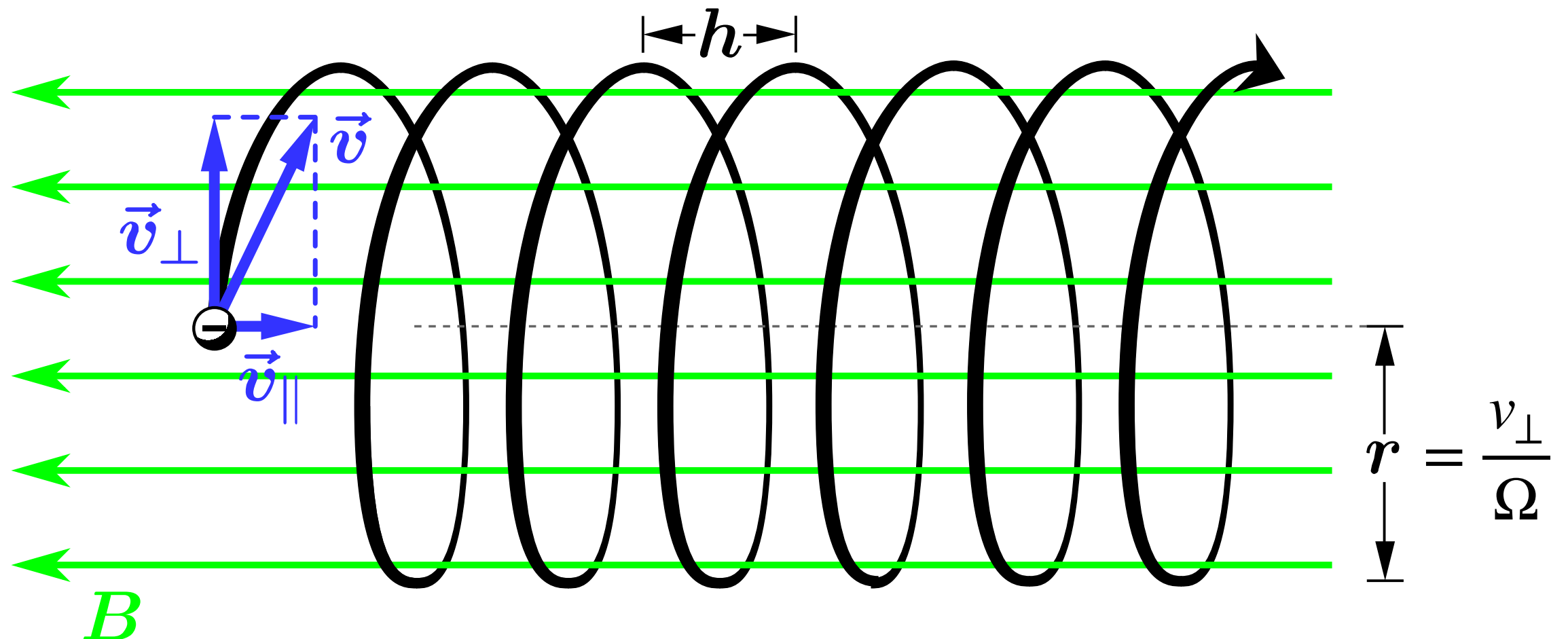
- The **power spectrum** $\mathcal{P}(k)$ is normalized to the energy density of the turbulence:

$$U_{\delta B} = \frac{1}{2} \langle \delta \mathbf{B}^2 \rangle = \int dk \mathcal{P}(k)$$

- For instance, in **Kolmogorov turbulence**:

$$\mathcal{P}(k) \propto k^{-5/3} \quad (k_{\min} < k < k_{\max})$$

Particle Gyration

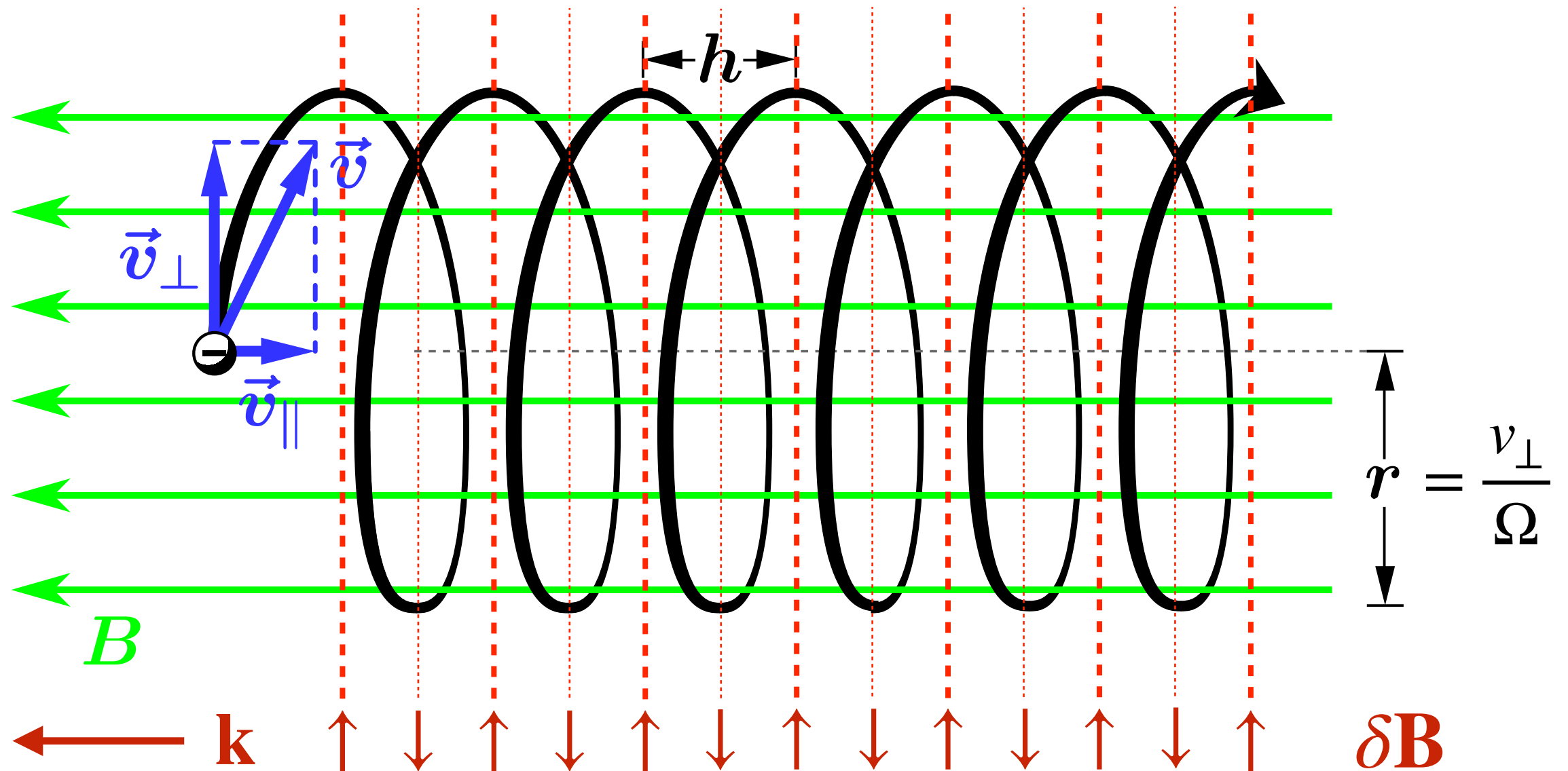


The **pitch angle** θ between $\mathbf{v}(t)$ and \mathbf{B}_0 remains constant in time.

The path is a superposition of circular motion in the plane perpendicular to \mathbf{B}_0 and linear motion along \mathbf{B}_0 with velocity:

$$v_{\parallel} = \cos \theta v \equiv \mu v.$$

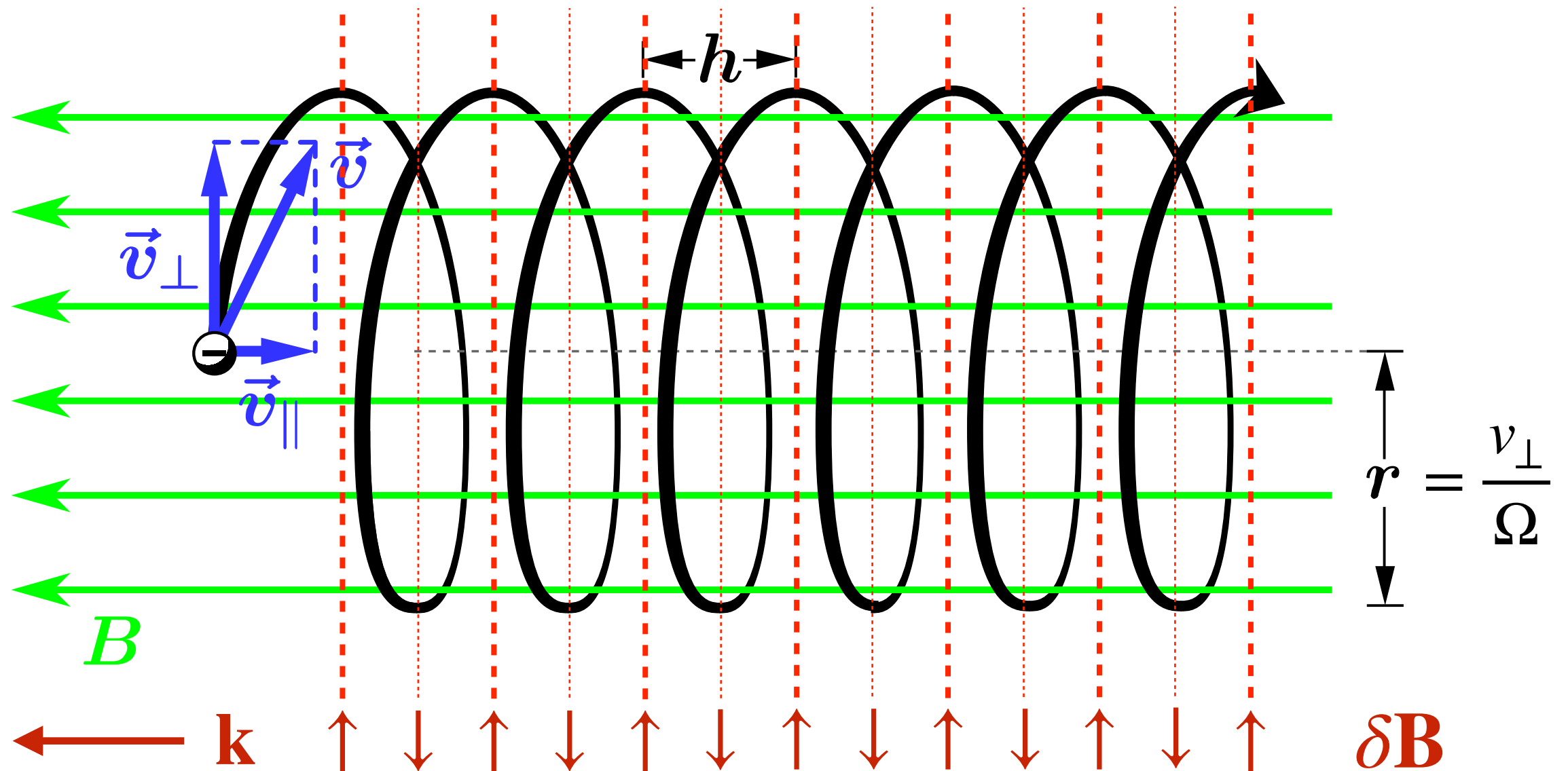
Particle Gyration



Consider now a **magnetic perturbation** in form of a plane wave:

$$\delta \mathbf{B} = \delta B \mathbf{e}_x \cos(kz + \alpha)$$

Particle Gyration



The time-averaged Lorentz force $\delta\mathbf{F}_L = q\boldsymbol{\beta} \times \delta\mathbf{B}$ along the path has the strongest contribution at the **resonance**:

$$kv_\parallel = \pm \Omega$$

Phase-Space Density

- We will work in the following with the CR **phase-space density** (PSD):

$$f(t, \mathbf{r}, \mathbf{p}) \equiv \frac{dN}{d^3r d^3p}$$

- for cosmic rays moving into solid angle Ω with momentum $p = \gamma\beta m$:

$$d^3r \times d^3p \rightarrow \beta dt dA_{\perp} \times d\Omega p^2 dp$$

- cosmic ray **intensity** ("spectral flux"):

$$F(t, \mathbf{r}, E, \Omega) \equiv \frac{dN}{dt dA_{\perp} d\Omega dE} = \beta p^2 \frac{dp}{dE} f(t, \mathbf{r}, \mathbf{p}) = p^2 f(t, \mathbf{r}, \mathbf{p})$$

- cosmic ray **spectral density**:

$$n(t, \mathbf{r}, E) \equiv \frac{dN}{d^3r dE} = \frac{1}{\beta} \int d\Omega F(t, \mathbf{r}, E, \Omega) = \frac{4\pi}{\beta} p^2 \langle f(t, \mathbf{r}, \mathbf{p}) \rangle_{4\pi}$$

Liouville's Theorem

- Let's assume that CRs propagate in static magnetic fields without dissipation or sources.

- Number of CRs per PS volume is constant: $\dot{f}(t, \mathbf{r}, \mathbf{p}) = 0$

- Equivalent to **Liouville's equation**: $\partial_t f + \dot{\mathbf{r}} \nabla_{\mathbf{r}} f + \dot{\mathbf{p}} \nabla_{\mathbf{p}} f = 0$

- **Lorentz force** in magnetic field:

$$\dot{\mathbf{p}} = \mathbf{p} \times (\underbrace{\boldsymbol{\Omega} + \boldsymbol{\omega}}_{\text{background field}}) \quad \text{with} \quad \underbrace{\boldsymbol{\Omega} \equiv e\mathbf{B}/p_0}_{\text{background field}} \quad \text{and} \quad \underbrace{\boldsymbol{\omega} \equiv e\delta\mathbf{B}/p_0}_{\text{turbulence}}$$

- **Vlasov equation**: $\partial_t f + \beta \nabla_{\mathbf{r}} f + [\mathbf{p} \times (\boldsymbol{\Omega} + \boldsymbol{\omega})] \nabla_{\mathbf{p}} f = 0$

Vlasov Equation

- We can express the Vlasov equation in the form ($\mathbf{L} \equiv i\mathbf{p} \times \nabla_{\mathbf{p}}$):

$$\partial_t f + \beta \nabla_{\mathbf{r}} f - i [\boldsymbol{\Omega} + \boldsymbol{\omega}] \mathbf{L} f = 0 \quad (\text{A})$$

- We now look at the **ensemble-average PSD**: $\langle f \rangle$
- Expanding $f = \langle f \rangle + \delta f$ and averaging (A) over magnetic ensemble:

$$\partial_t \langle f \rangle + \beta \nabla_{\mathbf{r}} \langle f \rangle - i\boldsymbol{\Omega} \mathbf{L} \langle f \rangle = \underbrace{i\langle \boldsymbol{\omega} \mathbf{L} \delta f \rangle}_{\text{collision term}} \equiv \left(\frac{\partial f}{\partial t} \right)_c \quad (\text{B})$$

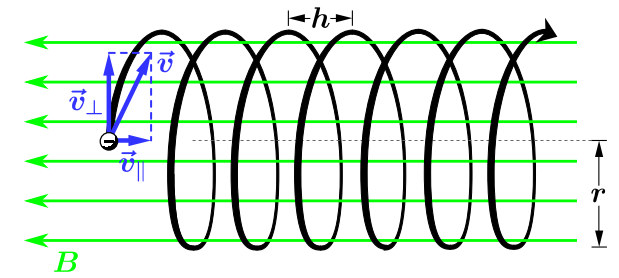
- The evolution of δf follows from the difference **(A)** - **(B)**:

$$\partial_t \delta f + \beta \nabla_{\mathbf{r}} \delta f - i\boldsymbol{\Omega} \mathbf{L} \delta f = i\boldsymbol{\omega} \mathbf{L} \langle f \rangle - \underbrace{[i\langle \boldsymbol{\omega} \mathbf{L} \delta f \rangle - i\boldsymbol{\omega} \mathbf{L} \delta f]}_{\simeq 0}$$

Collision Term

- We can solve along **unperturbed particle paths** \mathcal{P}_0 :

$$\delta f(t, \mathbf{r}_0(t), \mathbf{p}'_0(t)) \simeq - \int_{-\infty}^t dt' [i\omega \mathbf{L} \langle f \rangle]_{\mathcal{P}_0(t')}$$



- This allows to derive a formal solution to the collision term:

$$\left(\frac{\partial f}{\partial t} \right)_c \simeq \left\langle \omega \mathbf{L} \int_{-\infty}^t dt' [\omega \mathbf{L} \langle f \rangle]_{\mathcal{P}(t')} \right\rangle$$

- The collision term on the R.H.S. depends on the form of the magnetic turbulence and can, in general, not be solved analytically.
- In **BGK approximation** we can simplify it as: [Bhatnagar, Gross & Krook'54]

$$\left(\frac{\partial f}{\partial t} \right)_c \rightarrow -\nu \left[\langle f \rangle - \frac{1}{4\pi} \int d\Omega \langle f \rangle \right]$$

Diffusion Approximation

- We will work with the **BGK approximation** in the following.
- Consider the **monopole** and **dipole** contribution of the ensemble averaged PSD:

$$\phi(t, \mathbf{r}, p) = \frac{1}{4\pi} \int d\Omega \langle f(t, \mathbf{r}, \mathbf{p}(\Omega)) \rangle \quad \& \quad \Phi(t, \mathbf{r}, p) = \frac{1}{4\pi} \int d\Omega \hat{\mathbf{p}}(\Omega) \langle f(t, \mathbf{r}, \mathbf{p}(\Omega)) \rangle$$

- Ignoring higher harmonics we can re-write the Vlasov equation as:

$$\partial_t \phi + \beta \nabla \Phi = 0 \quad \& \quad \partial_t \Phi + \frac{\beta}{3} \nabla \phi + \mathbf{\Omega} \times \Phi = -\nu \Phi$$

- Assuming that $\partial_t |\Phi| \ll \partial_t \phi$ we arrive at the **diffusion equation**:

$$\partial_t \phi - \partial_i \left(K_{ij} \partial_j \phi \right) = 0 \quad \mathbf{K} = \frac{\beta^2}{3} \begin{pmatrix} \nu_{\perp}^{-1} & \nu_A^{-1} & 0 \\ -\nu_A^{-1} & \nu_{\perp}^{-1} & 0 \\ 0 & 0 & \nu_{\parallel}^{-1} \end{pmatrix} \quad \begin{aligned} \nu_{\parallel} &= \nu \\ \nu_{\perp} &= \nu + \Omega^2 / \nu \\ \nu_A &= \Omega + \nu^2 / \Omega \end{aligned}$$

Diffusion Approximation

- Consider now a CR source term:

$$\partial_t \phi - \partial_i \left(K_{ij} \partial_j \phi \right) = Q(t, \mathbf{r}, p)$$

- **Green's function** for $Q(t, \mathbf{r}, p) = \delta(\mathbf{r} - \mathbf{r}_s) \delta(t - t_s)$:

$$G(t, \mathbf{r}; t_s, \mathbf{r}_s) = (4\pi\Delta t)^{-3/2} (\det \mathbf{K}_s)^{-1/2} \exp \left(-\frac{\Delta \mathbf{r}^T \mathbf{K}_s^{-1} \Delta \mathbf{r}}{4\Delta t} \right)$$

- General solution:

$$n_{\text{CR}}(t, \mathbf{r}, p) = \int d^3 r_s \int dt_s G(t, \mathbf{r}; t_s, \mathbf{r}_s) Q(t_s, \mathbf{r}_s, p)$$

- Impulsive source, $Q = Q_\star(p) \delta(t) \delta(\mathbf{r} - \mathbf{r}_s)$, in isotropic diffusion:

$$n_{\text{CR}}(t, p) = \frac{Q_\star(p)}{(4\pi t K_{\text{iso}})^{3/2}} \exp \left(-\frac{\Delta r^2}{4t K_{\text{iso}}} \right) \quad \lambda_{\text{diff}}^2 \simeq \langle \mathbf{r}^2 \rangle = 6K_{\text{iso}} t$$

Quasi-Linear Approximation

- In the case of a strong background magnetic field and rapid gyration, the **CR anisotropy is expected to align with \mathbf{B}_0** .
- We can evaluate the turbulence at the **location of the gyrocenter**.
- Ignoring any spatial gradient of the anisotropy, we then approximate the collision term as:

$$\left(\frac{\partial f}{\partial t}\right)_c \simeq -L_i \mathcal{D}_{ij} L_j \langle f \rangle$$

- For homogenous (and isotropic) turbulence we expect:

$$\mathcal{D}_{ij} = \frac{\Omega^2}{B_0^2} \int_0^\infty d\tau C_{ij}(\mathbf{e}_z \mu \beta \tau) e^{-i\Omega\tau L_z}$$

Sidenote : AM Operators

- definition and commutation relation:

$$L_i \equiv i\epsilon_{ijk}p_j \frac{\partial}{\partial p_k} \quad \& \quad [L_i, L_j] = i\epsilon_{ijk}L_k$$

- in spherical coordinates:

$$L_x = -i \left(-\sin \varphi \frac{\partial}{\partial \theta} - \cot \theta \cos \varphi \frac{\partial}{\partial \varphi} \right)$$

$$L_y = -i \left(\cos \varphi \frac{\partial}{\partial \theta} - \cot \theta \sin \varphi \frac{\partial}{\partial \varphi} \right)$$

$$L_z = -i \frac{\partial}{\partial \varphi}$$

$$\mathbf{L}^2 = -\frac{1}{\sin^2 \theta} \frac{\partial^2}{\partial \varphi^2} + \frac{1}{\sin \theta} \frac{\partial}{\partial \theta} \left(\sin \theta \frac{\partial}{\partial \theta} \right)$$

Pitch-Angle Diffusion

- The product of angular momentum operators can be evaluated, e.g.

$$e^{-i\Omega\tau L_z} L_x = (\cos \Omega\tau L_x + \sin \Omega\tau L_y) e^{-i\Omega\tau L_z}$$

- If we assume that $\langle f \rangle$ is **only** a function of **pitch-angle** ($\mu = \cos \theta$):

$$\partial_t \langle f \rangle + v\mu \frac{\partial}{\partial \mu} \langle f \rangle \simeq \frac{\partial}{\partial \mu} \left(D_{\mu\mu} \frac{\partial}{\partial \mu} \langle f \rangle \right)$$

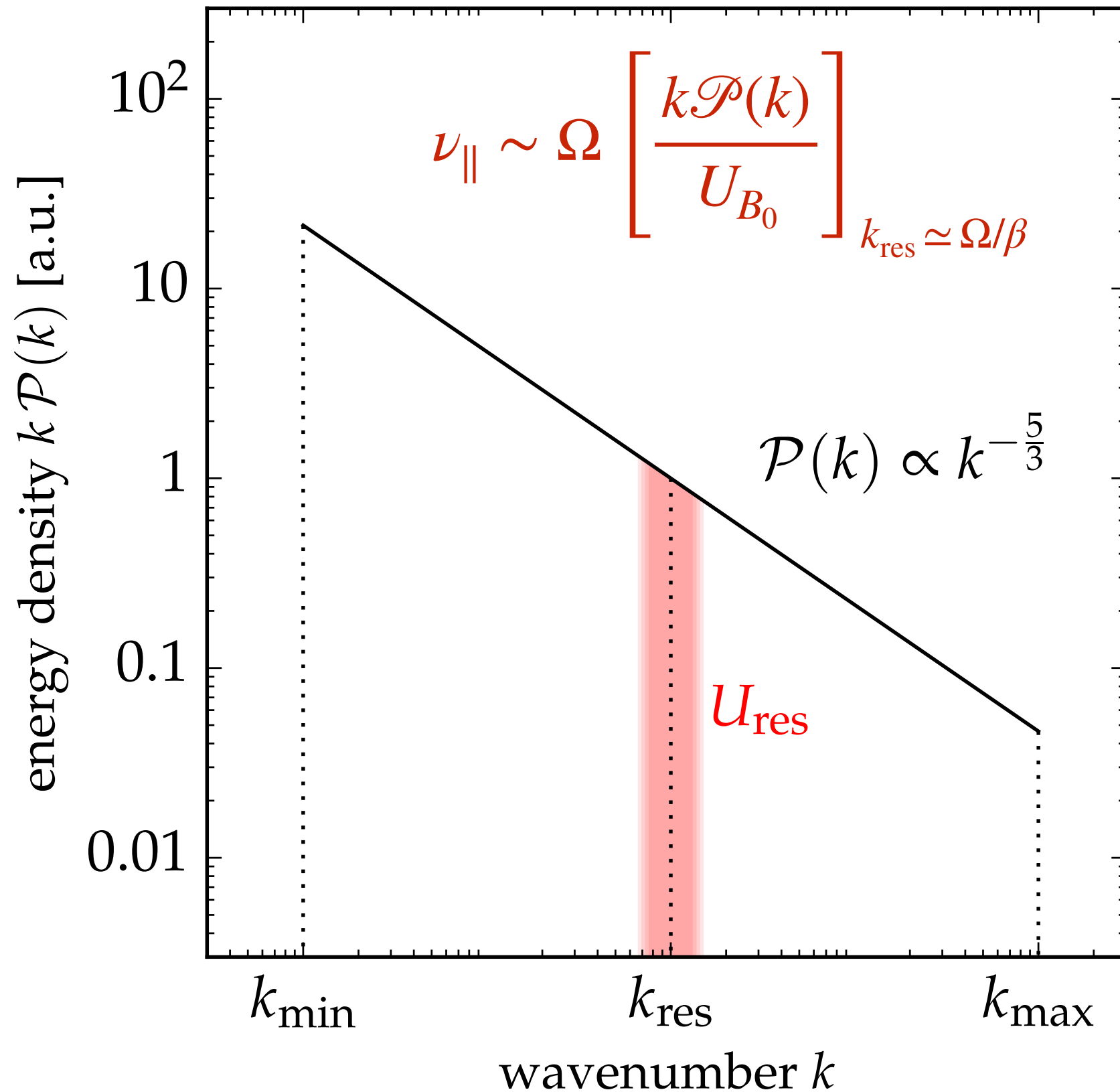
- The **pitch-angle diffusion** coefficient can be written as:

$$\frac{D_{\mu\mu}}{1 - \mu^2} \propto \frac{\Omega^2}{B_0^2} \int d^3k \frac{\mathcal{P}(k)}{4\pi k^2} A(\hat{k}_\perp, \hat{k}_\parallel) \int_0^\infty d\tau \left[e^{i(k_\parallel \mu \beta + \Omega)\tau} + e^{i(k_\parallel \mu \beta - \Omega)\tau} \right]$$

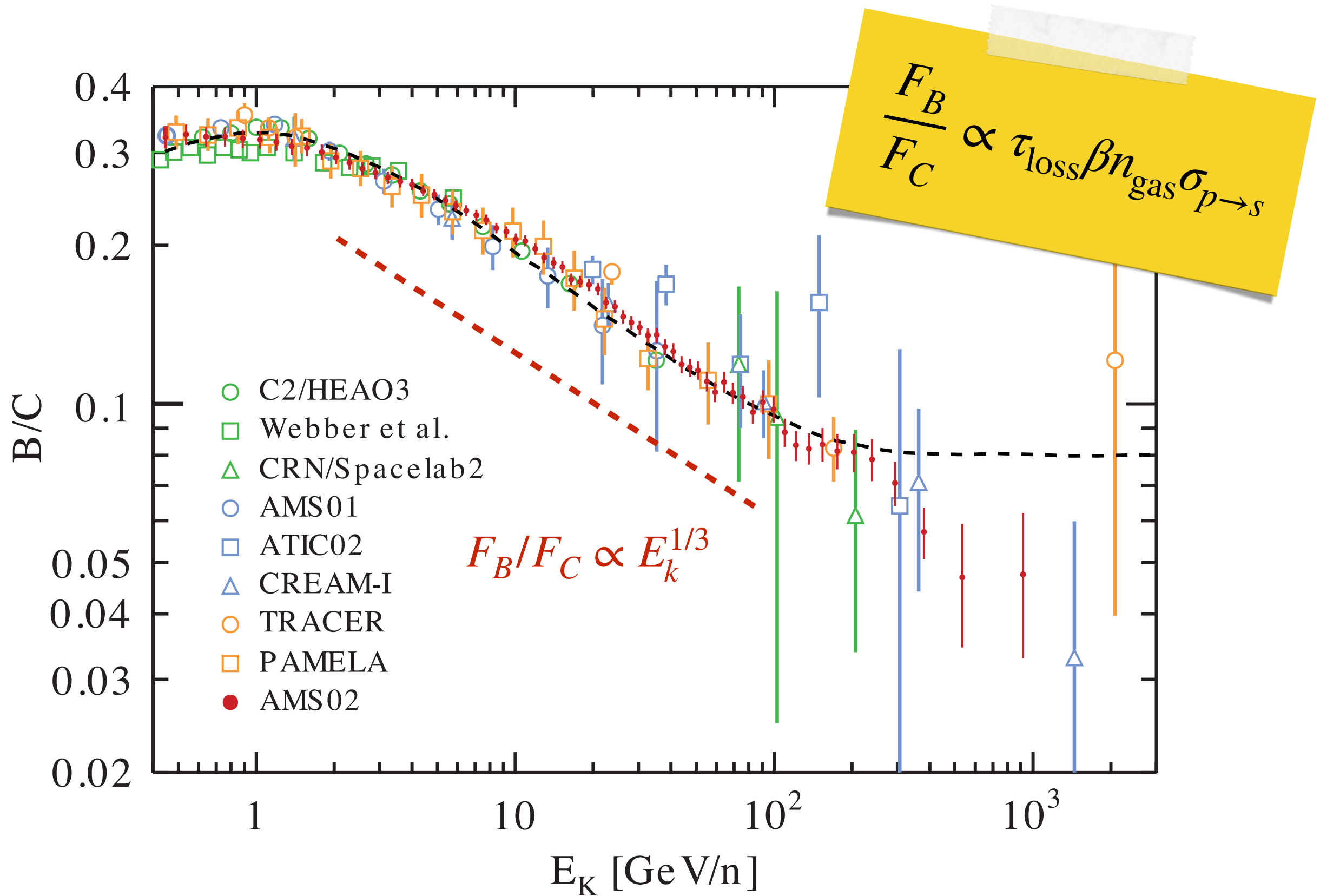
- This expression has the **expected resonance** we discussed earlier:

$$\nu_\parallel \propto D_{\mu\mu} \propto \Omega [k \mathcal{P}(k)]_{k_{\text{res}} \simeq \Omega/|\mu|\beta} \propto \Omega^{1/3} \propto \mathcal{R}^{-1/3}$$

Resonant Scattering



Boron-to-Carbon Ratio



Compton-Getting Effect

- PSD is Lorentz-invariant:

$$f(t, \mathbf{r}, \mathbf{p}) = f^*(t, \mathbf{r}^*, \mathbf{p}^*)$$

- relative motion of observer ($\boldsymbol{\beta} = \mathbf{v}/c$) in plasma rest frame:

$$\mathbf{p}^* = \mathbf{p} + p\boldsymbol{\beta} + \mathcal{O}(\beta^2)$$

- Taylor expansion:

$$f(\mathbf{p}) \simeq f^*(\mathbf{p}) + p\boldsymbol{\beta} \nabla_{\mathbf{p}} f^*(\mathbf{p}) + \mathcal{O}(\beta^2)$$

- dipole term Φ is not invariant:

$$\phi = \phi^* \quad \Phi = \Phi^* + \frac{1}{3}\boldsymbol{\beta} \frac{\partial \phi^*}{\partial \ln p} = \Phi^* + \underbrace{(2 + \Gamma)\boldsymbol{\beta}}_{\text{Compton-Getting effect}}$$

- *What is the plasma rest-frame?* LSR or ISM : $v \simeq 20 \text{ km/s}$

Summary : Dipole Anisotropy

- Spherical harmonics expansion of **relative intensity**:

$$I(\Omega) = 1 + \boldsymbol{\delta} \cdot \mathbf{n}(\Omega) + \sum_{\ell \geq 2} \sum_{m=-\ell}^{\ell} a_{\ell m} Y_{\ell m}(\Omega)$$

- **cosmic ray density** $n_{\text{CR}} \propto E^{-\Gamma}$ and **dipole vector** $\boldsymbol{\delta}$ from diffusion theory:

$$\underbrace{\partial_t n_{\text{CR}} \simeq \nabla(\mathbf{K} \nabla n_{\text{CR}}) + Q_{\text{CR}}}_{\text{diffusion equation}}$$

$$\underbrace{\boldsymbol{\delta} \simeq 3\mathbf{K} \nabla n_{\text{CR}} / n_{\text{CR}}}_{\text{Fix's law}}$$

- **diffusion tensor** \mathbf{K} in general anisotropic along background field \mathbf{B} :

$$K_{ij} = \kappa_{\parallel} \hat{B}_i \hat{B}_j + \kappa_{\perp} (\delta_{ij} - \hat{B}_i \hat{B}_j) + \kappa_A \epsilon_{ijk} \hat{B}_k$$

- relative motion of the observer in the plasma rest frame (\star):

[Compton & Getting '35]

$$\boldsymbol{\delta} \simeq \boldsymbol{\delta}^{\star} + (2 + \Gamma)\boldsymbol{\beta}$$

TeV-PeV Dipole Anisotropy

- **CG-corrected** dipole:

$$\delta^* \simeq \delta - (2 + \Gamma)\beta = 3\mathbf{K} \nabla n_{\text{CR}} / n_{\text{CR}}$$

- **projection** onto equatorial plane:

$$\delta^* \rightarrow (\delta_{0h}^*, \delta_{6h}^*, 0)$$

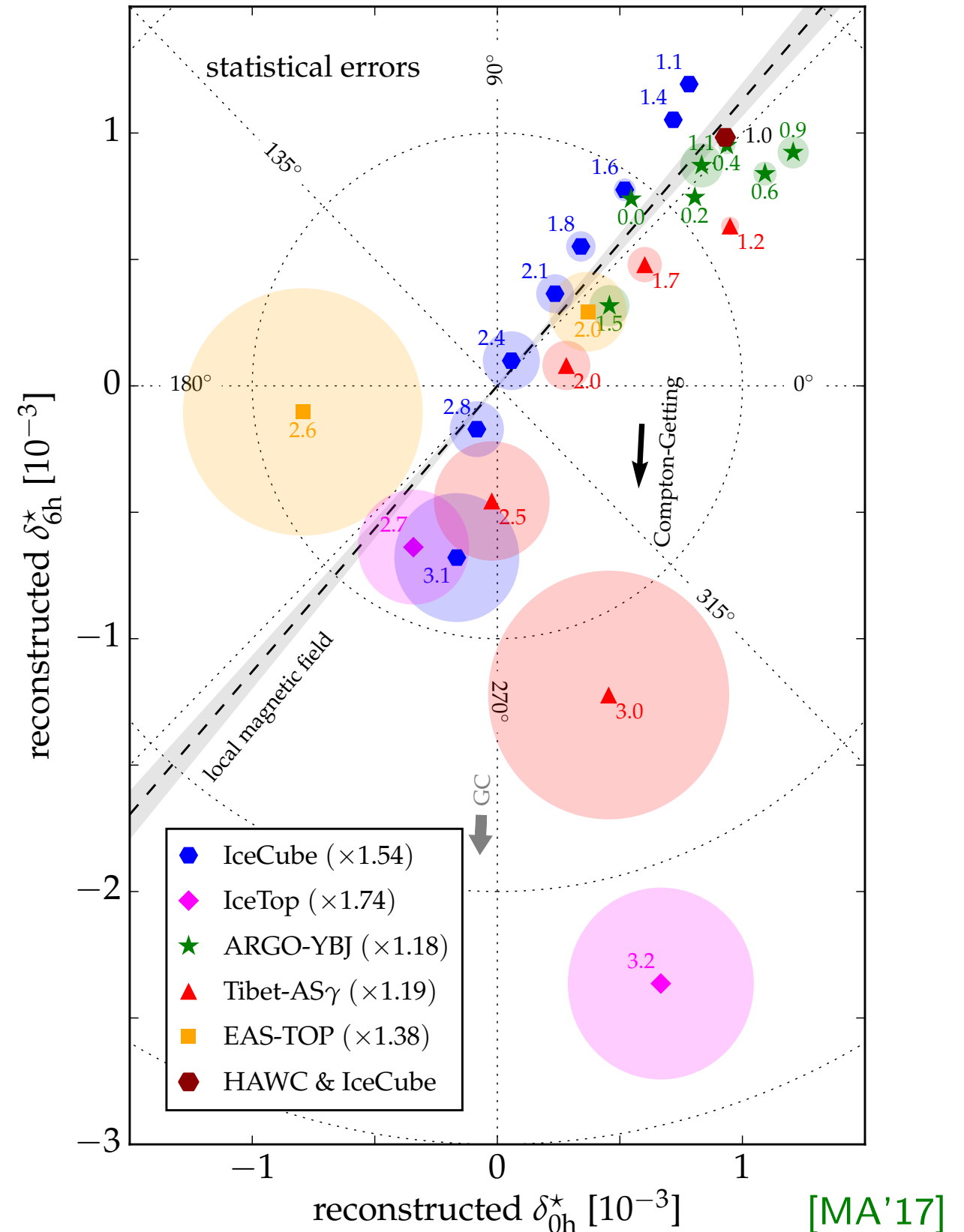
- **projection** along strong regular magnetic fields:

[Mertsch & Funk'14; Schwadron *et al.*'14]

$$K_{ij} \simeq \kappa_{\parallel} \hat{B}_i \hat{B}_j$$

- TeV-PeV dipole data consistent with magnetic field direction inferred from IBEX data.

[McComas *et al.*'09]



Local Magnetic Field

- **IBEX ribbon:** enhanced emission of energetic neutral atoms (ENAs) observed with the **I**nterstellar **B**oundary **E**Xplorer [McComas *et al.*'09]

- interpreted as local magnetic field ($\lesssim 0.1$ pc) draping the heliopause

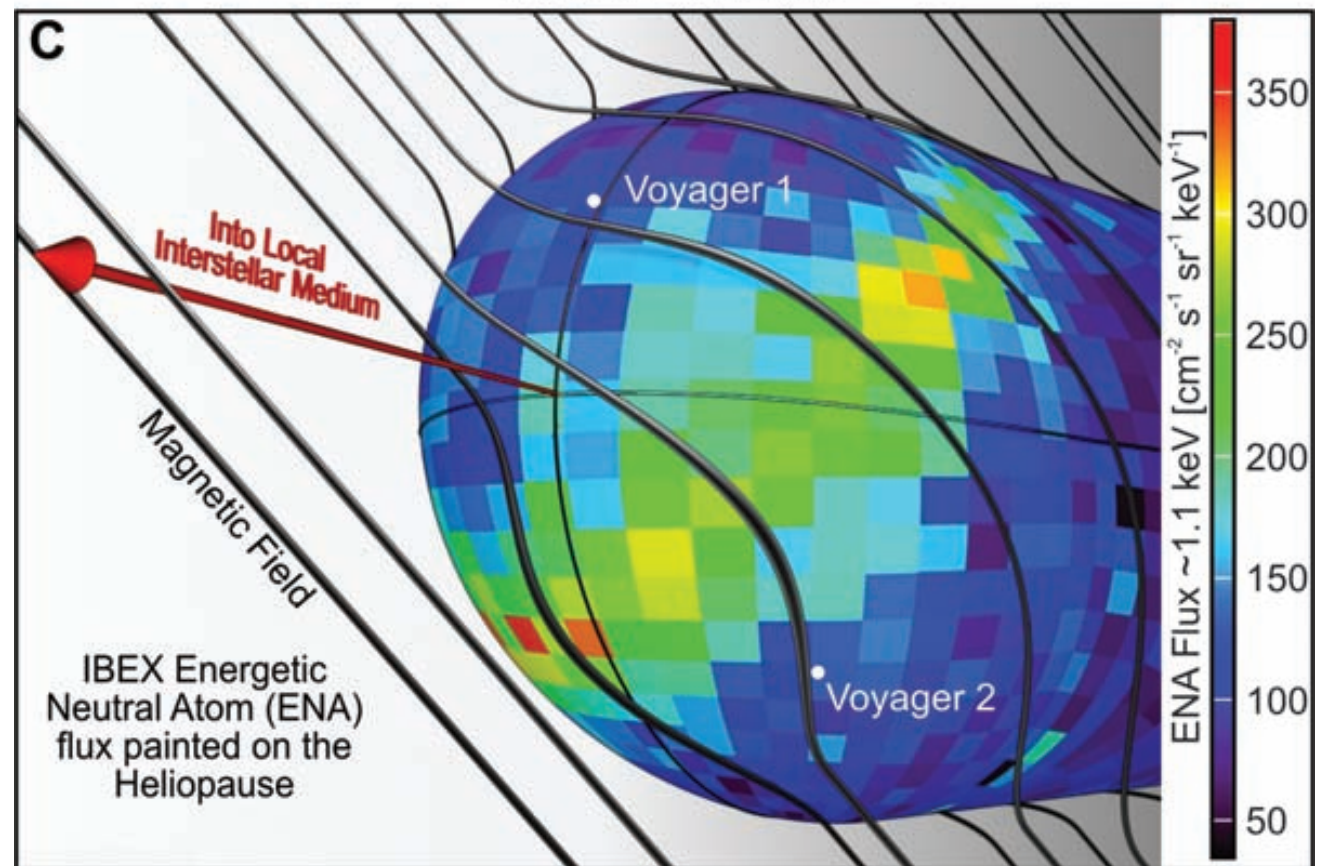
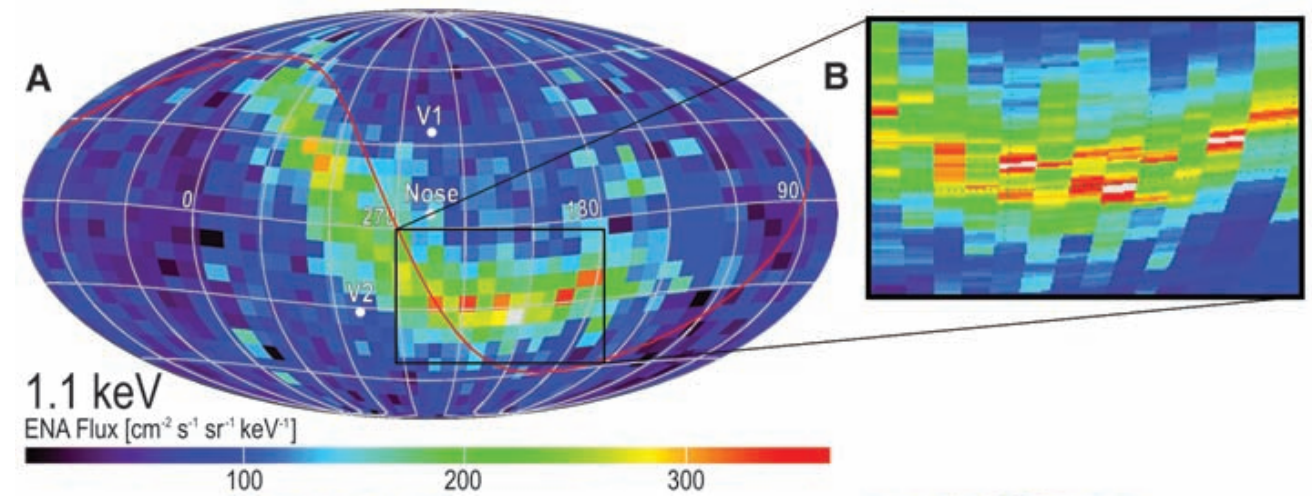
- ribbon center defines field orientation (Galactic coordinates): [Funsten *et al.*'13]

$$l \simeq 210.5^\circ \quad \& \quad b \simeq -57.1^\circ$$

- consistent with field inferred from polarization of starlight by interstellar dust ($\lesssim 40$ pc):

[Frisch *et al.*'15]

$$l \simeq 216.2^\circ \quad \& \quad b \simeq -49.0^\circ$$



[McComas *et al.*'09]

Known Local SNRs

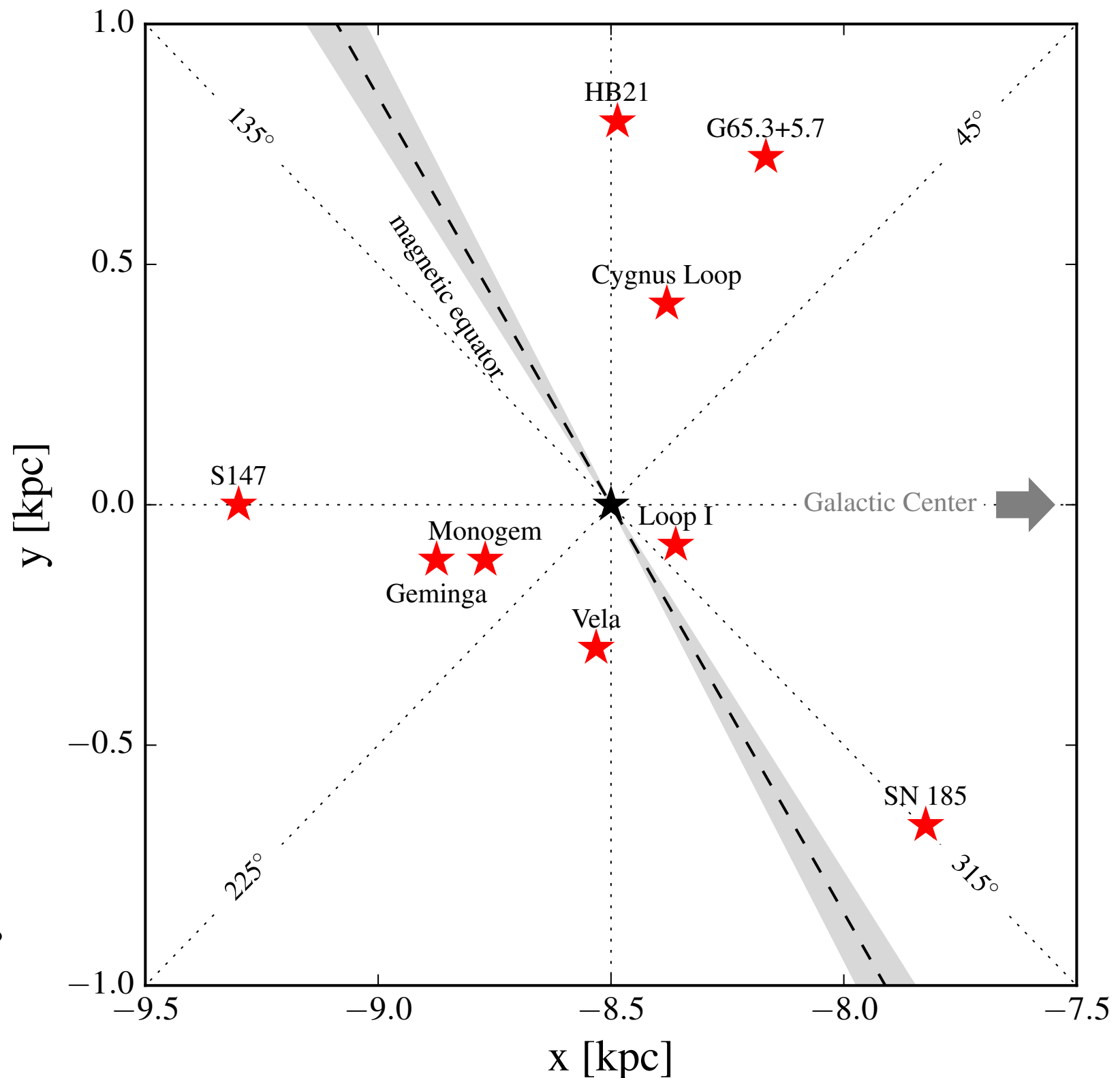
- projection along magnetic field leaves two possible dipole directions:

$$\delta \propto \pm \hat{\mathbf{B}}_0$$

- **Intersection of magnetic equator with Galactic Plane** defines two regions where CR sources contribute to the dipole with opposite phases:

$$120^\circ \leq l \leq 300^\circ \rightarrow \alpha_1 \simeq 49^\circ$$

$$-60^\circ \leq l \leq 120^\circ \rightarrow \alpha_1 \simeq 229^\circ$$



Phase-Flip by Vela SNR?

- Observed 1-100 TeV phase indicates dominance of a local source with:

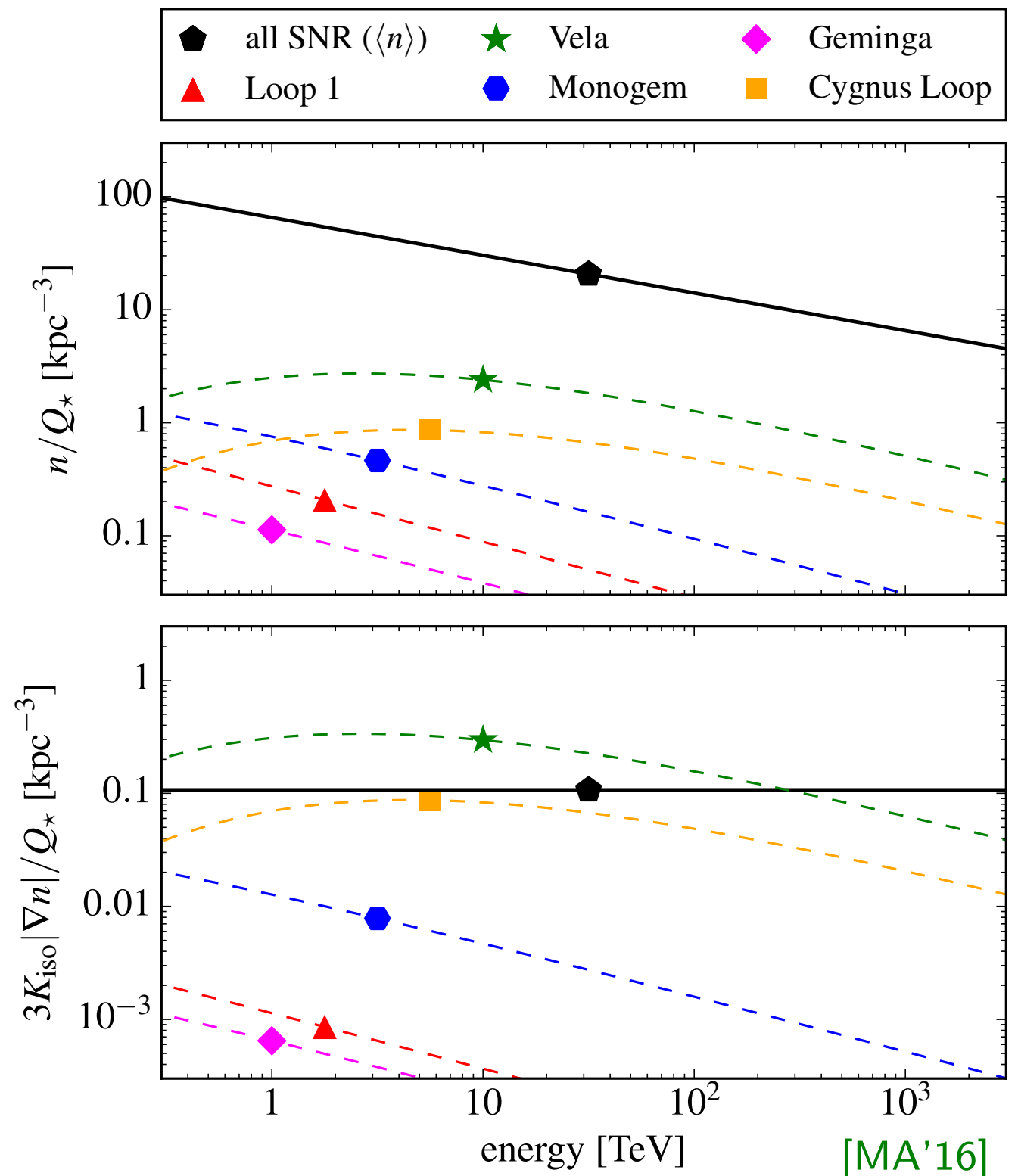
$$120^\circ \leq l \leq 300^\circ$$

- **plausible scenario: Vela SNR**

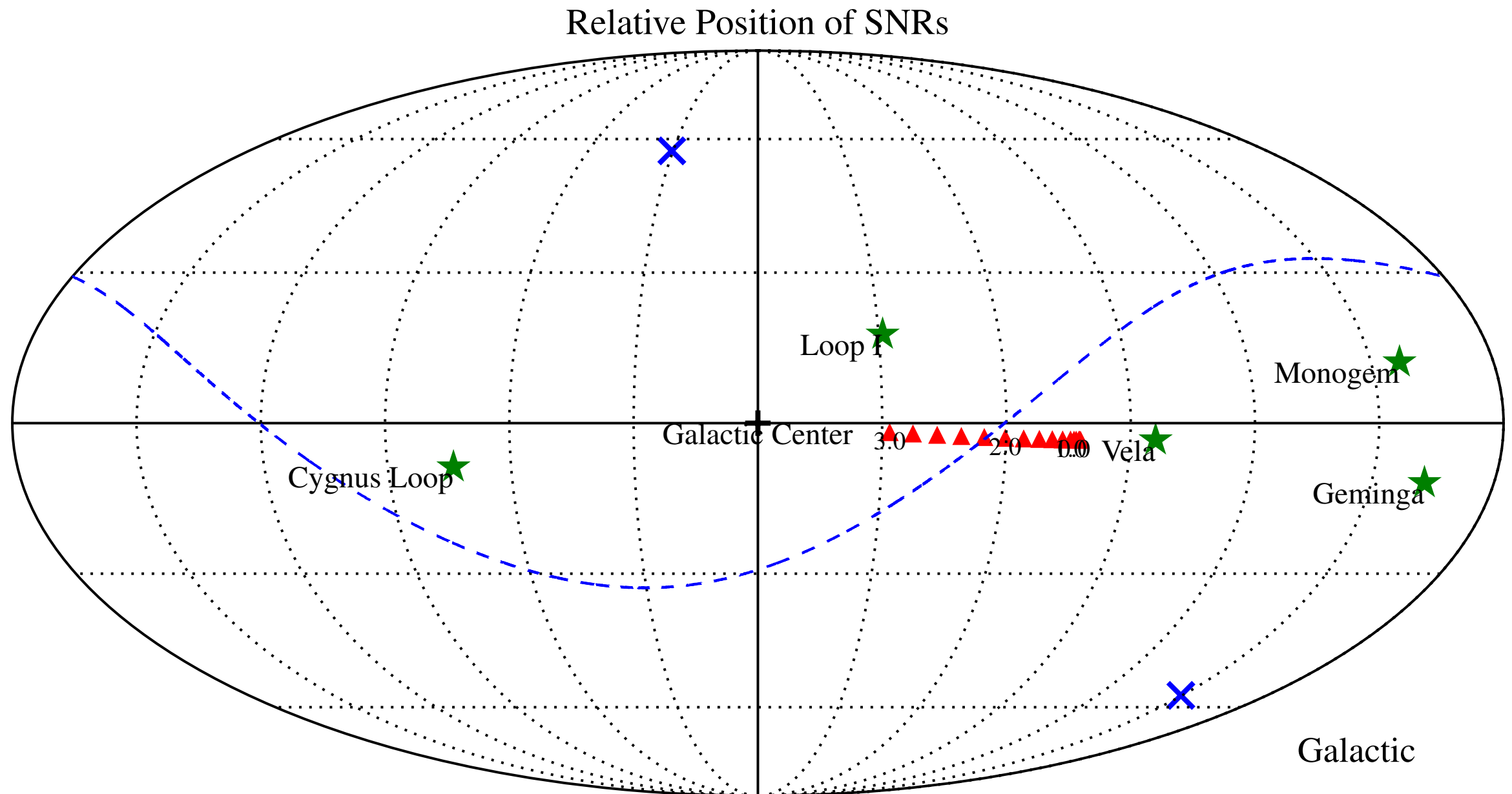
- age: $\simeq 11,000$ yrs
- distance: $\simeq 1,000$ lyrs
- SNR rate: $\simeq 1/30 \text{ yr}^{-1}$
- (effective) isotropic diffusion:

$$K_{\text{iso}} \simeq 3 \times 10^{28} E_{\text{GeV}}^{1/3} \text{cm}^2/\text{s}$$

- Galactic halo width: $\simeq 3$ kpc
- instantaneous CR emission Q_\star

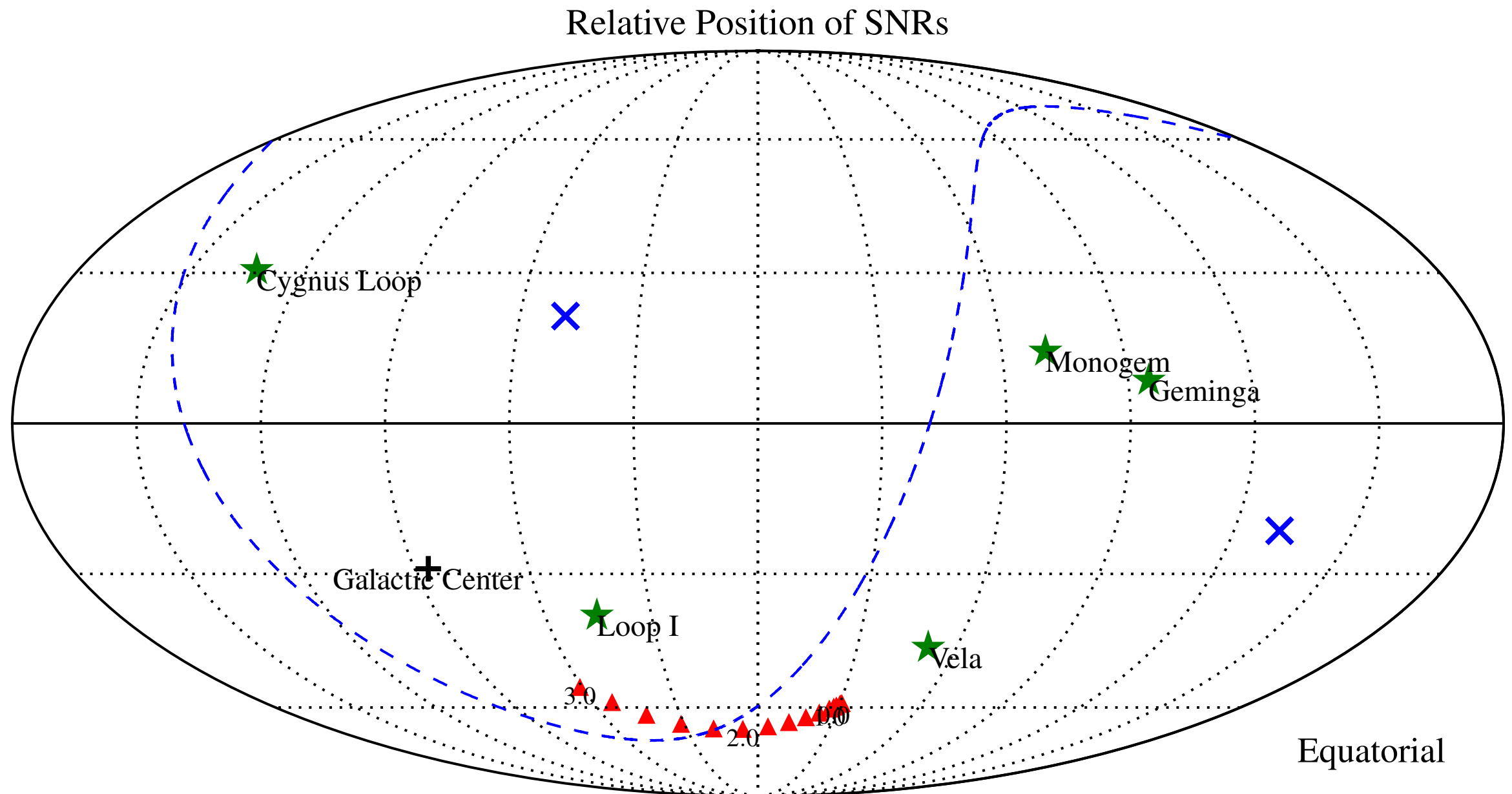


Position of SNR



Relative position of the five closest SNRs. The magnetic field direction (IBEX) is indicated by \times and the **magnetic equator** by a dashed line.

Position of SNR



Relative position of the five closest SNRs. The magnetic field direction (IBEX) is indicated by \times and the **magnetic equator** by a dashed line.

Phase-Flip by Vela SNR?

- Observed 1-100 TeV phase indicates **dominance of a local source** with:

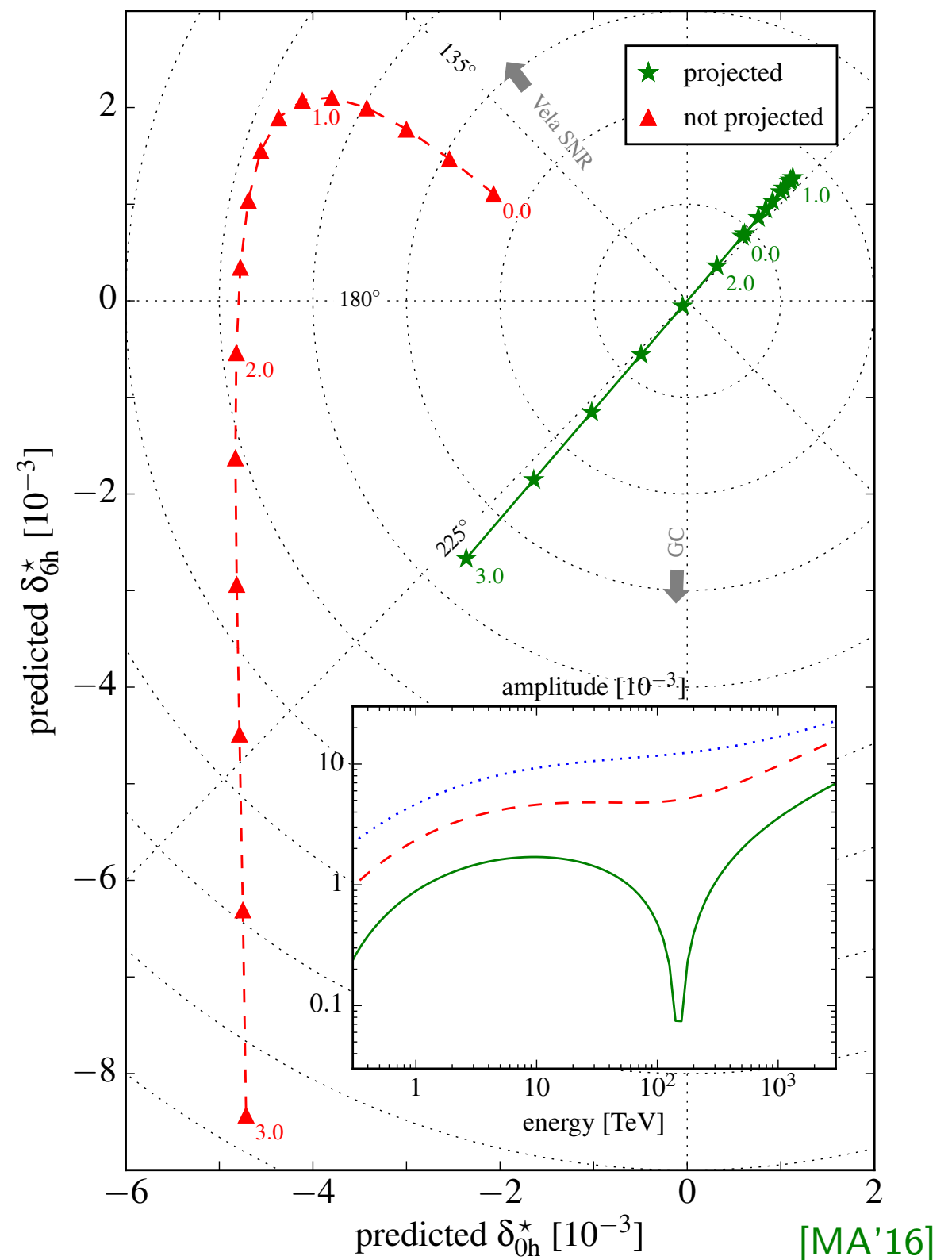
$$120^\circ \leq l \leq 300^\circ$$

- **plausible scenario: Vela SNR**

- age: $\simeq 11,000$ yrs
- distance: $\simeq 1,000$ lyrs
- SNR rate: $\simeq 1/30 \text{ yr}^{-1}$
- (effective) isotropic diffusion:

$$K_{\text{iso}} \simeq 3 \times 10^{28} E_{\text{GeV}}^{1/3} \text{cm}^2/\text{s}$$

- Galactic halo width: $\simeq 3$ kpc
- instantaneous CR emission Q_\star



[MA'16]

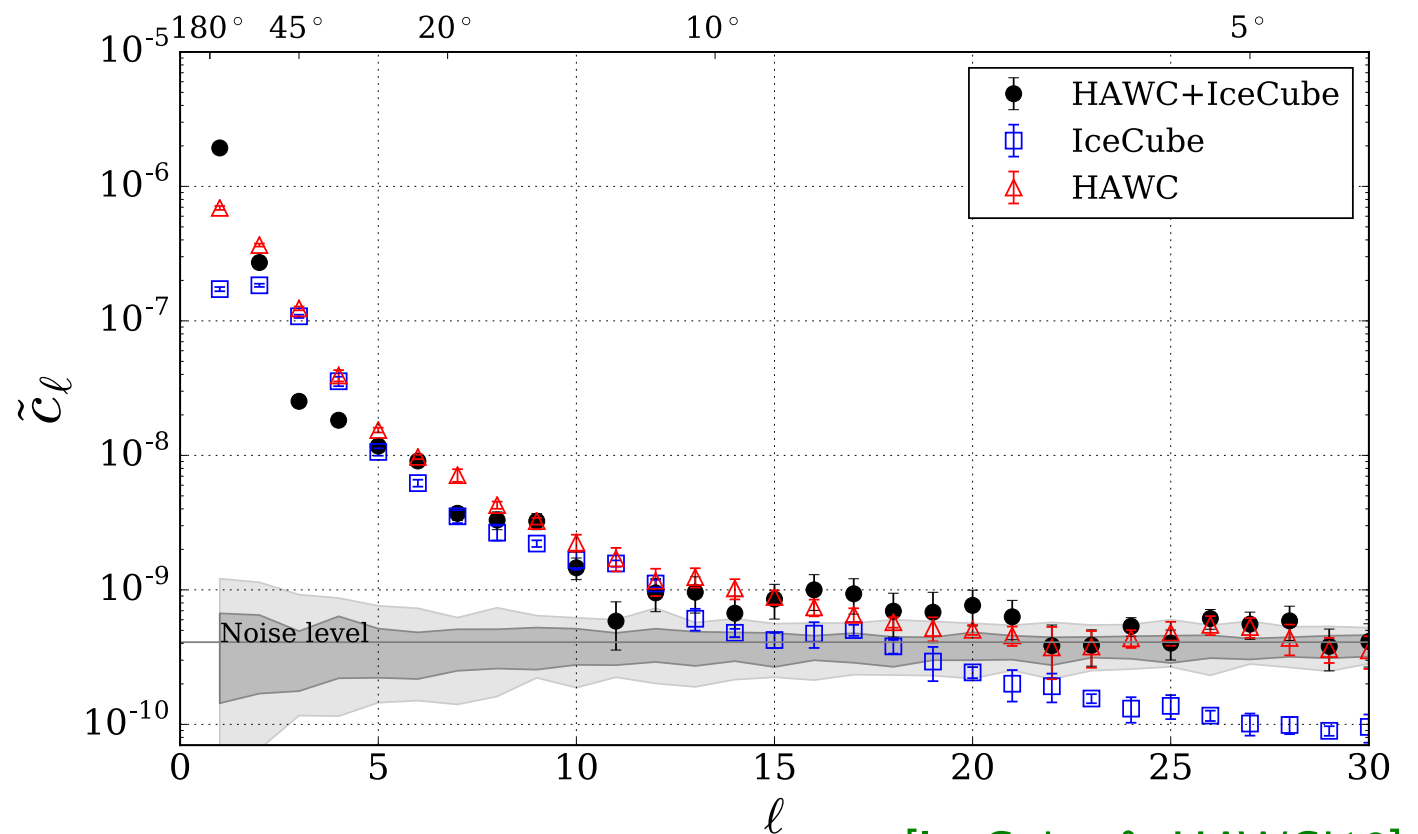
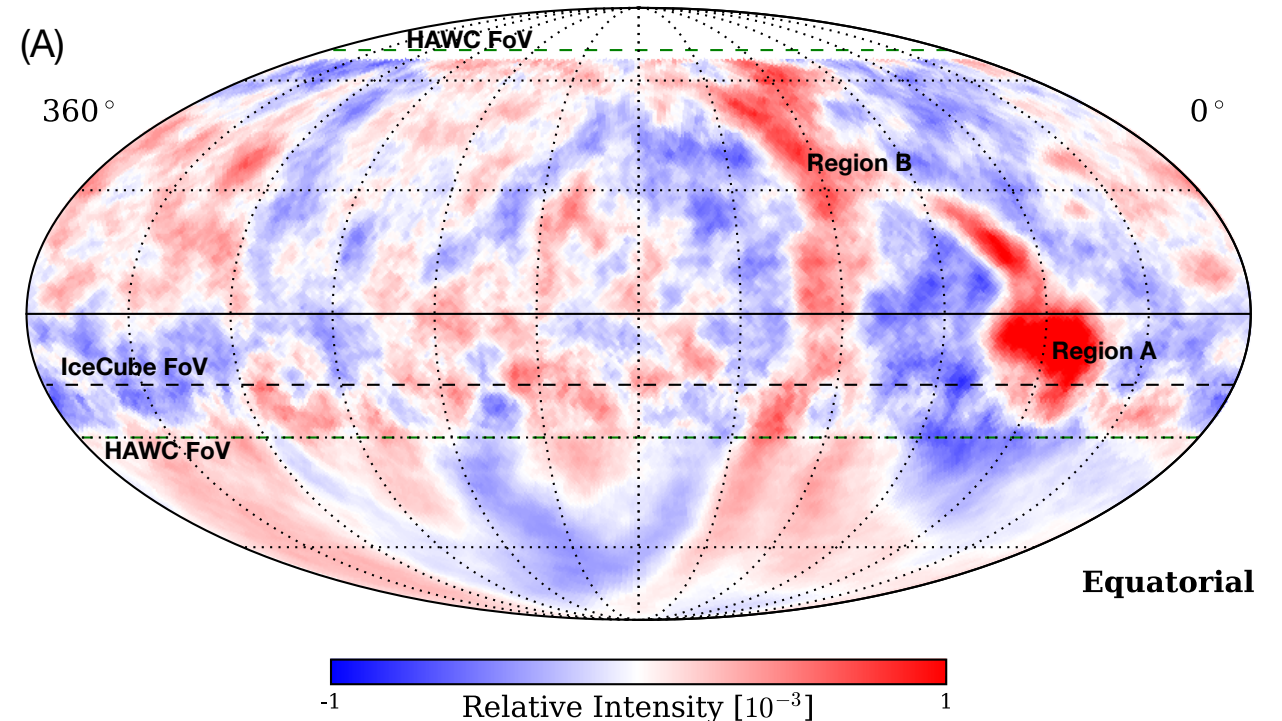
Small-Scale Anisotropy

- Significant TeV small-scale anisotropies down to angular scales of $\mathcal{O}(10^\circ)$.
- Strong local excess (*region A*) observed by Northern observatories.

[Tibet-AS γ '06; Milagro'08]
 [ARGO-YBJ'13; HAWC'14]

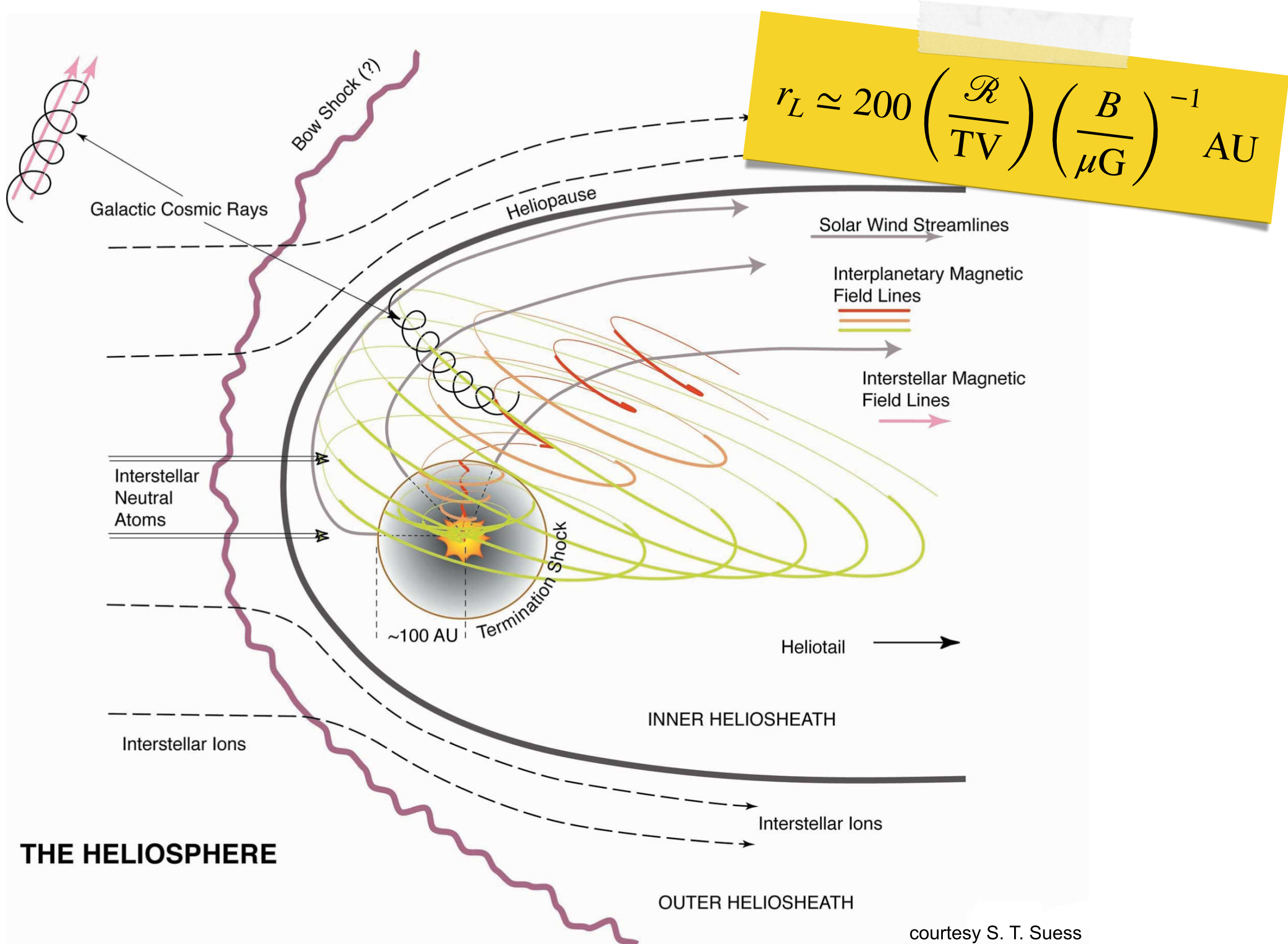
- Angular power spectra of IceCube and HAWC data show excess compared to isotropic arrival directions. [IC'11; HAWC'14]

$$C_\ell = \frac{1}{2\ell + 1} \sum_{m=-\ell}^{\ell} |a_{\ell m}|^2$$

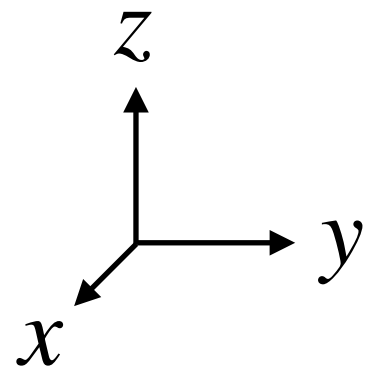


[IceCube & HAWC'18]

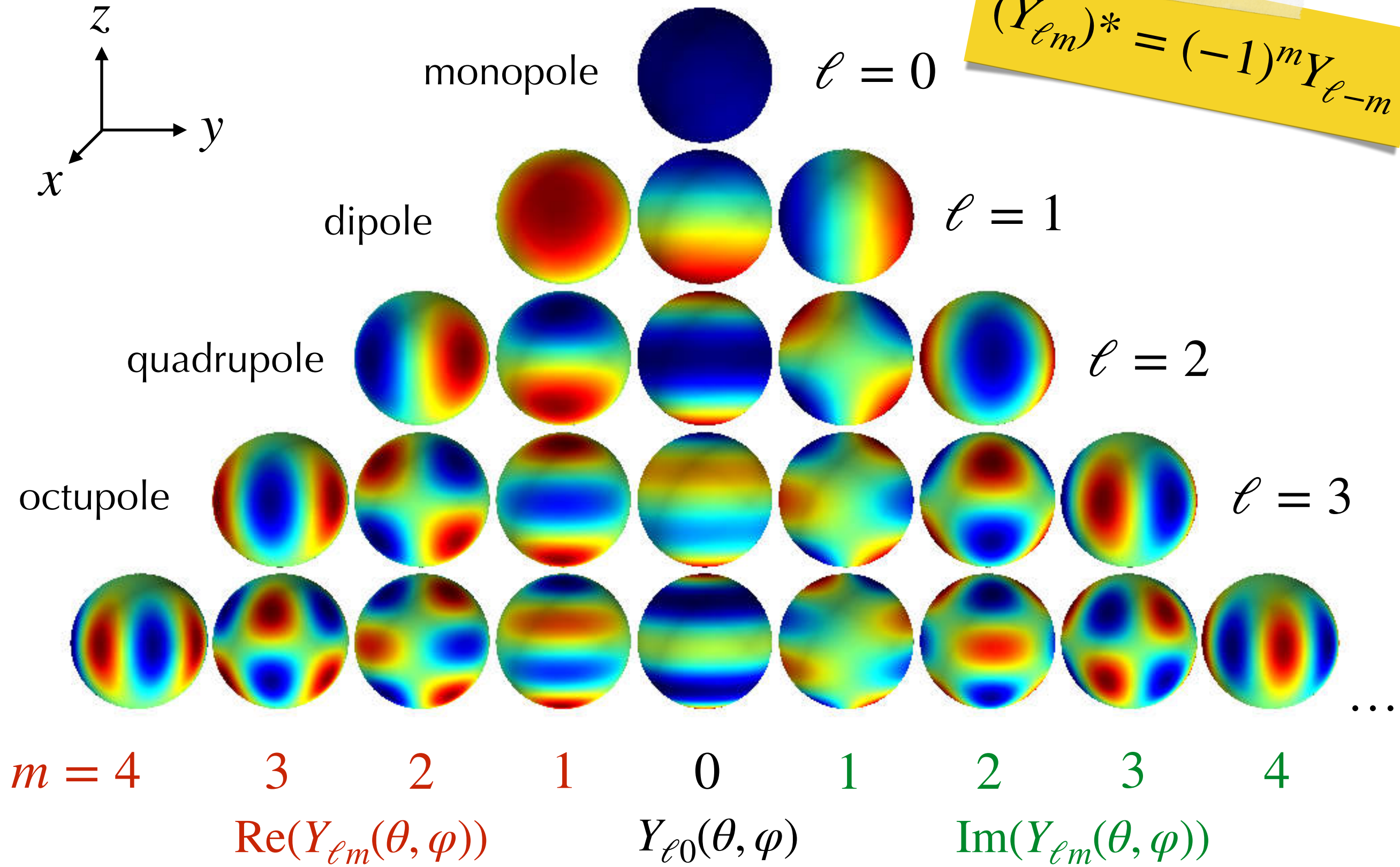
Influence of Heliosphere?



Spherical Harmonics



$$(Y_{\ell m})^* = (-1)^m Y_{\ell -m}$$



Angular Power Spectrum

- Every smooth function $g(\theta, \varphi)$ on a sphere can be decomposed in terms of spherical harmonics $Y_{\ell m}(\theta, \varphi)$:

$$g(\theta, \varphi) = \sum_{\ell=0}^{\infty} a_{\ell m} Y_{\ell m}(\theta, \varphi) \quad \leftrightarrow \quad a_{\ell m} = \int d \cos \theta \int d\varphi Y_{\ell m}^*(\theta, \varphi) g(\theta, \varphi)$$

- **angular power spectrum:**

$$C_{\ell} = \frac{1}{2\ell + 1} \sum_{m=-\ell}^{\ell} |a_{\ell m}|^2$$

- related to the two-point **auto-correlation function:**

$$\xi(\eta) = \frac{1}{8\pi^2} \int d\Omega_1 \int d\Omega_2 \delta(\mathbf{n}_1 \cdot \mathbf{n}_2 - \cos \eta) g(\Omega_1) g(\Omega_2) = \frac{1}{4\pi} \sum_{\ell=0}^{\infty} (2\ell + 1) C_{\ell} P_{\ell}(\cos \eta)$$

- Note that power C_{ℓ} is invariant under rotations (assuming 4π coverage).

Non-Uniform Pitch-Angle Diffusion

- stationary pitch-angle diffusion:

$$v\mu \frac{\partial}{\partial z} \langle f \rangle = \frac{\partial}{\partial \mu} \left(D_{\mu\mu} \frac{\partial}{\partial \mu} \langle f \rangle \right)$$

- non-uniform diffusion:**

$$\frac{D_{\mu\mu}}{1 - \mu^2} \neq \text{const}$$

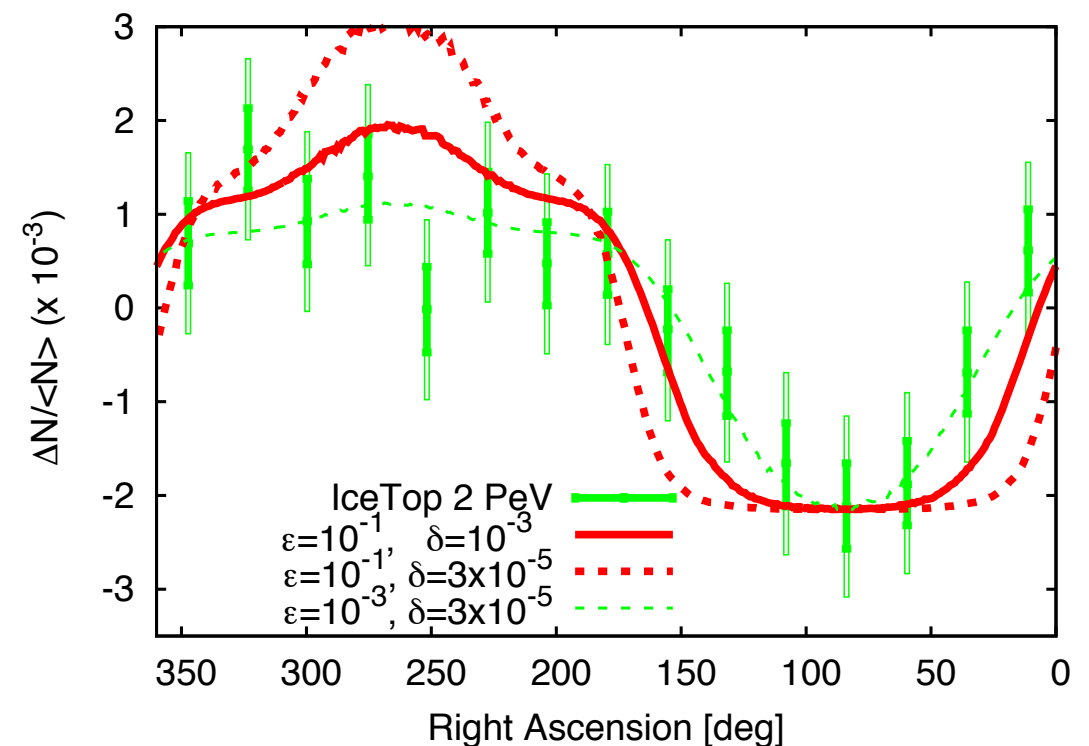
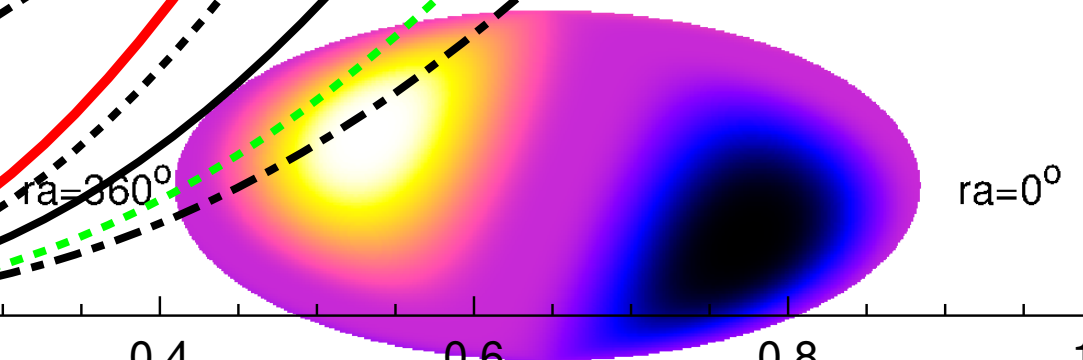
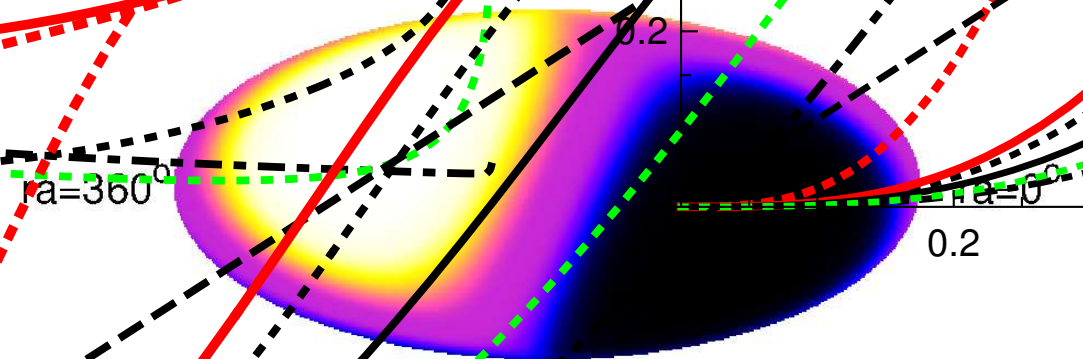
- non-uniform pitch-angle diffusion modifies the large-scale anisotropy aligned with background field

- small-scale** excess/deficits for enhanced diffusion towards $\mu = \pm 1$

[Malkov *et al.*'10]

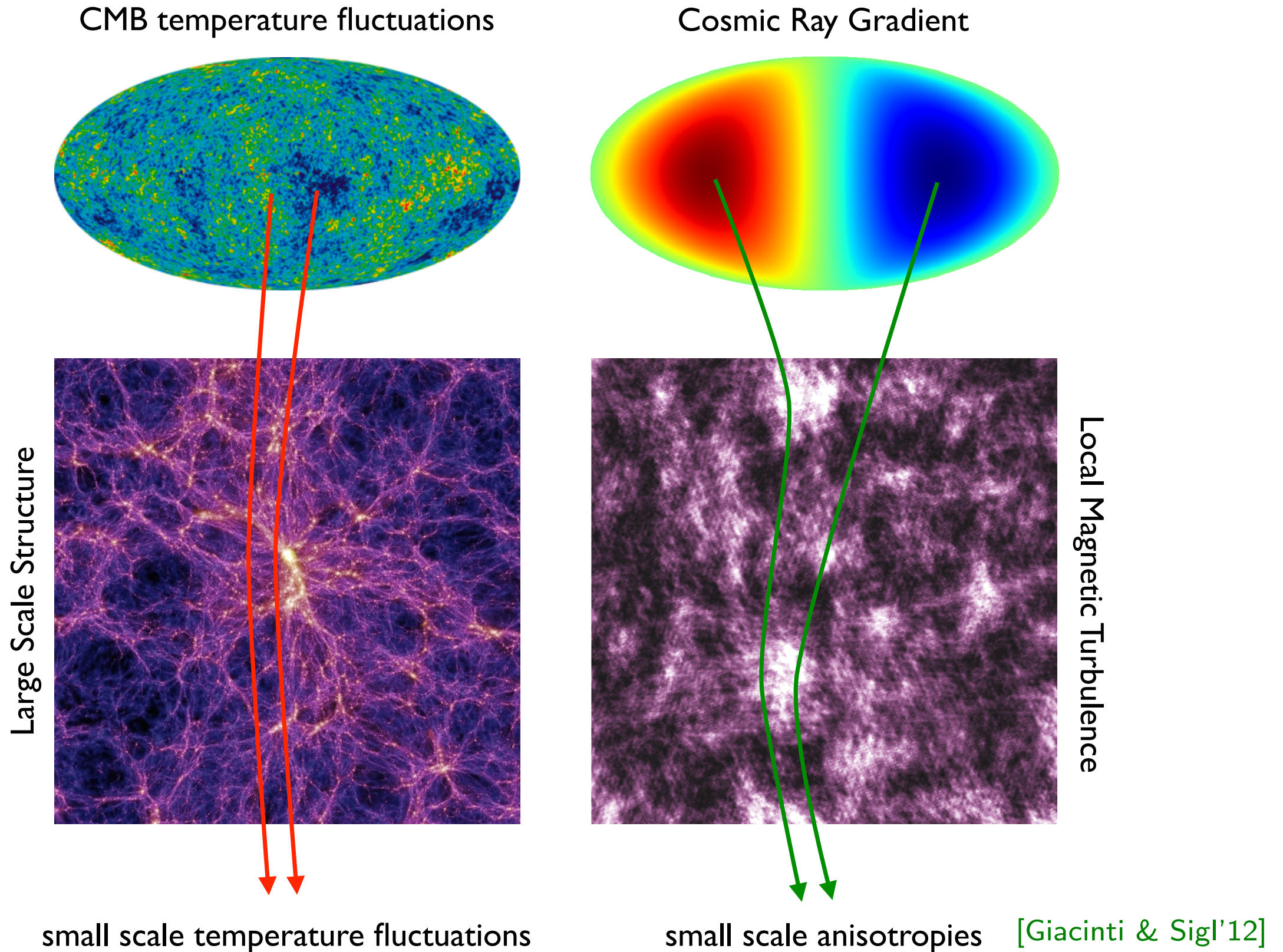
- large-scale** features for enhanced diffusion at $\mu = 0$

[Giacinti & Kirk'17]



[Giacinti & Kirk'17]

Anisotropy from Local Turbulence



Small-Scale Theorem

- **Assumptions:**

- absence of CR sources and sinks
- isotropic and static magnetic turbulence
- initially, homogenous phase space distribution

- **Theorem:** *The sum over the ensemble-averaged angular power spectrum is constant:*

[MA'14]

$$\sum_{\ell=0}^{\infty} (2\ell + 1) \langle C_{\ell} \rangle \propto \langle \xi(1) \rangle \propto \text{const}$$

- **Proof:** by angular auto-correlation function.
- Wash-out of individual moments by diffusion (rate $\nu_{\ell} \propto \mathbf{L}^2 \propto \ell(\ell + 1)$) has to be compensated by generation of small-scale anisotropy.
- Theorem implies small-scale angular features from large-scale average dipole anisotropy.

[Giacinti & Sigl'12; MA'14; MA & Mertsch'15,'20]

Evolution Model

- Diffusion theory motivates that each $\langle C_\ell \rangle$ decays exponentially with an effective relaxation rate:

$$\nu_\ell \simeq \nu \mathbf{L}^2 = \nu \ell(\ell + 1)$$

- A linear $\langle C_\ell \rangle$ evolution equation with **partial rates** $\nu_{\ell \rightarrow \ell'}$ requires:

$$\partial_t \langle C_\ell \rangle = -\nu_\ell \langle C_\ell \rangle + \sum_{\ell' \geq 0} \nu_{\ell' \rightarrow \ell} \frac{2\ell' + 1}{2\ell + 1} \langle C_{\ell'} \rangle \quad \text{with} \quad \nu_\ell \equiv \sum_{\ell' \geq 0} \nu_{\ell \rightarrow \ell'}$$

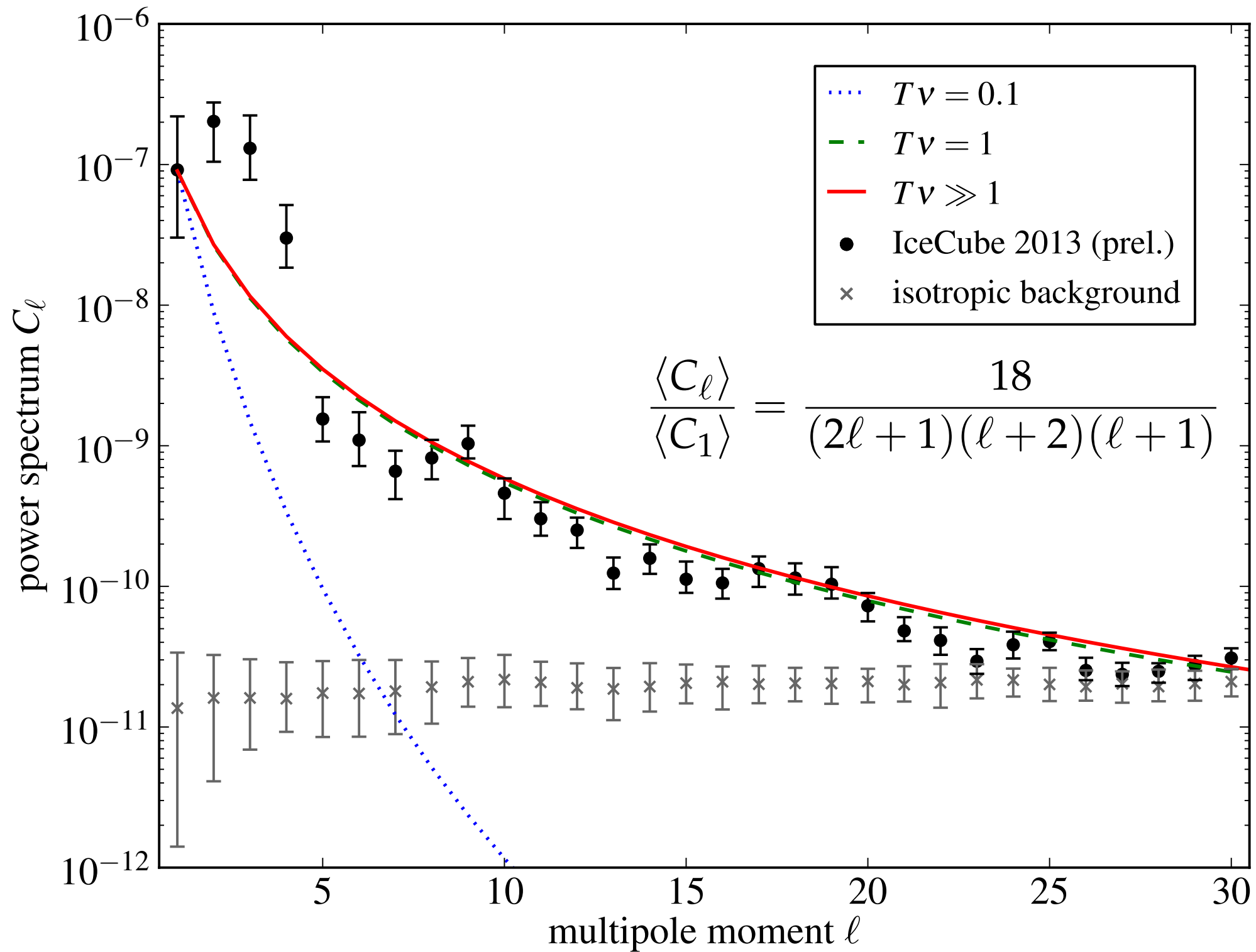
- For $\nu_\ell \simeq \nu_{\ell \rightarrow \ell+1}$ and, initially, $C_\ell(t = 0) = C_1 \delta_{\ell 1}$ this has an analytic solution:

$$\langle C_\ell \rangle(T) = \frac{3C_1}{2\ell + 1} \prod_{m=1}^{\ell-1} \nu_m \sum_n \prod_{p=1(\neq n)}^{\ell} \frac{e^{-T\nu_n}}{\nu_p - \nu_n}$$

- At large times we arrive at the asymptotic ratio:

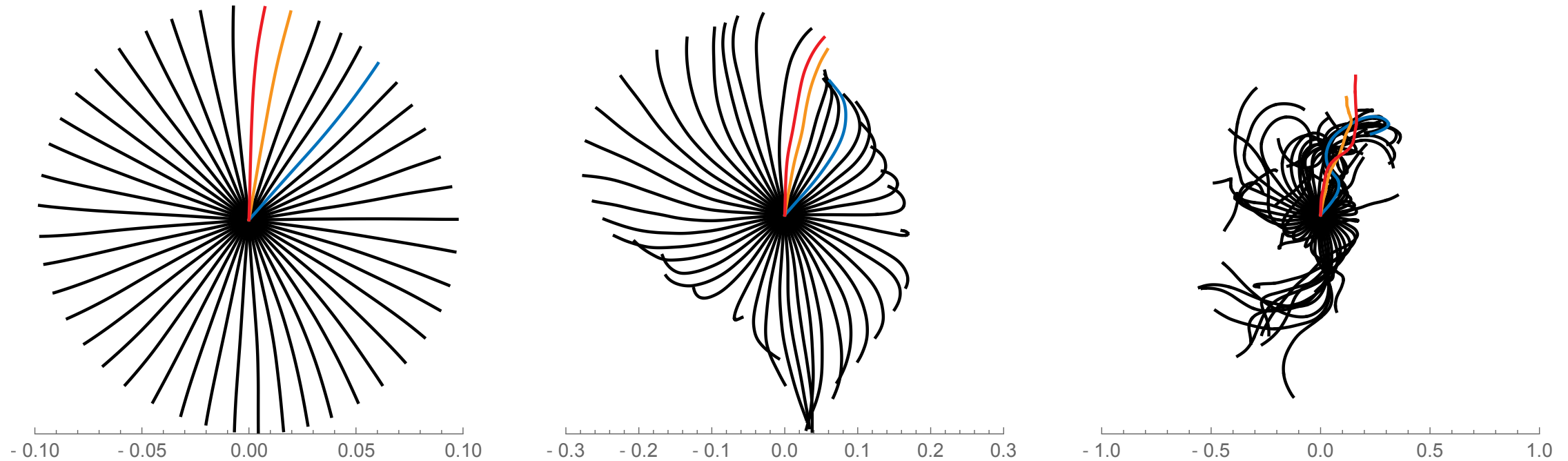
$$\lim_{T \rightarrow \infty} \frac{\langle C_\ell \rangle(T)}{\langle C_1 \rangle(T)} \simeq \frac{18}{(2\ell + 1)(\ell + 2)(\ell + 1)}$$

Comparison with Data



[MA'14]

Cosmic Ray Backtracking



- Consider a local (quasi-)stationary solution of the diffusion approximation:

[MA & Mertsch'15]

$$\langle f \rangle \simeq \phi + (\mathbf{r} - 3\hat{\mathbf{p}}\mathbf{K}) \nabla \phi$$

- Ensemble-averaged C_ℓ 's ($\ell \leq 1$) from backtracking:

$$\frac{\langle C_\ell \rangle}{4\pi} \simeq \int \frac{d\hat{\mathbf{p}}_1}{4\pi} \int \frac{d\hat{\mathbf{p}}_2}{4\pi} P_\ell(\mathbf{p}_1\mathbf{p}_2) \lim_{T \rightarrow \infty} \langle \mathbf{r}_{1i}(-T) \mathbf{r}_{2j}(-T) \rangle \frac{\partial_{r_i} n_{\text{CR}} \partial_{r_j} n_{\text{CR}}}{n_{\text{CR}}^2}$$

Cosmic Ray Backtracking

- simulation in isotropic & static magnetic turbulence with:

$$\overline{\delta \mathbf{B}^2} = \mathbf{B}_0^2$$

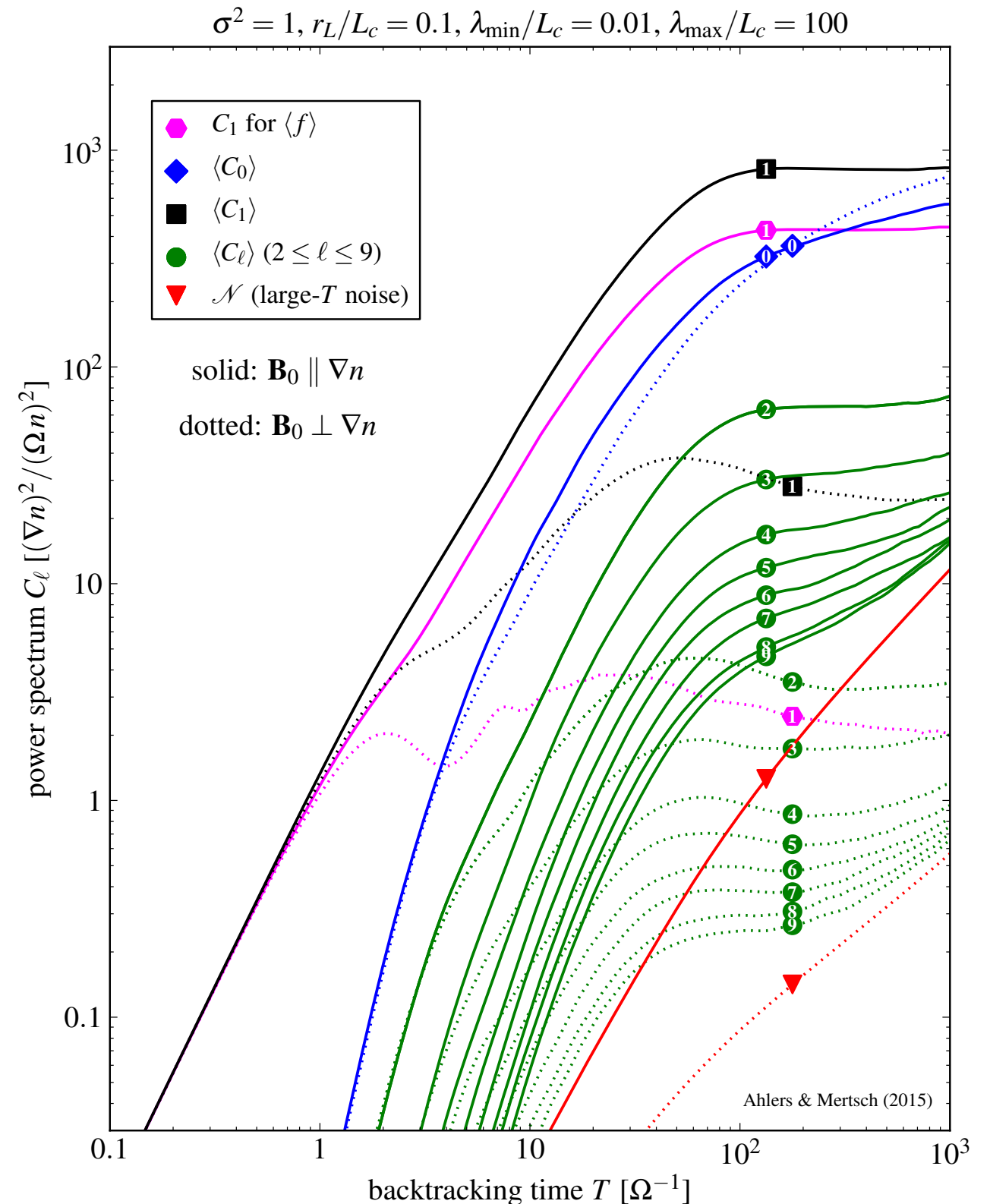
- relative orientation of CR gradient:

- *solid lines* : $\mathbf{B}_0 \parallel \nabla n_{\text{CR}}$

- *dotted lines* : $\mathbf{B}_0 \perp \nabla n_{\text{CR}}$

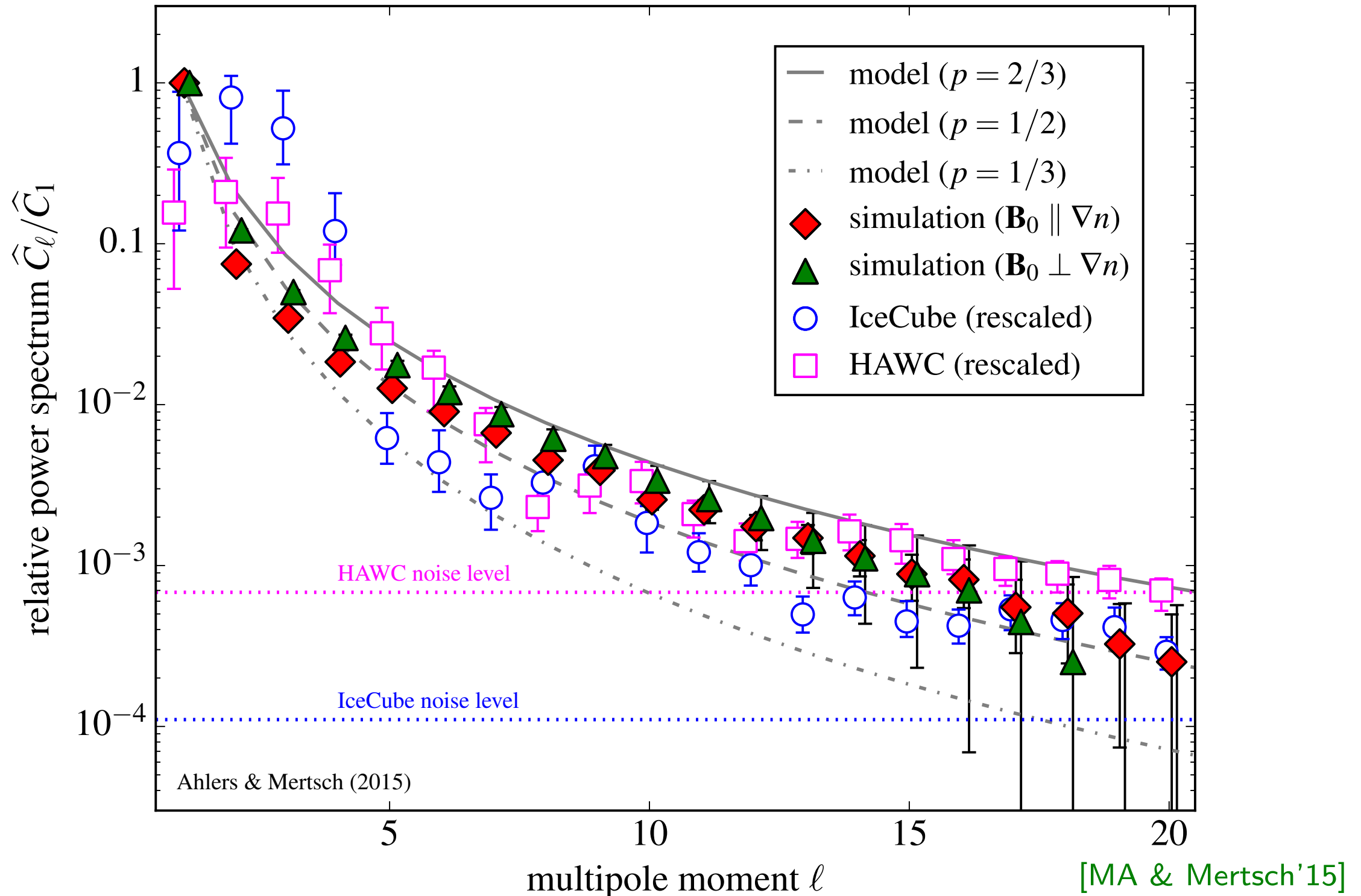
- diffusive regime at $T\Omega \gtrsim 100$
- slightly enhanced dipole compared to standard diffusion
- asymptotically limited by simulation noise:

$$\mathcal{N} \simeq \frac{4\pi}{N_{\text{pix}}} 2TK_{ij} \frac{\partial_i n_{\text{CR}} \partial_j n_{\text{CR}}}{n_{\text{CR}}^2}$$

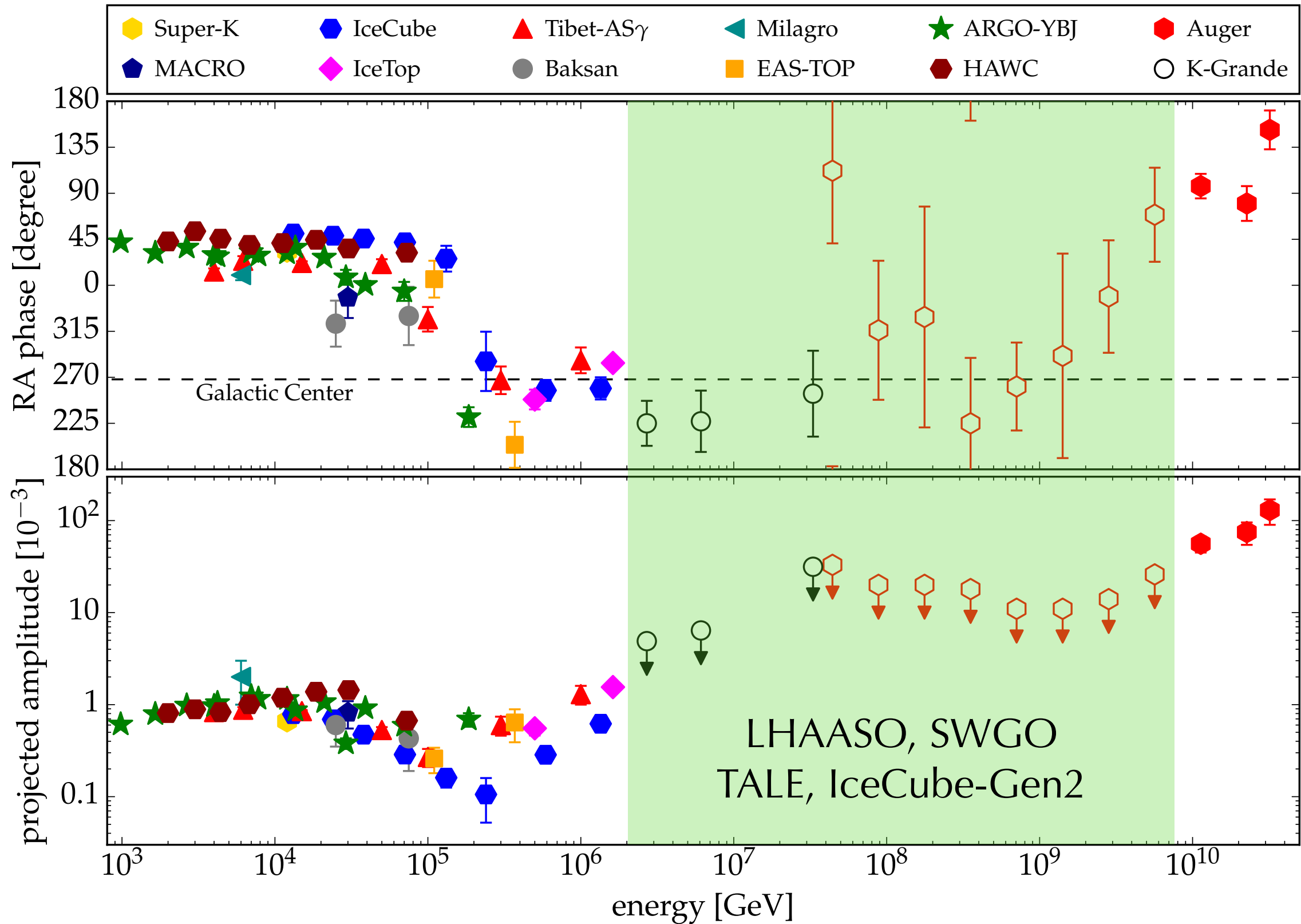


Simulation vs. Data

$$\sigma^2 = 1, r_L/L_c = 0.1, \lambda_{\min}/L_c = 0.01, \lambda_{\max}/L_c = 100, \Omega T = 100$$



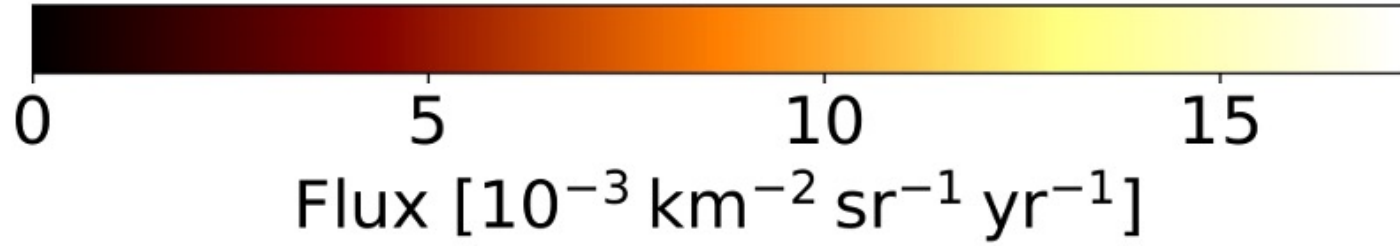
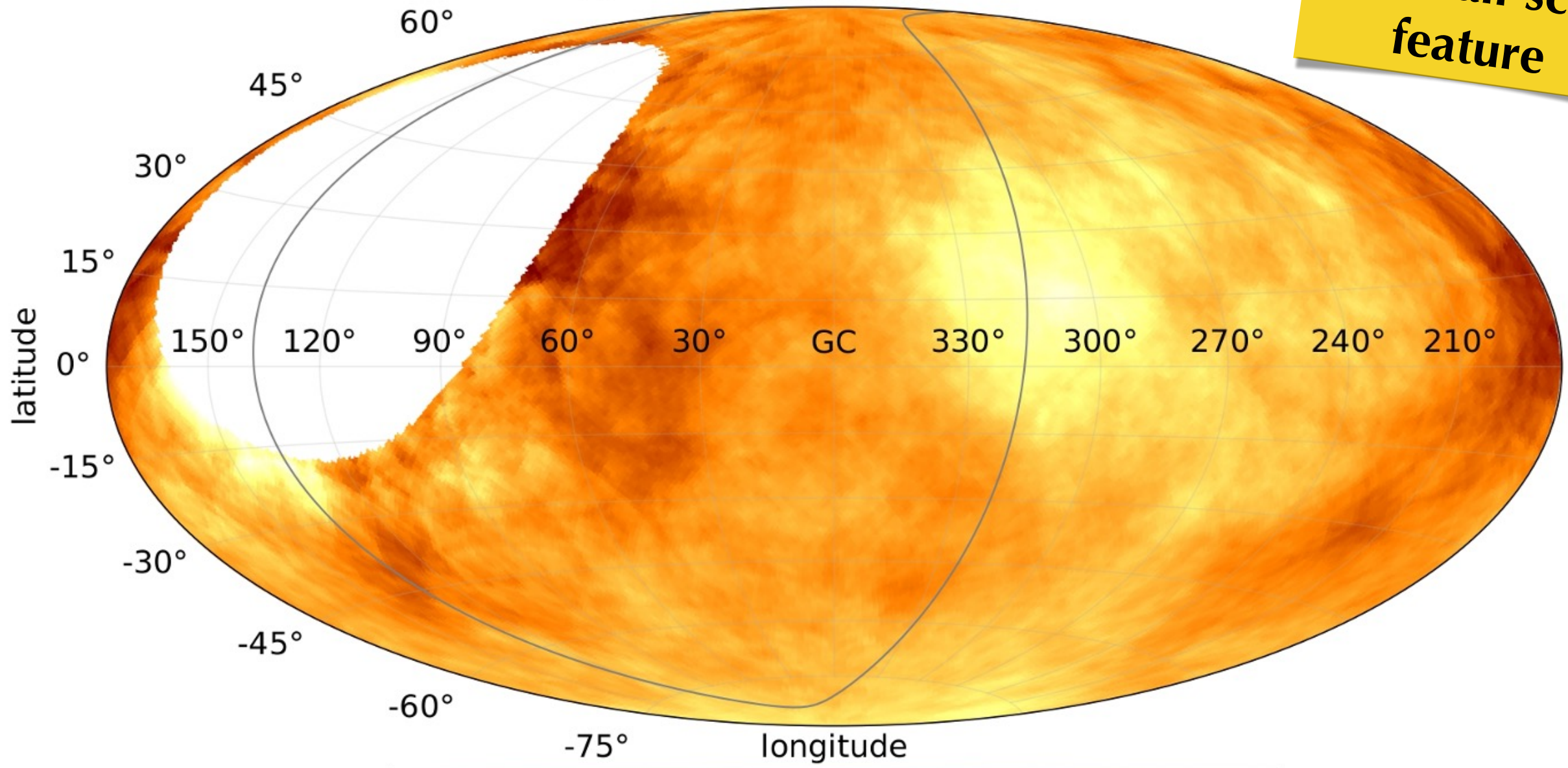
"Via Lactea Incognita"



More UHE CR Anisotropies

$\Phi(E_{\text{Auger}} \geq 41 \text{ EeV}) - \Psi = 25^\circ$
Galactic

**4 σ evidence
for small-scale
feature**

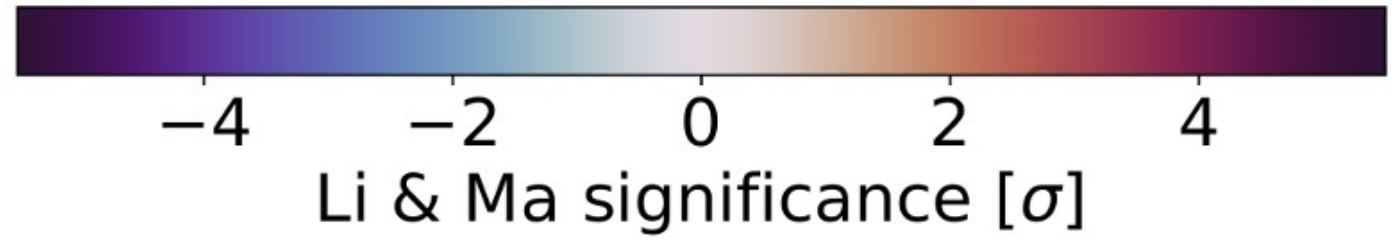
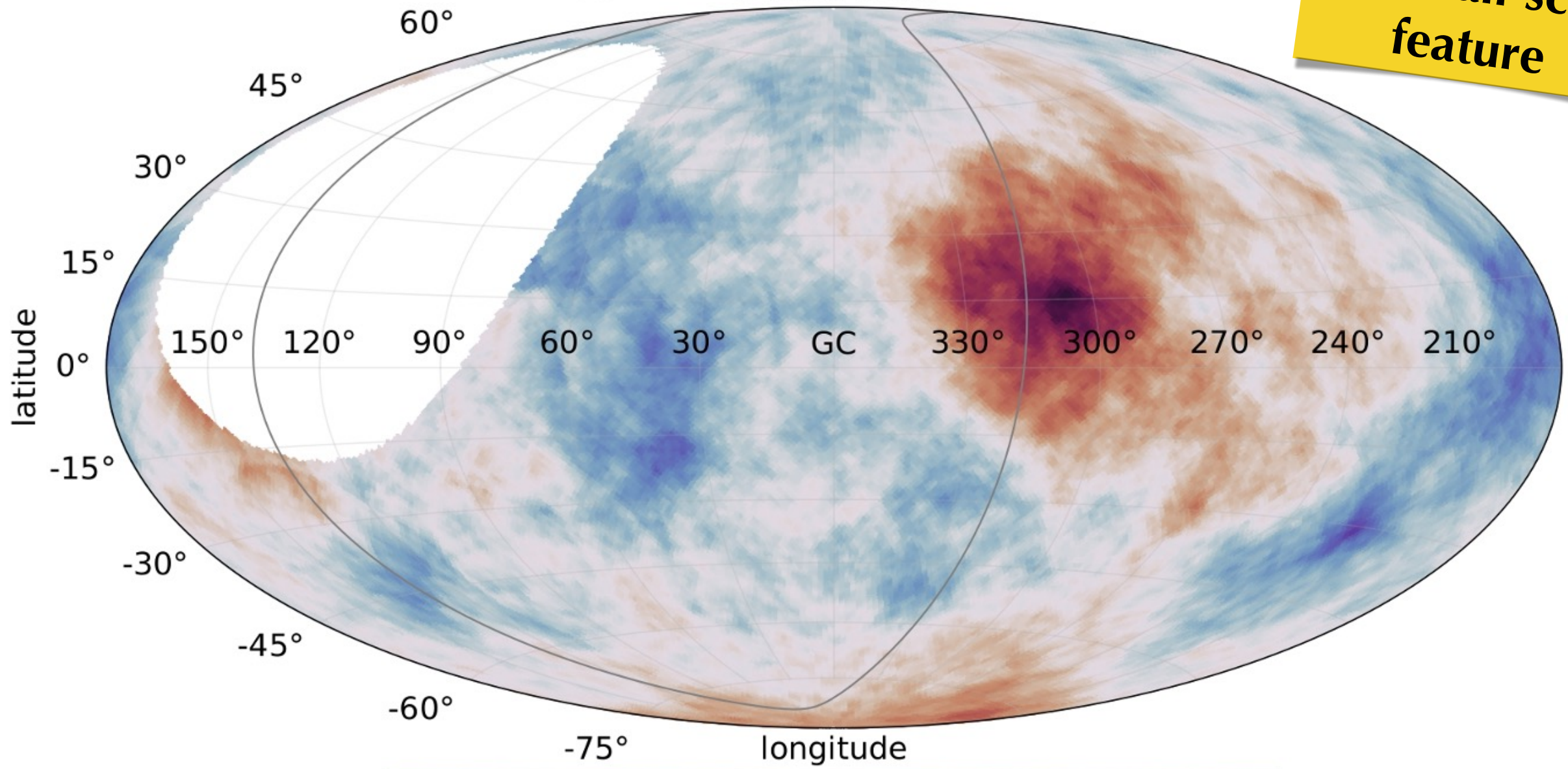


[Auger Collaboration'22]

More UHE CR Anisotropies

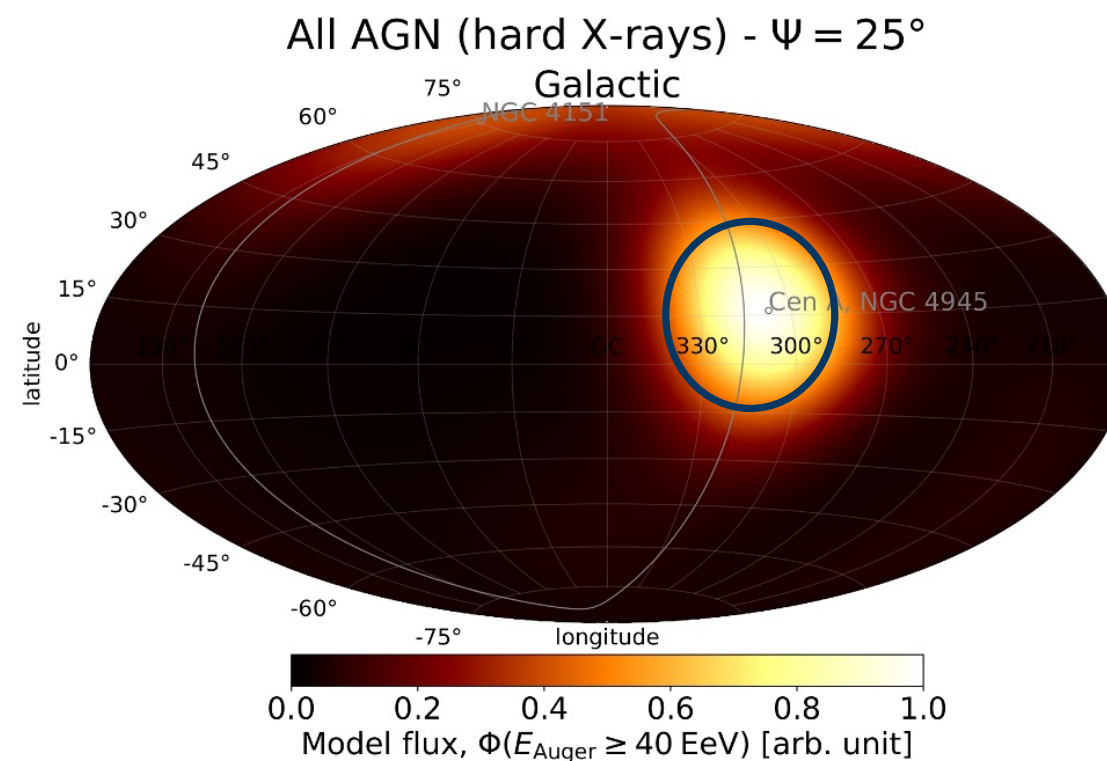
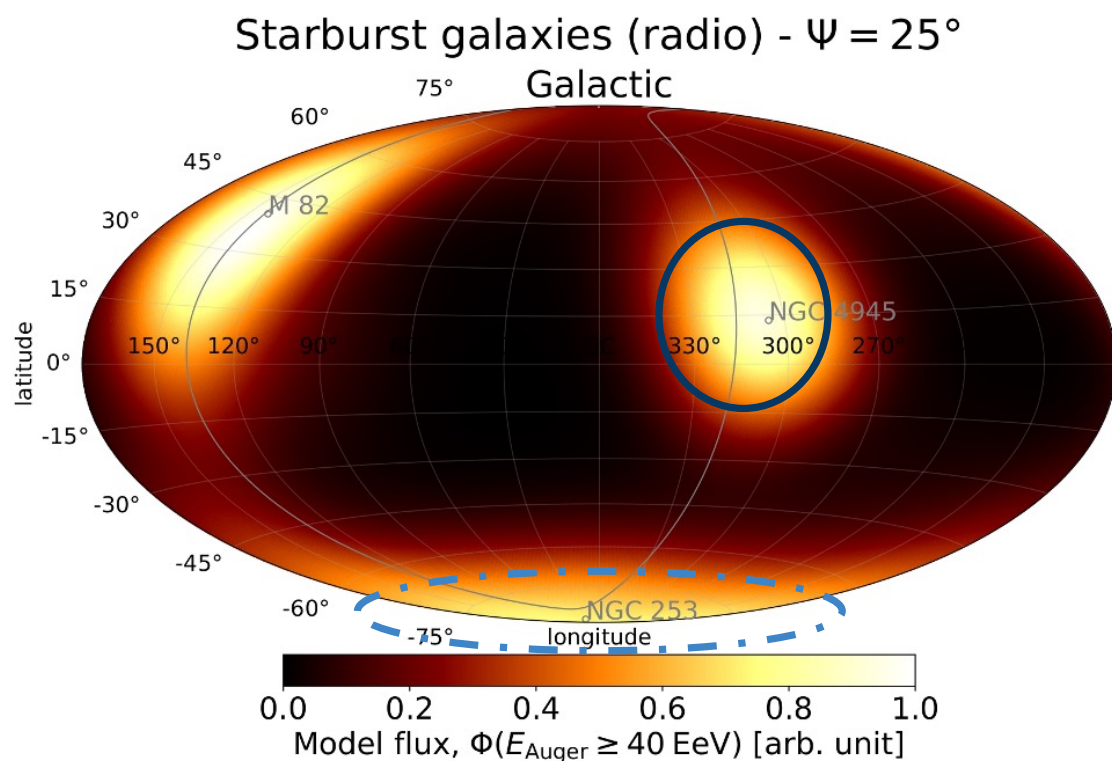
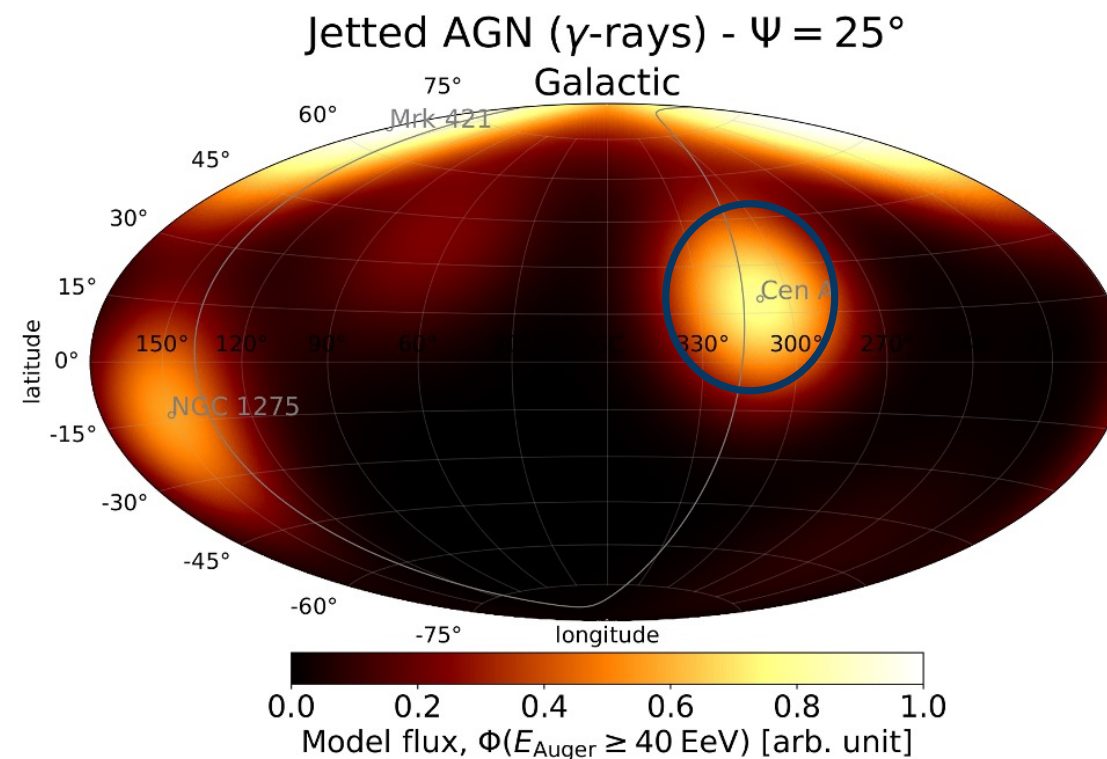
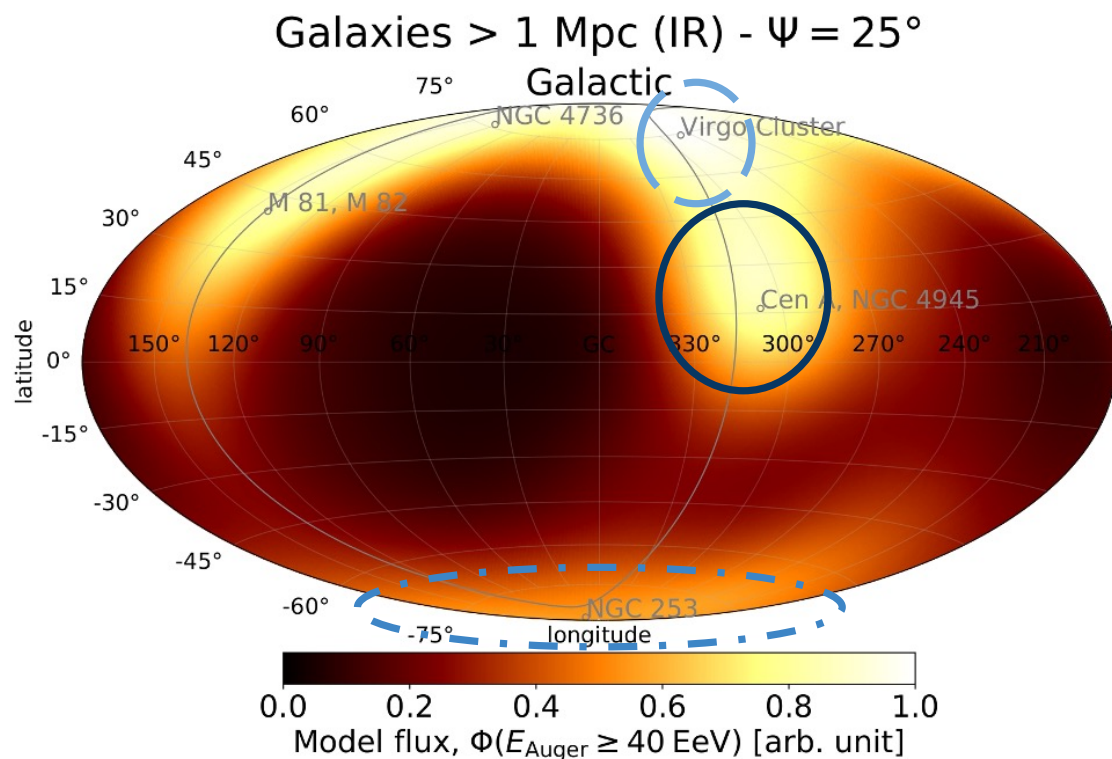
$\sigma(E_{\text{Auger}} \geq 41 \text{ EeV}) - \Psi = 24^\circ$
Galactic

**4 σ evidence
for small-scale
feature**



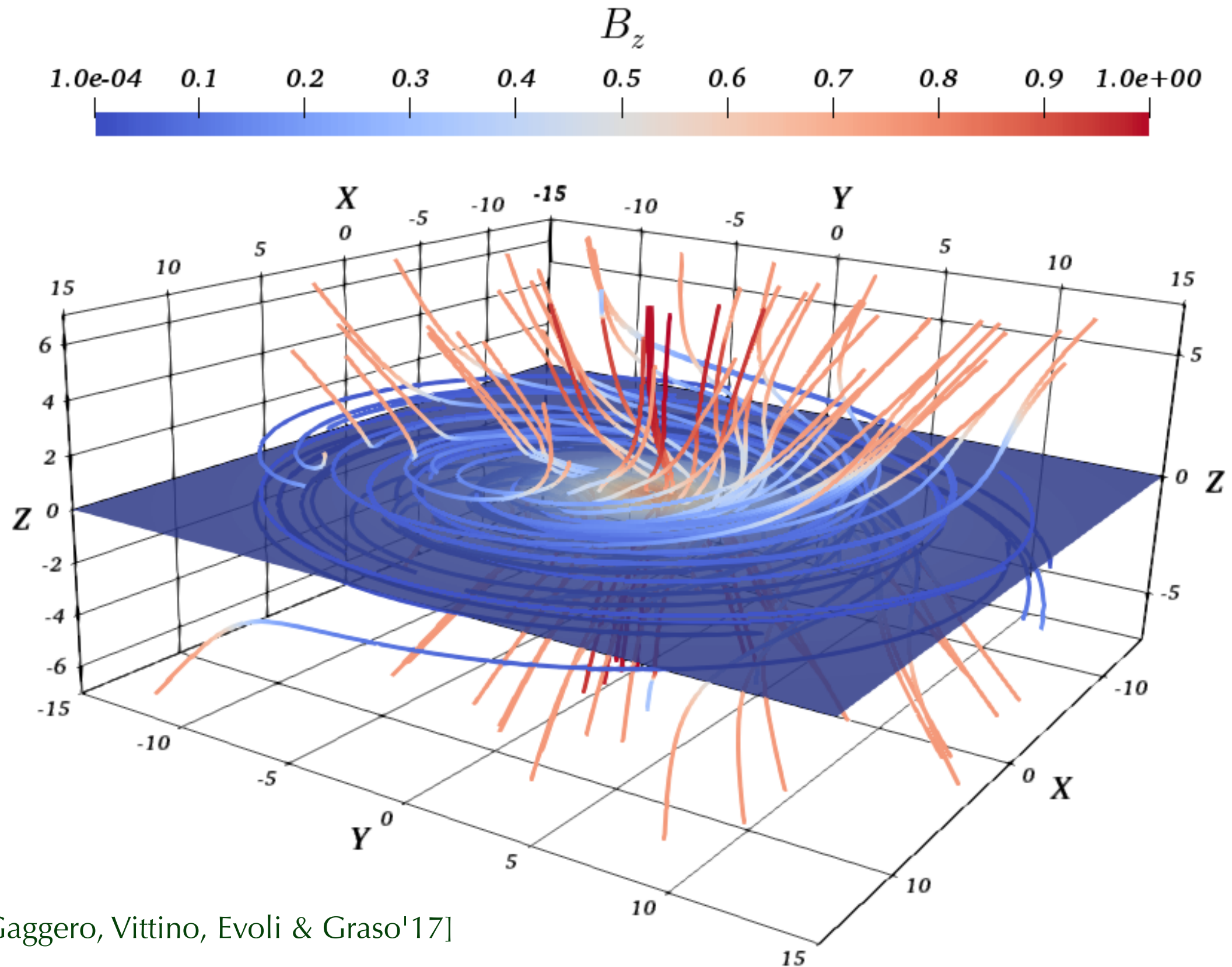
[Auger Collaboration'22]

More UHE CR Anisotropies



[Auger Collaboration'22]

Galactic Magnetic Field



[Cerri, Gaggero, Vittino, Evoli & Graso'17]

Summary

A. Observation of CR anisotropies at the level of one-per-mille is challenging.

- large statistical and systematic uncertainties
- multipole analysis can introduce bias, sometimes not stated or corrected for

B. Dipole anisotropy can be understood in the context of diffusion theory.

- TV-PV dipole phase aligns with the local ordered magnetic field
- amplitude variations as a result of local sources
- plausible candidates are local SNRs, e.g. Vela
- *What is the expected dipole anisotropy in the PV-EV range?*

C. Observed CR data shows also evidence for small-scale anisotropy.

- induces cross-talk with dipole anisotropy in limited field of view
- constitutes a probe of local magnetic turbulence
- *What can we learn about our heliosphere from TV small-scale features?*
- *What is the effect of local ($\lesssim 10$ pc) magnetic turbulence?*
- *How do we disentangle global CR transport features from local turbulence?*

Backup Slides

Turbulence Simulation

- 3D-isotropic turbulence:

[Giacalone & Jokipii'99]

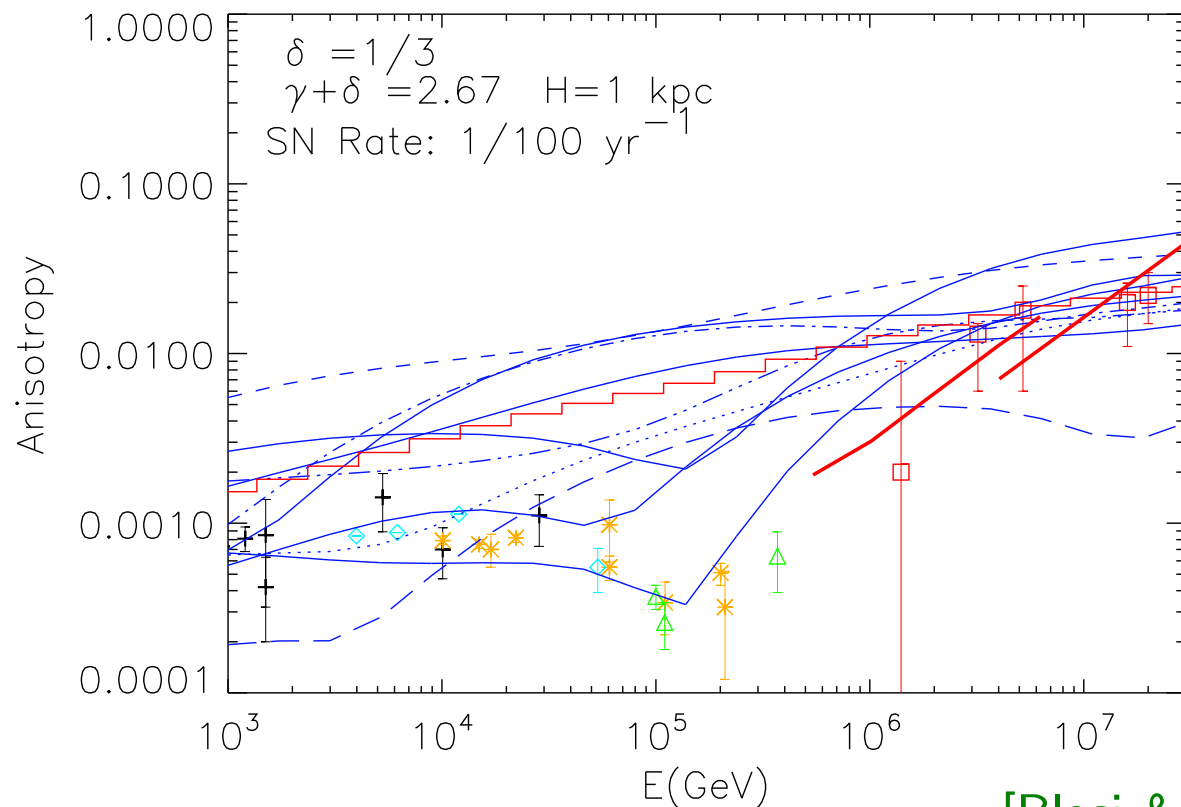
$$\delta\mathbf{B}(\mathbf{x}) = \sum_{n=1}^N A(k_n) (\mathbf{a}_n \cos \alpha_n + \mathbf{b}_n \sin \alpha_n) \cos(\mathbf{k}_n \mathbf{x} + \beta_n)$$

- α_n and β_n are random phases in $[0, 2\pi)$, unit vectors $\mathbf{a}_n \propto \mathbf{k}_n \times \mathbf{e}_z$ and $\mathbf{b}_n \propto \mathbf{k}_n \times \mathbf{a}_n$
- with amplitude

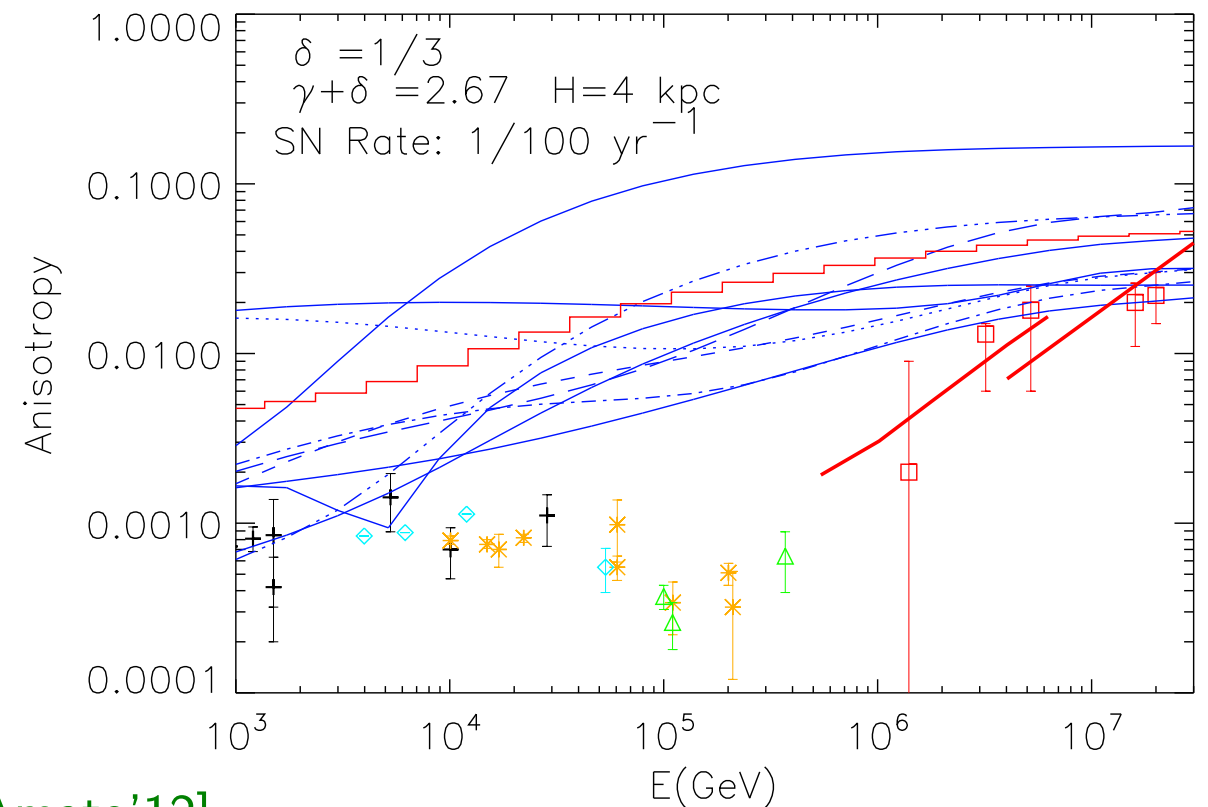
$$A^2(k_n) = \frac{2\sigma^2 B_0^2 G(k_n)}{\sum_{n=1}^N G(k_n)} \quad \text{with} \quad G(k_n) = 4\pi k_n^2 \frac{k_n \Delta \ln k}{1 + (k_n L_c)^\gamma}$$

- Kolmogorov-type turbulence: $\gamma = 11/3$
- $N = 160$ wavevectors \mathbf{k}_n with $|\mathbf{k}_n| = k_{\min} e^{(n-1)\Delta \ln k}$ and $\Delta \ln k = \ln(k_{\max}/k_{\min})/N$
- $\lambda_{\min} = 0.01L_c$ and $\lambda_{\max} = 100L_c$ [Fraschetti & Giacalone'12]
- rigidity: $r_L = 0.1L_c$
- turbulence level: $\sigma^2 = \mathbf{B}_0^2 / \langle \delta\mathbf{B}^2 \rangle = 1$

Local Sources



[Blasi & Amato'12]



- Distribution of local cosmic ray sources (SNR) in position and time induces variation in the anisotropy.

[Erlykin & Wolfendale'06; Blasi & Amato'12]

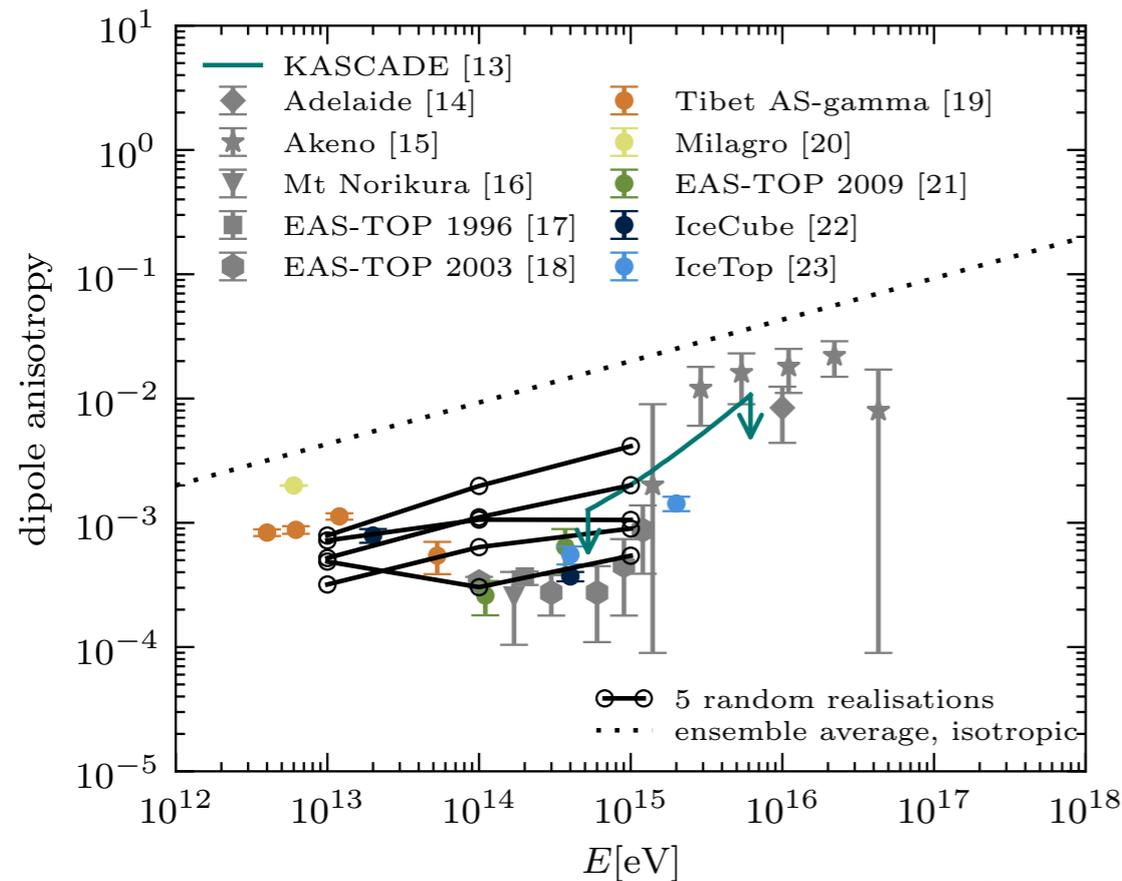
[Sveshnikova *et al.*'13; Pohl & Eichler'13]

- variance of amplitude can be estimated as:

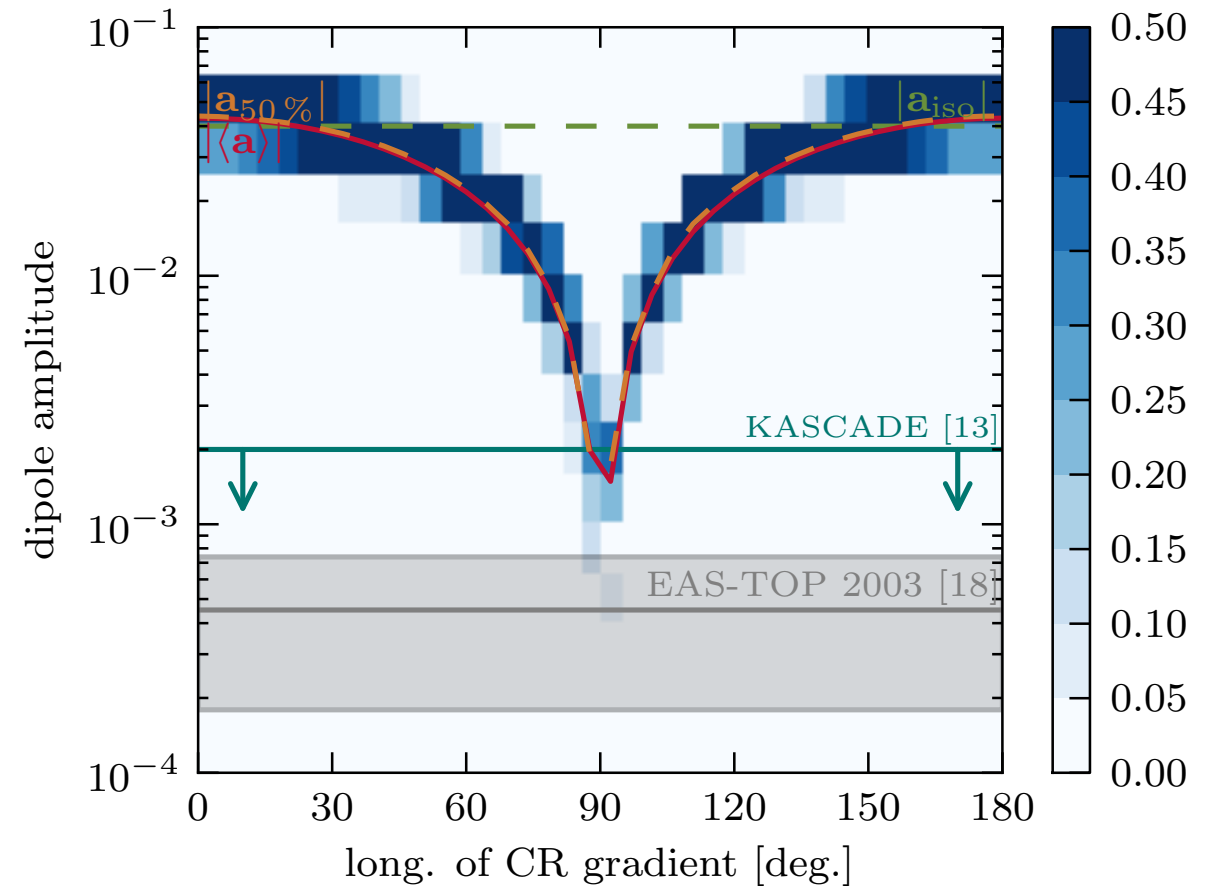
[Blasi & Amato'12]

$$\sigma_A \propto \frac{K(E)}{cH} \quad \rightarrow \quad \frac{\sigma_A}{A} = \text{const}$$

Local Magnetic Field



[Mertsch & Funk'14]



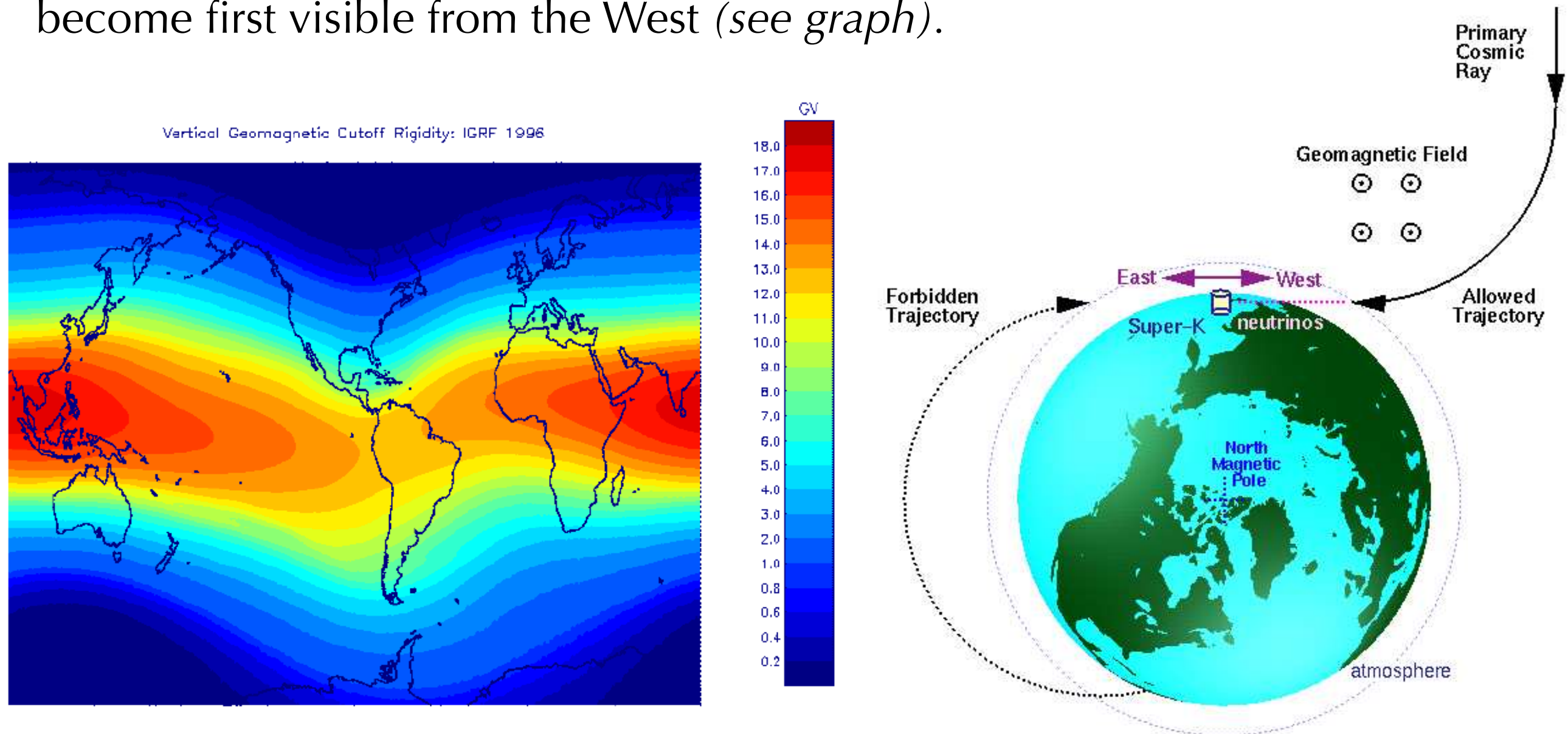
- strong regular magnetic fields in the local environment
- diffusion tensor reduces to **projector**: [e.g. Mertsch & Funk'14; Schwadron *et al.*'14; MA'17]

$$K_{ij} \rightarrow \kappa_{\parallel} \hat{B}_i \hat{B}_j$$

- reduced dipole amplitude and alignment with magnetic field: $\delta \parallel \mathbf{B}$

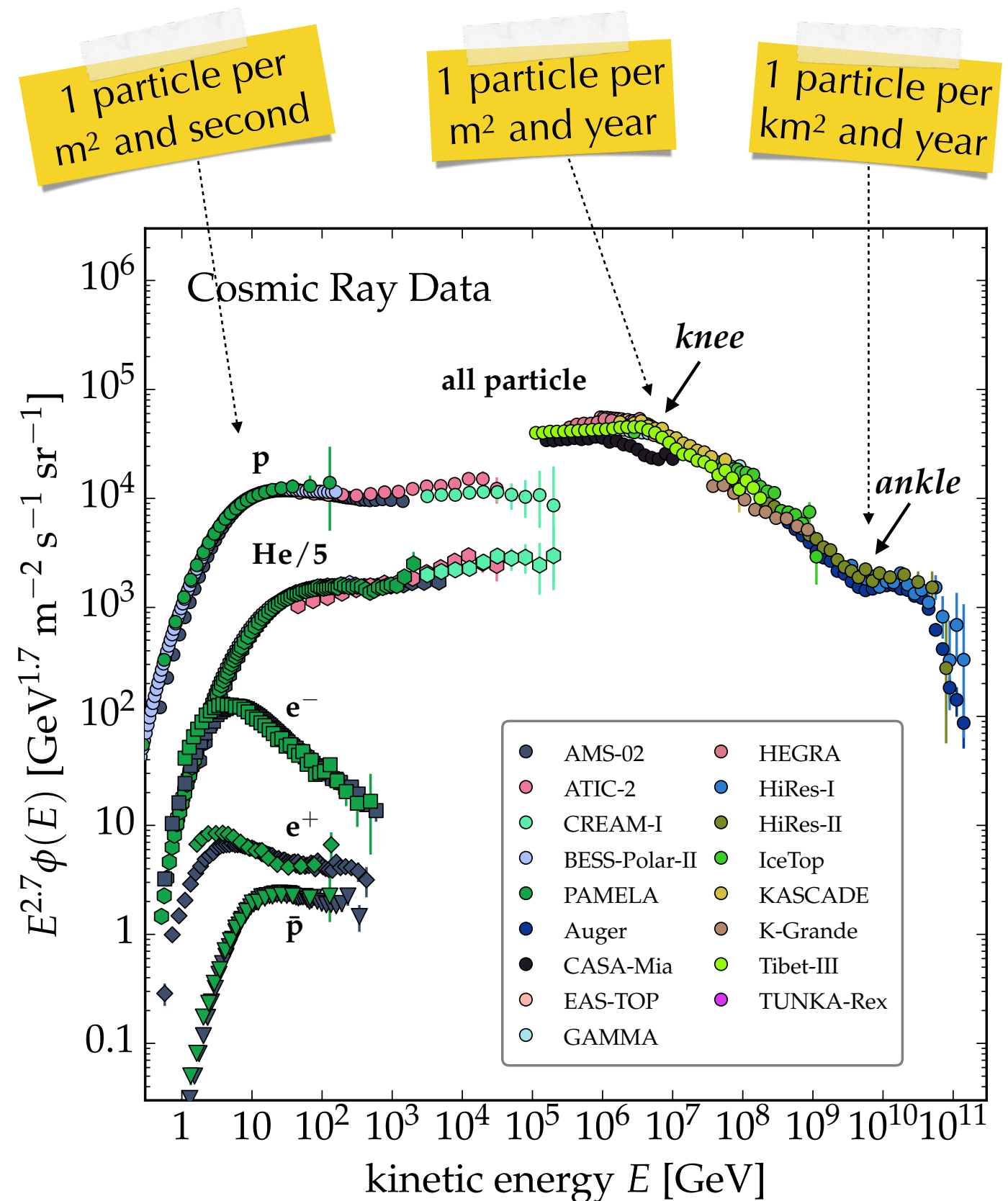
Rigidity Cutoff & East-West Effect

- **Rigidity cutoff:** Low-rigidity cosmic rays can not enter the atmosphere from vertical direction (*see plot*).
- **East-West effect:** Close to the rigidity cutoff, cosmic rays with positive charge become first visible from the West (*see graph*).



Cosmic Rays

- Cosmic rays (CRs) are energetic nuclei and (at a lower level) leptons.
- Spectrum follows a **power-law** over many orders of magnitude, indicating a **non-thermal origin**.
- **Direct observation** with satellite and balloon-borne experiments up to TeV energies (small detectors with good resolution for individual elements).
- **Indirect observation** as air showers above 10 TeV (large detectors with poor resolution).



Conventions and Units

Cosmic ray physics is tightly connected to the advent of particle physics.

Unit of energy used in astroparticle physics: **electron-Volt (eV)**

$$10^6 \text{ eV} = 1 \text{ MeV} \quad m_e c^2 \simeq \frac{1}{2} \text{ MeV}$$

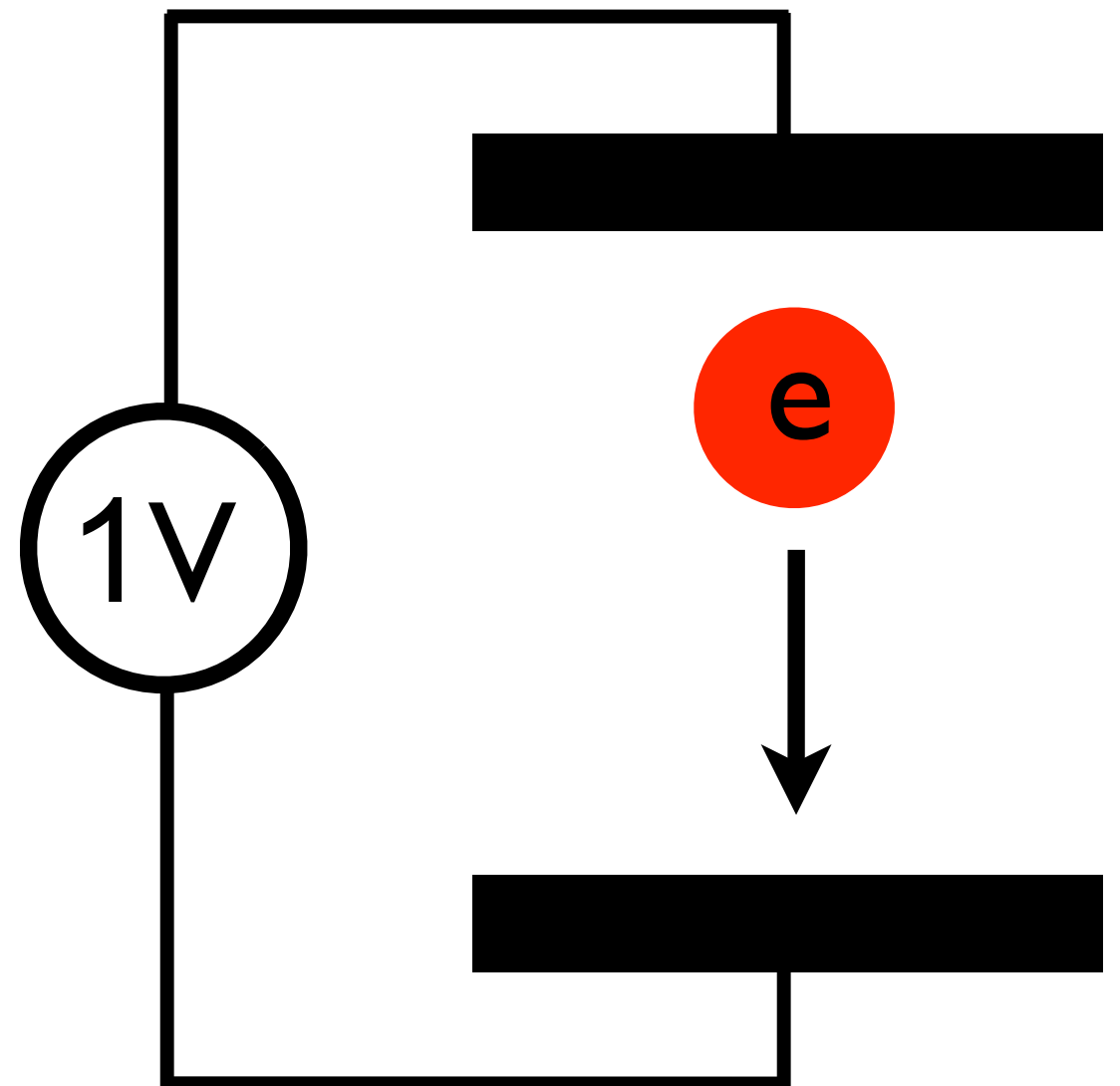
$$10^9 \text{ eV} = 1 \text{ GeV} \quad m_p c^2 \simeq 1 \text{ GeV}$$

$$10^{12} \text{ eV} = 1 \text{ TeV} \quad \sqrt{s_{\text{LHC}}} \simeq 7 \text{ TeV}$$

$$10^{15} \text{ eV} = 1 \text{ PeV} \quad E_{\text{max,Earth}} \simeq 2 \text{ PeV}$$

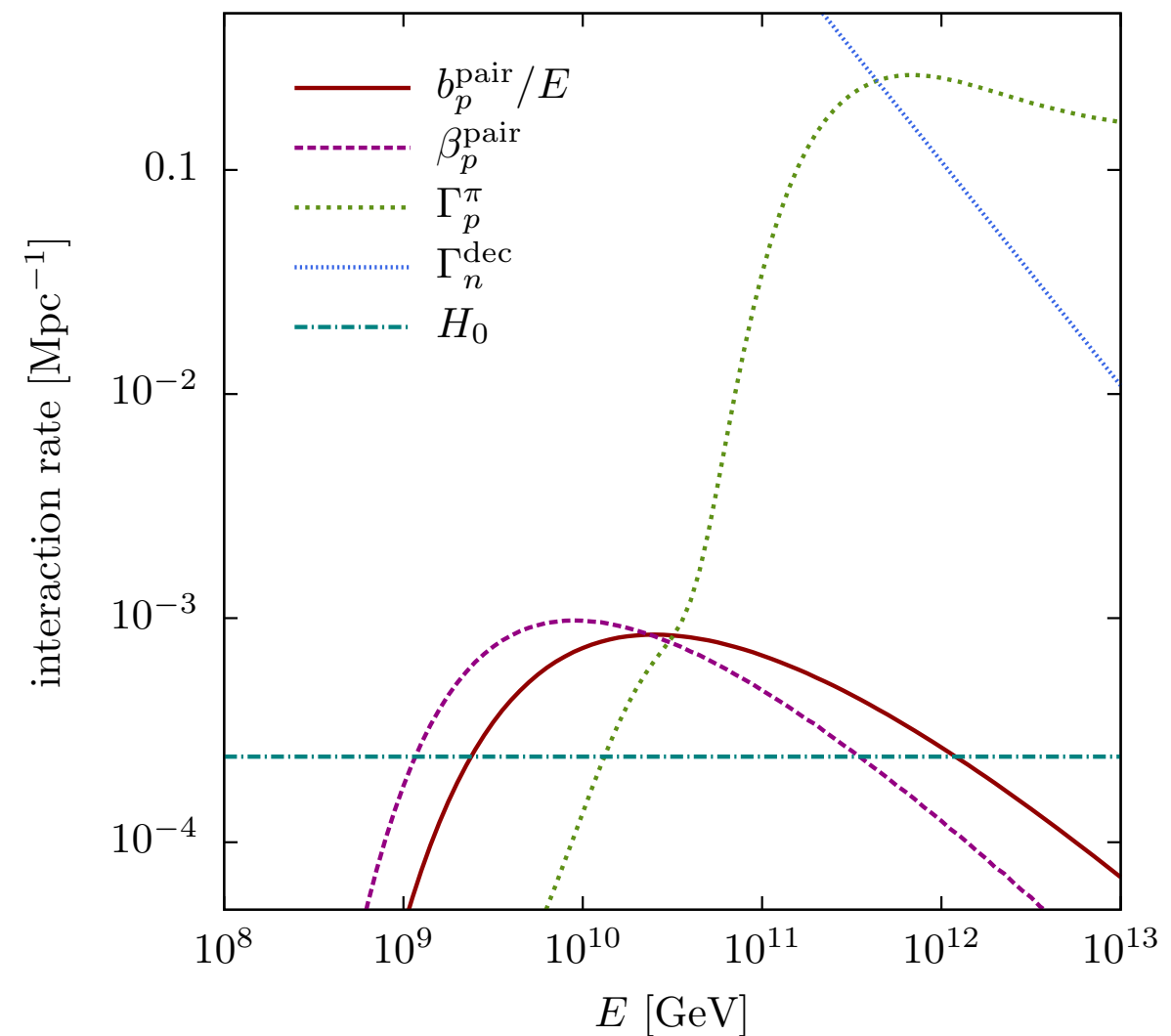
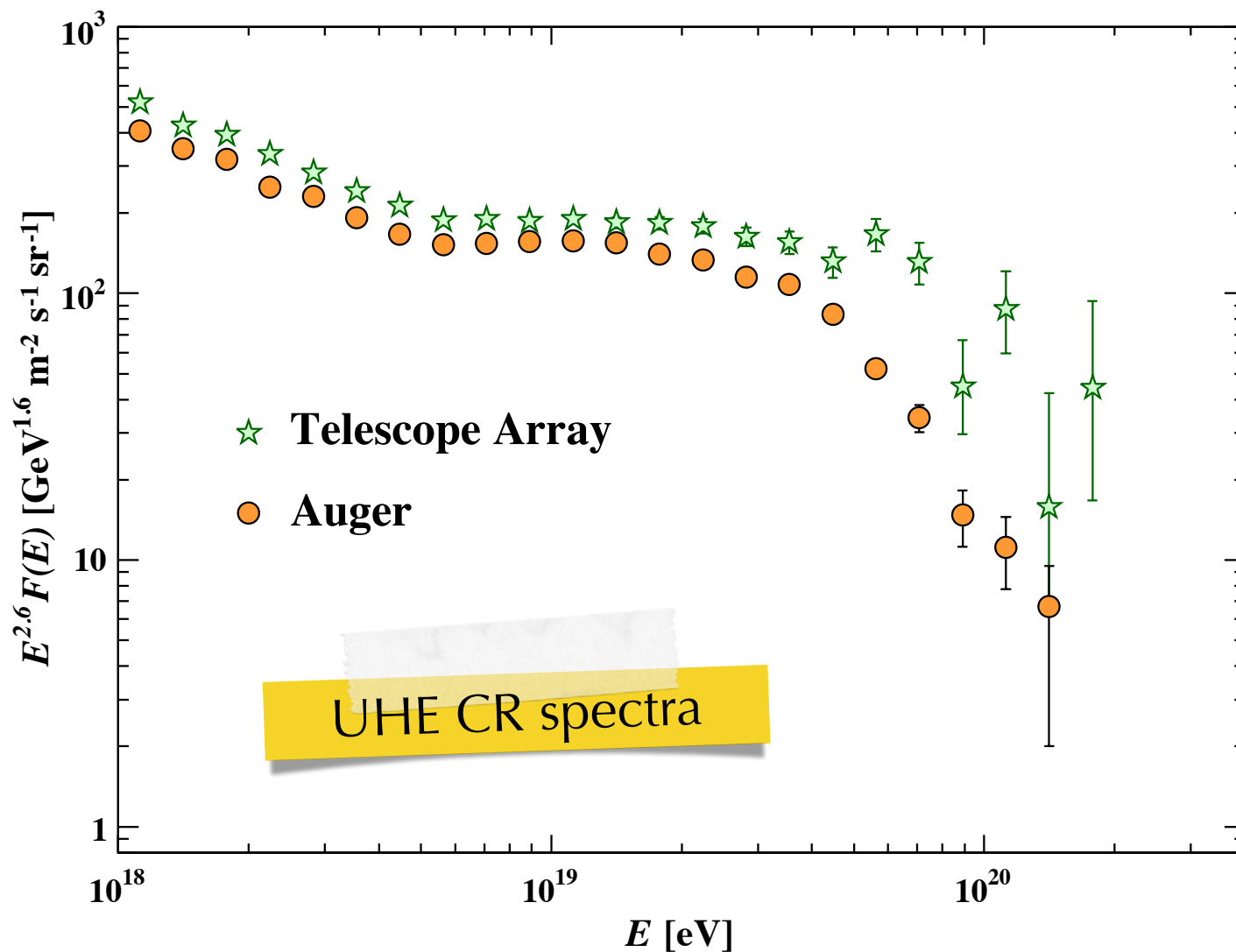
$$10^{18} \text{ eV} = 1 \text{ EeV} \quad \text{Joule} \simeq 6 \text{ EeV}$$

$$10^{21} \text{ eV} = 1 \text{ ZeV} \quad ???$$

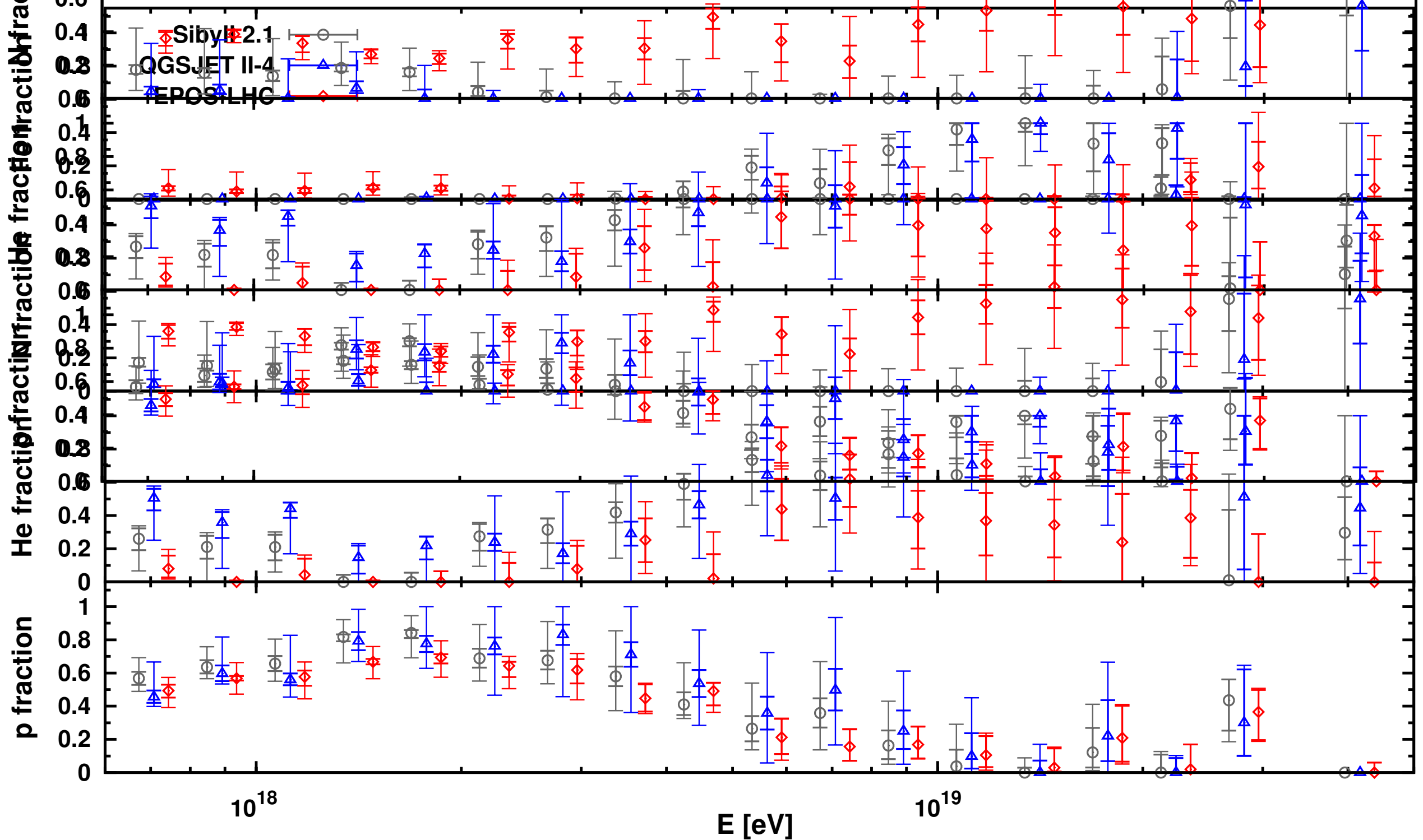


UHE CR Spectrum

- UHE CR spectrum expected to show *GZK cutoff* due to interactions with cosmic microwave background. [Greisen & Zatsepin'66; Kuzmin'66]
- resonant interactions $p + \gamma_{\text{CMB}} \rightarrow \Delta^+ \rightarrow X$ lead to $E_{\text{GZK}} \simeq 40 \text{ EeV}$
- UHE CR propagation limited to less than about 200 Mpc.

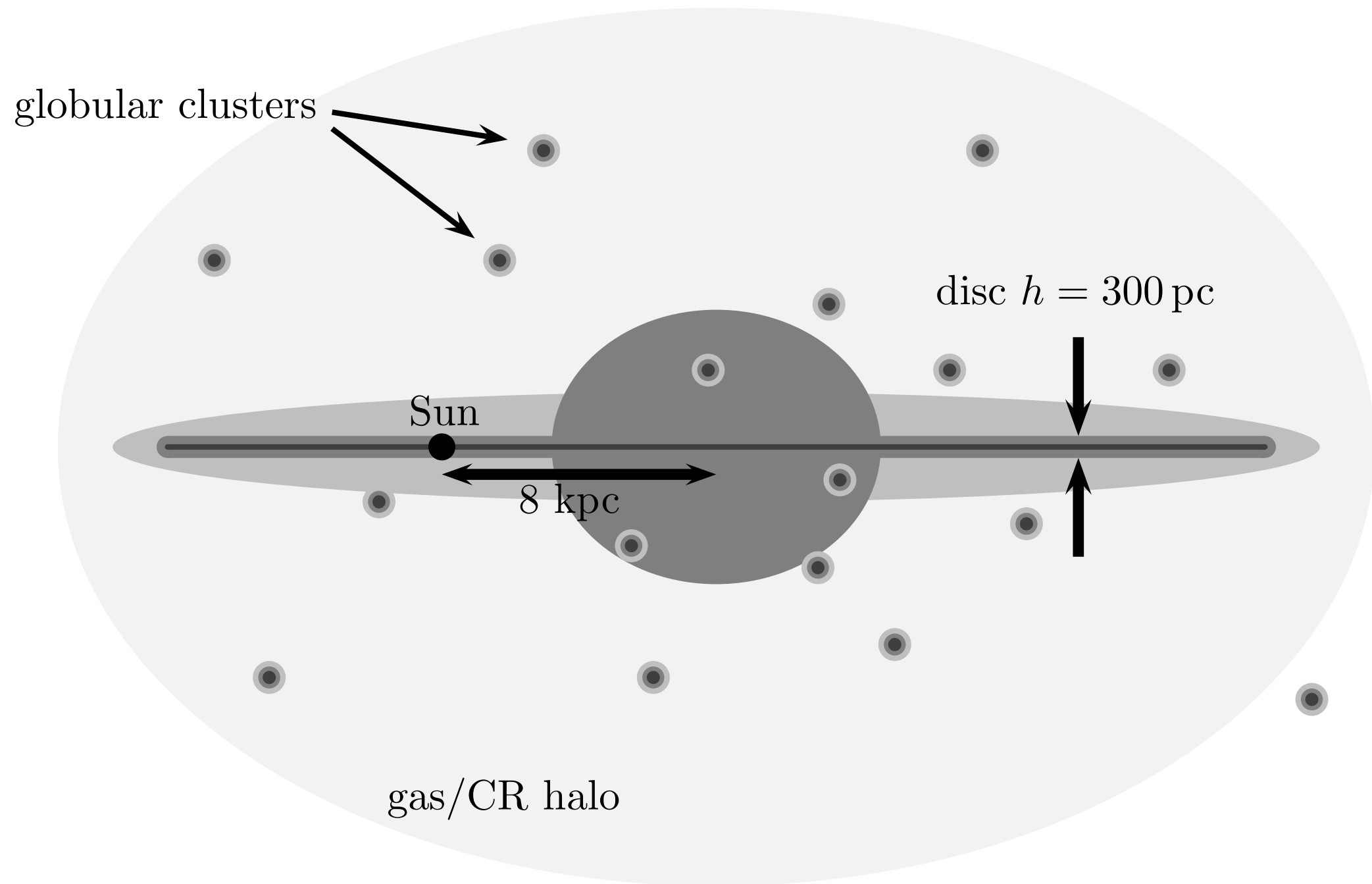


UHE CR Composition



Composition of UHE CRs is uncertain; depends on details of CR interactions in atmosphere.

Leaky-Box Model



[from Kachelriess'08]

Leaky Box Model

- Cosmic ray diffusion in our Galaxy is mainly limited to a volume \mathcal{V} that support turbulent magnetic fields.
- The **total number** of CRs in this volume is given by the integral:

$$N_{\text{CR}}(t, E) = \int_{\mathcal{V}} d\mathbf{r} n(t, \mathbf{r}, E)$$

- In steady-state ($\partial_t N_{\text{CR}} = 0$) the loss through the surface of the volume has to be balanced by the newly generated CRs from sources:

$$\int_{\partial\mathcal{V}} d\mathbf{A}_{\perp} \cdot \mathbf{K} \cdot \nabla n = \int_{\mathcal{V}} d\mathbf{r} Q(t, \mathbf{r}, E) = Q_{\text{tot}}(t, E)$$

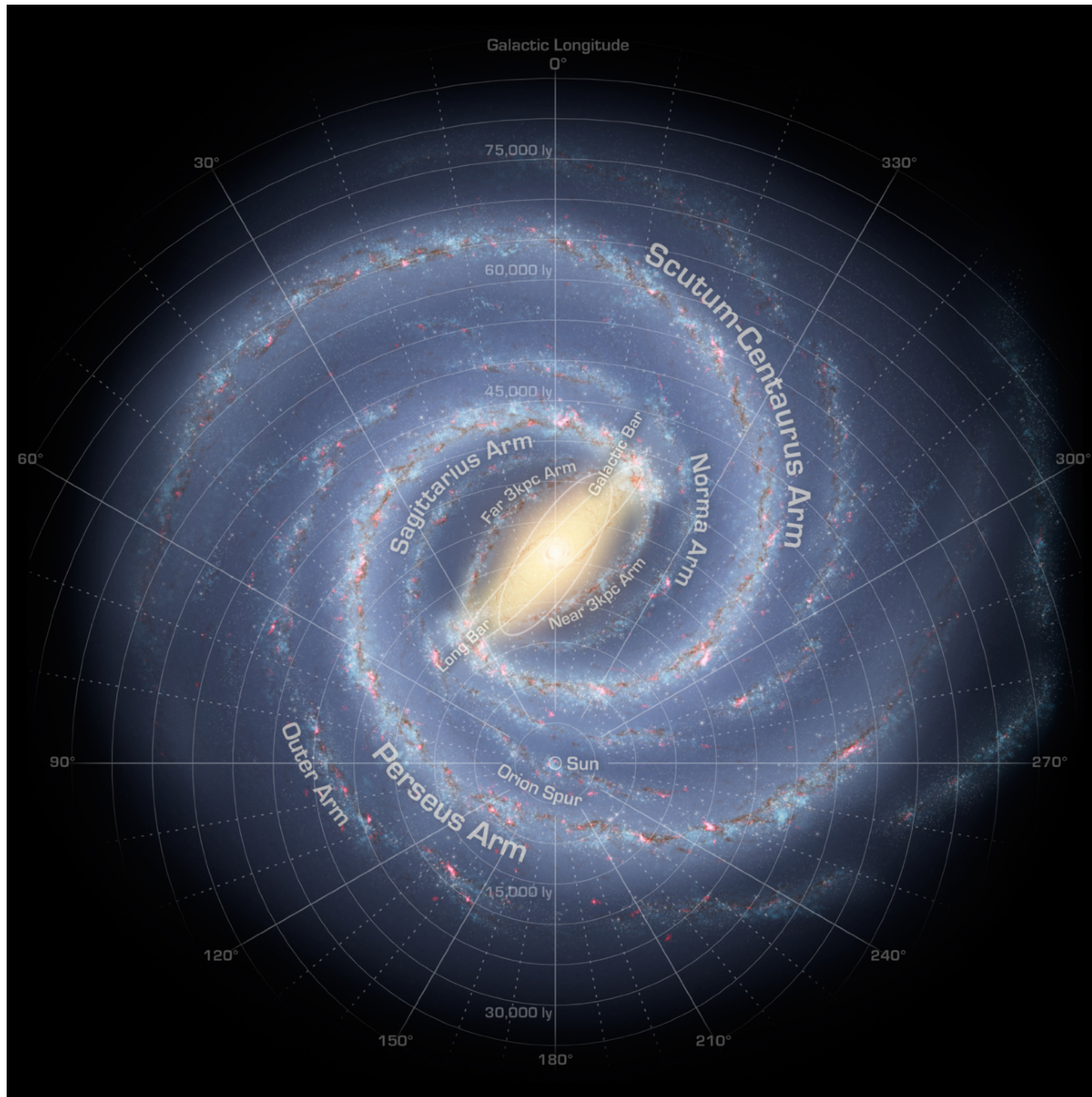
- In the “leaky-box” approximation, the loss is parametrized by an effective loss time:

$$\frac{N_{\text{CR}}(E)}{\tau_{\text{loss}}(E)} \simeq \int_{\partial\mathcal{V}} d\mathbf{A}_{\perp} \cdot \mathbf{K} \cdot \nabla n$$

- For diffusion coefficient $K(E) \propto E^{\delta}$, the loss time scales as $\tau_{\text{loss}}(E) \propto E^{-\delta}$.
- If the source spectrum $Q_{\text{tot}} \propto E^{-\alpha}$ then the observed CR spectrum is:

$$N_{\text{CR}}(E) \simeq \tau_{\text{loss}}(E) Q_{\text{tot}}(t, E) \propto E^{-\alpha-\delta}$$

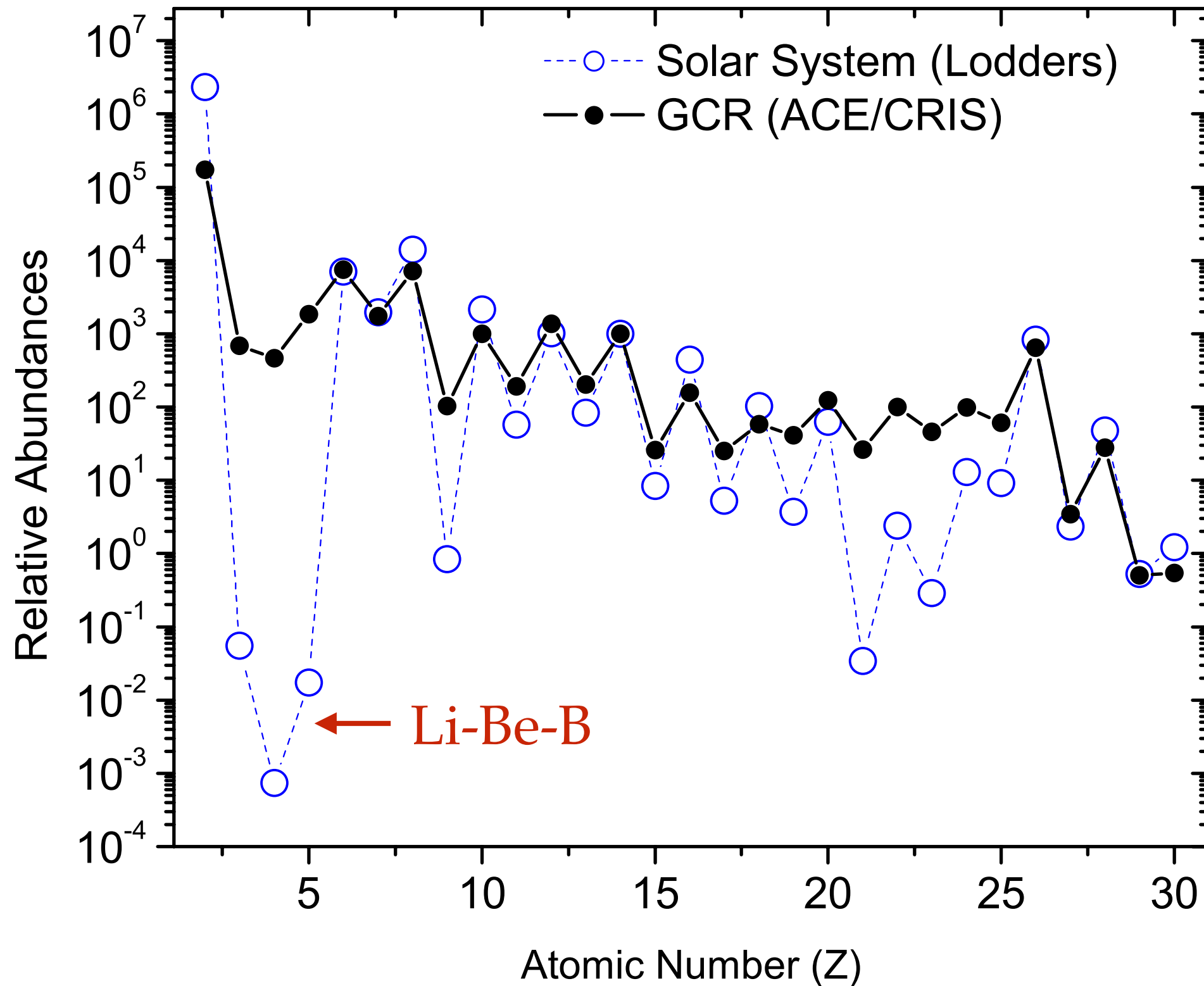
Galactic Cosmic Rays



General Transport Equation

$$\begin{aligned}
 \frac{\partial n_i}{\partial t} = & \frac{\partial}{\partial r_a} \left(K_{ab} \frac{\partial}{\partial r_b} n_i \right) && \text{(spatial diffusion)} \\
 & + \frac{\partial}{\partial p} \left[p^2 \tilde{K} \frac{\partial}{\partial p} \left(\frac{n_i}{p^2} \right) \right] && \text{(momentum diffusion)} \\
 & - \frac{\partial}{\partial r_a} \left(V_a n_i \right) && \text{(convection)} \\
 & - \frac{\partial}{\partial p} \left(\dot{p} n_i - \frac{p}{3} \left(\frac{\partial V_a}{\partial r_a} \right) n_i \right) && \text{(continuous \& adiabatic loss)} \\
 & - \Gamma_i^{\text{dec}}(E_i) n_i && \text{(CR decay)} \\
 & - c \rho_{\text{ISM}} \sigma_i(E_i) n_i && \text{(loss from CR collisions)} \\
 & + c \rho_{\text{ISM}} \sum_j \int dE_j \frac{d\sigma_{j \rightarrow i}}{dE_i}(E_j, E_i) n_j(E_j) && \text{(gain from CR collisions)} \\
 & + Q_i && \text{(source term)}
 \end{aligned}$$

Relative Abundance of Elements



Secondary-To-Primary Ratio

- The abundance of cosmic rays in the Li-Be-B group ($Z = 3 - 5$) is larger than expected from solar abundance measurements.
- We can understand this phenomenon by considering the production of secondary cosmic rays (n_s) in primary cosmic ray (n_p) collisions in background molecular gas:

$$\partial_t N_s(E) = -\frac{N_s(E)}{\tau_{\text{loss}}(E)} + c\rho\sigma_{p\rightarrow s}N_p(E)$$

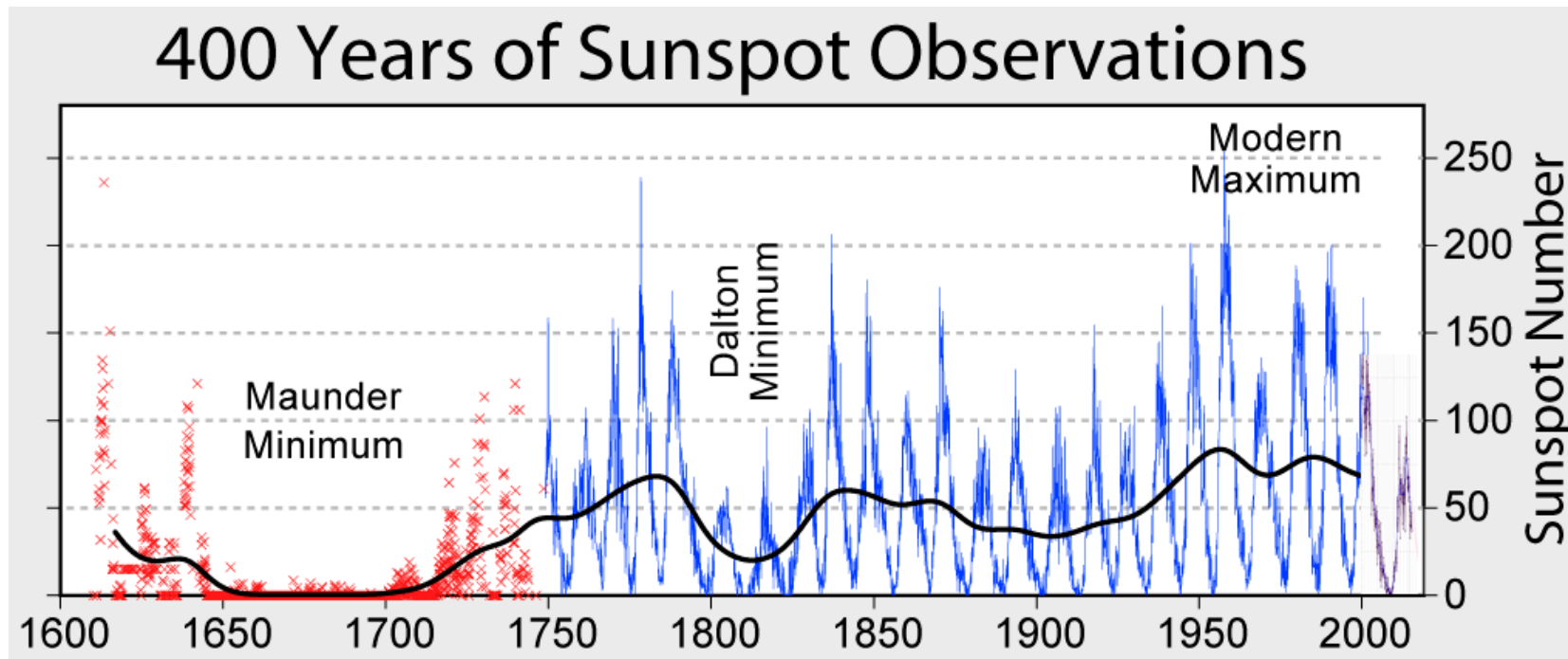
- We can again look for the steady-state solution ($\partial_t N_p = 0$ & $\partial_t N_s = 0$):
- The solution is

$$N_s(E) = \tau_{\text{loss}}(E)c\rho\sigma_{p\rightarrow s}N_p(E)$$

- The secondary-to-primary ratio is:

$$\frac{N_s(E)}{N_p(E)} = \tau_{\text{loss}}(E)c\rho\sigma_{p\rightarrow s} \propto E^{-\delta}$$

Solar Magnetic Field

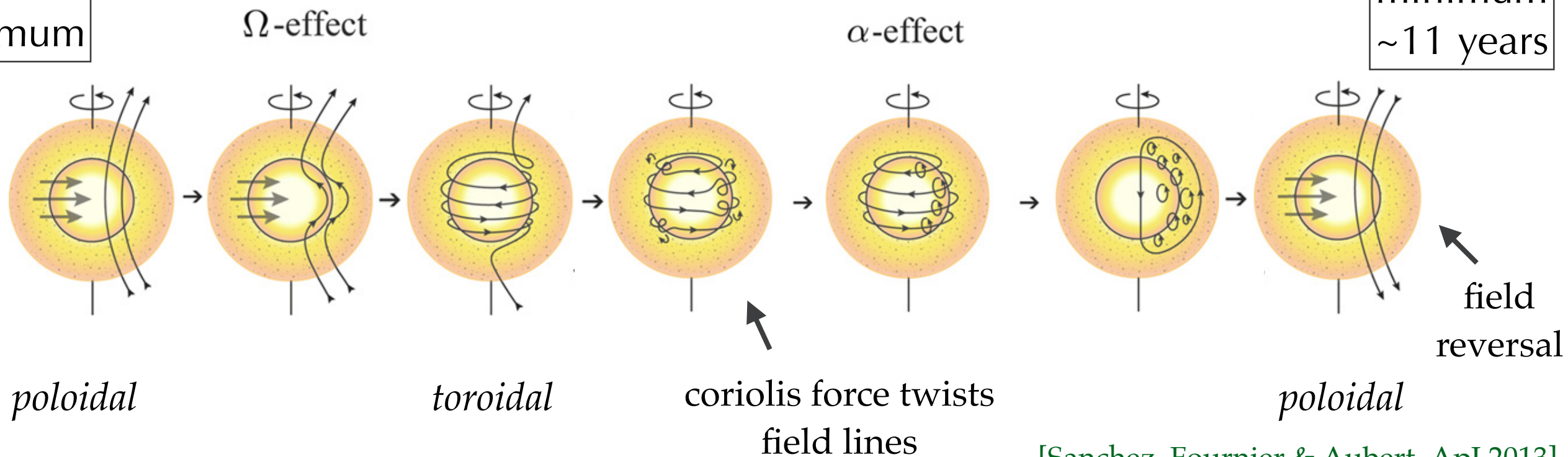


Solar cycle with period ~22 year

solar maximum
with sunspots
and flares (outflow)

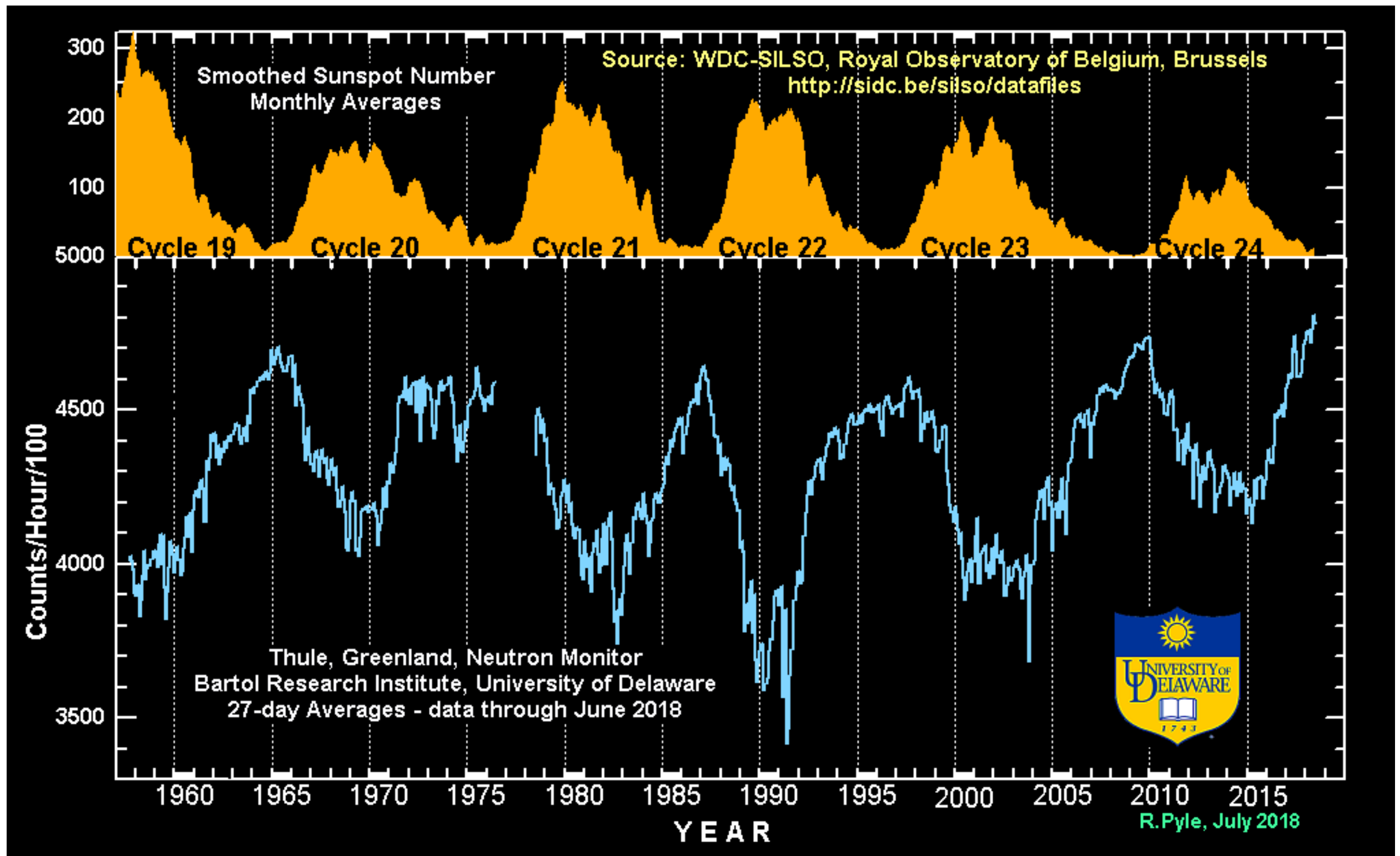
solar
minimum

next solar
minimum
~11 years



[Sanchez, Fournier & Aubert, ApJ 2013]

Solar Cycle



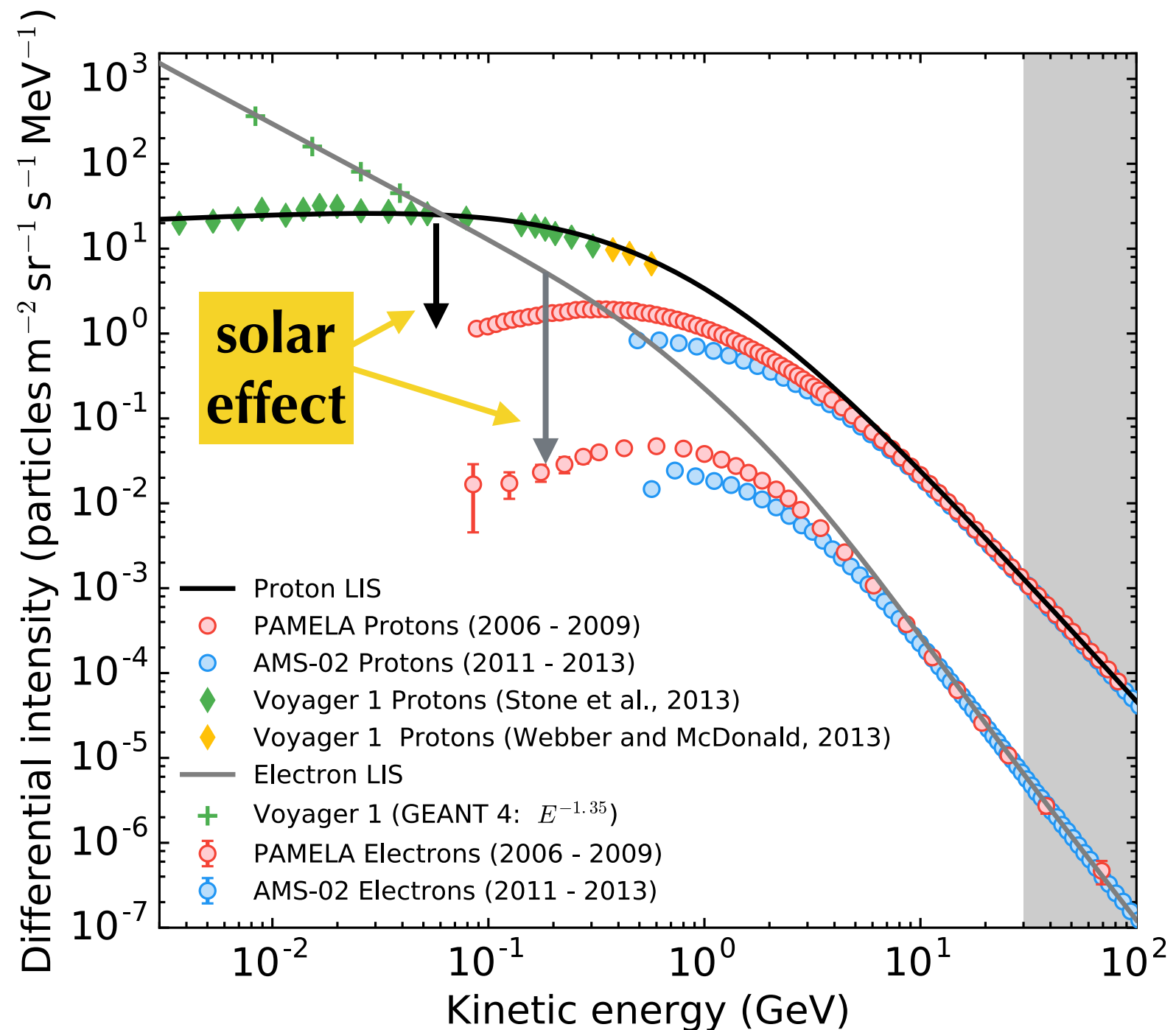
Solar Modulation

- Voyager satellite observes proton & electron spectra in local interstellar medium (LIS): **no solar effect**

PAMELA 2006-2009
solar minimum

AMS-02 2011-2013
solar maximum

- Effect can be treated via a *force field approximation* corresponding to a **solar potential**.



[Potgieter & Vos, A&A 2017]